ROLE OF PITUITARY ADENYLATE CYCLASE-ACTIVATING POLYPEPTIDE IN ENERGY EXPENDITURE INCLUDING THE THERMOGENIC RESPONSE

by

Daemon Lee Cline

B.Sc. (Hons.), University of Northern British Columbia, 2016

THESIS SUBMITTED IN PARTIAL FULFILLMENT OF
THE REQUIREMENTS FOR THE DEGREE OF
MASTER OF SCIENCE
IN
BIOCHEMISTRY

UNIVERSITY OF NORTHERN BRITISH COLUMBIA

February 2020

ABSTRACT

Obesity results when energy intake chronically exceeds energy expenditure, driving accumulation and malfunctioning of white adipose tissue and increasing risk for comorbidity. Brown adipose tissue (BAT) burns energy via adaptive thermogenesis, a process gaining therapeutic interest to restore energy balance in obesity. PACAP regulates energy expenditure including thermogenesis in BAT, but the neuronal circuits involved are not well known. Thus, we aim to develop a tool to safely restore PACAP in the hypothalamic ventromedial nucleus (VMN) of PACAP-null mice to assess the VMN's contribution. We also investigated whether PACAP directly regulates BAT function by binding at adipocytes. We discovered PACAP receptor expression in BAT and genetic regulation of receptor expression with cold acclimation. Acute *in vitro* studies did not show PACAP-stimulated thermogenesis in BAT. Studying adaptive thermogenesis and its hypothalamic regulation will contribute to the field of energy metabolism, and the pathophysiology of obesity and type 2 diabetes.

TABLE OF CONTENTS

LIST OF TABLES

LIST OF FIGURES

ACKNOWLEDGEMENT

I gratefully acknowledge the financial contributions of the Natural Sciences and Engineering Council of Canada (NSERC) and the University of Northern BC throughout my undergraduate and graduate studies so that I could focus my efforts on academic achievement and research, including this thesis. A sincere thank you to my MSc Supervisor, Dr. Sarah Gray, for her unwavering support as a mentor, advisor, and role model in all areas of my professional development throughout my graduate studies. She has fostered an inclusive, fair, and caring environment for everyone in the Gray Lab family and I cherish my time there. I thank Dr. Dezene Huber for being an excellent professor, supervisor, and Graduate Supervisory Committee Member to support my various academic and employment endeavors, including his unwavering patience through the unending requests for reference letters. I thank Dr. Geoff Payne for taking time out of his exceptionally busy schedule to guide my master's degree and thesis as a Graduate Supervisory Committee Member. Further, I thank both Drs. Payne and Gray for fostering an interest in physiology in me, which has focused my career interests in a positive way. I would also like to thank my undergraduate thesis supervisor Dr Daniel Erasmus for introducing me to research. I thank Lydia Troc, Sianne Vautour, and Natalie de Brun for taking exceptional care of our research animals and thank the mice for their sacrifice to make this research possible. I thank Dr. Alina Constantine for her expertise in neuroanatomy and contribution to the micrographs in Chapter 2. I thank Dr. James Johnson and Peter Overby at UBC for lending their help with the *in vitro* oxygen consumption measurements in Chapter 3. I thank Ryan Vander Werff at the Biomedical Research Centre, UBC, for teaching me the ropes of mRNA sequencing. Finally, thanks to my friends and colleagues Linda, Maeghan, Erik, Simon, and Landon for tolerating my eccentricities and for all their help in the lab.

DEDICATION

For Charmé, whose century of footsteps have guided our family well through the years.

Chapter One: Introduction to Energy Regulation and Obesity

1.1 THE OBESITY EPIDEMIC: CAUSES AND COMORBIDITY

Prevalence of overweight and obesity have been increasing at an alarming rate in developed and developing countries in the last four decades[1-3]. Body mass index (BMI) is the most commonly used metric for assessing overweight (25-29.9 kg/m^2) and obesity (≥ 30 kg/m^2) and is calculated by an individual's mass divided by the square of their height. While this metric has received criticism for its inability to account for lean mass and metabolic health at the individual level, BMI data are ubiquitous and useful for understanding population-level trends. In the years 1980-2013, the worldwide prevalence of obesity in adults increased by a total of 8%, and in 2013, almost 25% of children in the world were overweight or obese[4]. The rise of obesity has driven a concomitant increase in the prevalence of non-communicable diseases such as cardiovascular disease, certain cancers, and type 2 diabetes (T2D). There is a growing catalogue of such diseases that can arise as a result of the metabolic consequences of obesity, compounding patient suffering and the health care burden. In 2008 alone, obesity-related health care costs to the US and Canada mounted to an estimated $153 billion[1,5]. Therefore, body mass-related disease is now being recognized as an epidemic[6-8]. Obesity is neither confined to rich countries nor wealthy people. In fact, economically and socially disadvantaged groups are at greater risk for the development of obestiy[1,9] because low-quality, high-calorie diets are cheaper and more accessible than fresh, unprocessed food[10]. From 2006-2013, the incidence of overweight in developed countries decreased slightly, but with over 40% of adults already overweight in many countries, solutions are desperately needed[4].

The obesity epidemic coincides with a number of negative societal transitions, including sedentary lifestyle, increased consumption of processed foods, and urbanization[9]. In Canada, these factors coalesce to form environments that are conducive to a positive energy

balance, as reflected by the startling prevalence of obesity. Some First Nations in Canada are disproportionately affected by obesity and T2D due to genetic determinants and colonialism-driven destruction of their traditional diets[11] and way of life. This case illustrates how disadvantaged groups bear a disproportionate proportion of the burden of obesity-related disease. In 2006, an estimated $6 billion was spent by the Canadian health care system in treating obesity and its comorbidities, such as hypertension, T2D, and coronary heart disease[1].

Despite stigmatization that overweight and obese individuals face, many of the socioeconomic and biological causes of obesity are beyond individual control or awareness. A new study shows evidence that processed food, while it contains more calories per gram, may also drive excessive food consumption independent of calorie-seeking behaviour[12]. This study matched calories, macronutrients, sugar, sodium, and fiber between ultra-processed and unprocessed meals. They found that participants voluntarily ate more and gained more weight when exposed to the ultra-processed diet despite the fact that it did not contain more fats, sugar, or calories, which are often hypothesized to be the motivators of excessive eating habits[12]. This shows that there are still unknown mechanisms that contribute to excessive eating, and that further work is needed to fully understand the regulation of energy balance.

The built environment is another factor that is not under individual control and has driven a societal shift to a less active approach to completing activities of daily living. Roadways are not often designed to protect active commuters, thereby prohibiting bicyclist and pedestrian use[7]. Increased sedentary behaviour, described as any waking activity performed in a sitting or reclined position, correlates to poor weight status in children[13]. Poorly planned urban development combined with automated/digitized personal and professional environments have led to increased sedentary behaviour in both adults and children[7,9]. Increased availability of TVs and their incorporation into almost all types of rooms in the

household, including bedrooms, has likely contributed to childhood obesity since screen time accounts for one-third of sedentary behaviour in children aged 9 to 11 years old[13]. Taken together, poor eating habits and increased sedentary behaviour are the key environmental influences driving the obesity epidemic.

There are also biological influences that facilitate obesity in addition to and in concert with environmental drivers. Obesity has been the target of significant stigma due to a lack of understanding of its etiology. This is derived from the false assertion that low physical activity and high calorie consumption are the only contributors to the progression of obesity. However, there exists a known pathophysiology of obesity including molecular pathways that become disturbed and lead to weight gain, dispelling the notion that simple laziness is the culprit. Furthermore, the impact of environmental influences differs between individuals. Not all sedentary people who consume a high-calorie diet will develop obesity, and not all people with obesity will develop metabolic consequences, showing that the pathology of the disease cannot be explained by lifestyle factors alone or by a specific amount of adipose tissue accumulation[14]. A number of hormones regulate physical activity and feeding behaviour in times of caloric deficiency to maintain energy homeostasis. These behaviors are subject to reinforcement by similar circuitry as those that contribute to drug addiction[15] and can even override or bypass regulators of satiety in the central nervous system (CNS)[16]. Many neuronal and chemical satiety signals originate from the gastrointestinal tract, including cholecystokinin (CCK) and ghrelin[17]. CCK increases satiety and ghrelin opposes it by decreasing perceived fullness and increasing normal meal size. Many such processes of energy balance are regulated by both positive and negative signals to ensure control within a homeostatic range. The receptivity of the CNS to such signals is highly modulated by other organs via endocrine or neurological means and thus homeostasis is ensured through a multi-faceted, multi-organ approach.

Adipose tissue, for example, is an important regulator of satiety signal sensitivity in the hypothalamus and hindbrain. Leptin, a hormone produced and released from adipose tissue, circulates at levels proportional to adipose tissue mass and acts to reduce meal sizes and increase satiety signaling in the hindbrain and hypothalamus[18] when sufficient energy stores exist. However, pathologically high circulating levels of leptin seen in obesity cause leptin resistance in the brain and other tissues[19-21] through negative feedback mechanisms that decrease the expression[22] and sensitivity[23] of the leptin receptor. In this case, control of energy balance is lost, further perpetuating obesity. Understanding these physiological regulators of energy metabolism has identified the complex biological regulation of body weight that opens up a plethora of potential molecular targets that could contribute to therapeutics for obesity. Adipose tissue has thus received much more attention in recent years for its ability to affect energy regulating processes in the whole body.

1.2 ADIPOSE BIOLOGY IN METABOLIC DISEASE

Historically, white adipose tissue (WAT) has been known for its ability to sequester energy in the form of lipid in times of caloric intake and release lipids in times of fasting for energy production. This function arose as a consequence of fundamental mammalian biology: tissues require energy constantly, but meals are sporadic[24]. WAT bridges this discrepancy between energy supply and demand in its role as the primary organ for energy storage. White adipocytes are highly specialized for storing triglycerides in a large cytoplasmic lipid droplet. In most other tissues, cellular accumulation of lipid is correlated with processes such as inflammation[25] and fibrosis[26]. While some non-adipose tissues can safely store energy in the form of glycogen, it is not an efficient storage molecule and provides only a fraction of total body energy stores with most energy being stored as lipid in WAT. In humans, glycogen can

only provide enough energy to fuel the body for approximately 2-3 hours of intense physical activity[27], while lipid, accounting for 70% of stored energy, can sustain the body through days or weeks[28,29]. Adipose tissue responds to fluctuating nutrient availability by storage through lipogenesis or utilization through lipolysis and lipid oxidation[24]. Thus, the lipid droplets of adipocytes are in constant flux[30,31] to maintain high intracellular rates of processes driving anabolism and catabolism of lipids. As such, WAT is a dynamic organ that regulates energy homeostasis through modulation of metabolic pathways involved in lipid cycling.

In the fed state, insulin action and decreased sympathetic stimulation at the adipocyte cause a decrease in lipolysis and promote pathways involved in the import, packaging, and storage of energy[32]. The vast majority of lipid is stored as triglyceride in WAT. This critically important storage molecule is composed of one glycerol backbone with three fatty acids esterified to it. The free fatty acids (FFAs) used to form triglycerides in the WAT come primarily from the diet, but they can also be synthesized in the cytoplasm by the repeated addition of two-carbon subunits from acetyl-Coenzyme A (acetyl-CoA). The formation of new lipids from acetyl-CoA is called *de novo* lipogenesis and occurs mainly in the liver but is stimulated in adipocytes by insulin[33]. Glucose taken up by adipocytes in response to insulin action can also be converted to lipids for storage[24]. The process of glycolysis breaks glucose down into two-carbon units attached to CoA, forming acetyl-CoA that can be utilized in lipogenesis. Adipose tissue is therefore a bridge between carbohydrate and lipid metabolism, providing an important glucose sink to attenuate blood hyperglycemia.

To provide energy during fasting and sustained moderate exercise, stored lipids must be made accessible to the peripheral organs including cardiac and skeletal muscle[29]. Adipose tissue accomplishes this via lipolysis, the process of breaking triglycerides down again for oxidation or export to the circulatory system. Both glycerol and free fatty acids released from

WAT are potential energy sources that can be utilized through the glycolysis pathway and β-oxidation, respectively. The process is started by the CNS sensing low blood glucose and/or free fatty aid. Sympathetic nerves to adipose tissue increase their activity, and depolarization releases norepinephrine at the SNS-adipocyte synapse. Beta-3 adrenergic receptors (β_3-ARs), one type of G-coupled protein receptors (GPCRs) expressed on adipocytes, bind norepinephrine and become activated[30]. Stimulatory G proteins (G_s) associated with the β_3-ARs exchange guanosine diphosphate (GDP) for GTP and dissociate from the receptor to activate the enzyme adenylyl cyclase. Increased adenylyl cyclase enzymatic activity results in rising cytosolic levels of the secondary messenger cyclic adenosine monophosphate (cAMP). High cytosolic concentration of cAMP releases the autoinhibition of c-AMP dependent protein kinase A (PKA), which in turn phosphorylates hormone-sensitive lipase (HSL) in an activating manner[30]. HSL translocates to the interior of the cytoplasmic lipid droplet and performs hydrolysis of triglycerides[32]. The resulting FFAs and glycerol can then be exported to the plasma for uptake in energetically demanding tissues such as muscle and liver.

The current understanding of adipose biology has moved beyond the classical view that adipose tissues are semi-inert storage depots. In addition to controlling whole-organism energy status through carbohydrate and lipid metabolism, adipose tissue secretes endocrine factors to modulate energy homeostasis in other metabolic organs[34-39]. The identification of cytokines secreted by adipose tissue such as tumor necrosis factor alpha (TNFα)[40] and leptin[41] has sparked interest in adipose tissue's endocrine role in the last 25 years. This work has led to the discovery of a new class of adipose-derived signaling molecules termed adipokines, revealing an important role for adipose tissue in communicating the whole-body energy status and regulating energy intake and expenditure by secreting endocrine factors[34].

Friedman and colleagues (1994)[41] were the first to discover an adipose tissue derived hormone, leptin, promoting the expansion of research surrounding adipose derived endocrine regulation of energy balance. As discussed above, leptin decreases appetite and is a modulator of both acute and long-term energy status. During fasting in lean individuals, levels of leptin decrease, and food intake is promoted. During times of energy excess, leptin is released from adipocytes in proportion to the total adipose tissue mass and travels through the bloodstream to bind leptin receptors on neurons of the hypothalamus, where it signals satiety and reduces appetite[42]. In obese individuals, circulating leptin levels are high but tissues including adipose, hypothalamus, liver, and others become resistant to its effects. For example, levels of soluble leptin receptor are decreased in obesity, which may contribute to a state of leptin resistance[20,43]. Reduced leptin sensitivity may have evolved as an adaptation to allow accumulation of energy stores and thus more stable energy supply. This adaptation would be particularly important in times where excess energy stores are required for survival, such as pregancy[44] or hibernation[45]. In obesity, reduced leptin action at target tissues drives further expansion of the WAT through increased feeding that further contributes to the level of obesity and to the development of metabolic consequences of obesity.

While it is true that there are metabolically healthy obese individuals[46], a finding that can be replicated in genetically modified rodent models of healthy obesity[47], there is a well-characterized association of obesity with a number of life-threatening comorbidities that can develop as a result of metabolic syndrome[6,42,48]. The risk of cardiovascular disease is greatly increased in obese individuals, including stroke, heart attack, hypertension, and coronary artery disease[8]. Obesity drives insulin resistance[6] and is thus a primary risk factor in the development of T2D. Other comorbidities include osteoarthritis, respiratory illness, and some forms of cancer[9]. It should be noted that while comprehensive assessments of obesity-associated costs

to Canadian health care resources are rare, worldwide analyses show that Canada has both a comparatively high prevalence and overall cost of obesity[1-3]. Thus, developing pharmacological therapeutics aimed at reducing overweight and obesity has been identified as a promising approach to reduce health care costs and patient suffering in Canada, in combination with lifestyle modification.

Normal adipose tissue function is required for the maintenance of metabolic homeostasis and impairments in adipose tissue function contribute to the development of obesity and drive the majority of comorbidities associated with this disease. Adipose tissue has thus been identified as a key promising therapeutic target and the biology of this tissue must be explored in greater depth to help reduce the prevalence of obesity. To better characterize the participation of adipose tissue in whole-animal metabolism, a mouse model lacking adipose tissue was developed[49]. Adipose tissue development relies heavily on the transcription factors, Jun and CAAAT enhancer binding protein (C/EBP) for proliferation and differentiation of precursor cells into mature adipocytes, respectively[50]. Thus, the formation of adipose tissue is ablated in transgenic mice with adipose tissue-specific knockout of these transcription factors[49]. The absence of adipose tissue in these mice leads to severe metabolic dysfunction, displaying hyperphagia, polyuria, reproductive failure, fatty liver, uncontrolled (50-400 fold increase) insulin secretion leading to diabetes[49] and premature death. This study shows that normal adipose tissue functioning is essential to maintenance of homeostasis.

Adipose tissue is a complex organ, and many facets of adipocyte biology become perturbed in obesity, such as endocrine function, glucose uptake, and lipid metabolism. In obesity, adipose tissues can become over-capacity and therefore unable to take up lipids from the blood or manage internal lipids properly. This dysregulated lipid metabolism and resulting pro-inflammatory cytokine secretion elevate the inflammatory state in multiple other

tissues[51,52]. Thus, controlling circulating lipids through modulation of lipolysis has long been a target for anti-obesity drugs[53] due to its potential to remove stored lipid from WAT or, conversely, prevent their excretion into the blood. Circulating FFAs directly reduce insulin receptor sensitivity and exacerbate symptoms of diabetes[54].

Despite the critical role adipose tissue plays in the maintenance of metabolic health, the increase in obesity and obesity-induced comorbidities have resulted in adipose tissue being typically viewed negatively by society, with less attention being given to the positive effects of this tissue on metabolism. The adipose tissue is linked to the regulation of glucose metabolism, lipid metabolism, feeding behaviour, and inflammation in other tissues through the secretion of adipokines. Adiponectin is an example of an adipokine that has widespread beneficial effects on many organs and highlights the important role of adipose tissue in maintaining metabolic health (Figure 1.1). Adiponectin receptors are expressed in a variety of tissues and their transcription appears to be regulated in response to feeding[55], perhaps by insulin[55,56]. Autocrine actions of adiponectin include increased glucose uptake, adipogenesis, and lipid import in the adipose tissue[57]. Together, these function to allow the adipose tissue to expand while remaining metabolically healthy. Endocrine functions of adiponectin include increased insulin sensitivity and secretion, increased FA oxidation, reduced lipogenesis, and maintenance of viability in myocytes[35], β-cells[58], and hepatocytes[57]. Unlike most other adipokines, adiponectin's expression is very low in obesity. Since adiponectin is an important anti-fibrosis and anti-inflammatory cytokine, some facets of metabolic syndrome can be explained by its attenuated expression seen in obese individuals. Thus, adiponectin is an example of an adipokine that aids in opposing many of the pathophysiological processes seen in metabolic syndrome and the development of T2D, but it is only one of many hormones that are secreted by the adipose tissue.

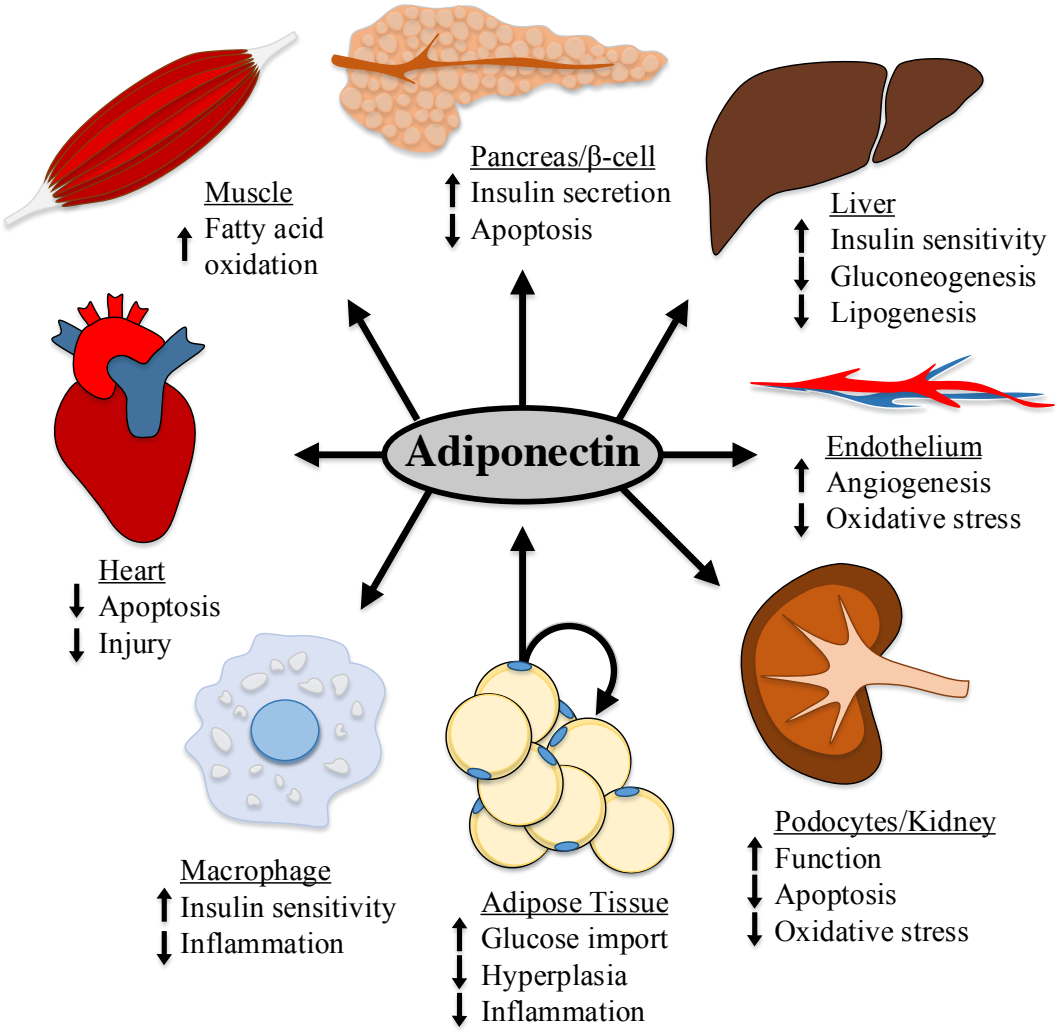

Figure 1.1. Metabolic, anti-inflammatory, and anti-apoptotic effects of adiponectin on multiple organ systems and cell types to highlight the importance of adipose tissue-derived endocrine/autocrine factors (adipokines) in whole body function. Modified from Ye, et al. (2013)[59] under Creative Commons license.

Hundreds of other peptides are secreted from the adipose tissue[36,39] and may also prove promising targets as anti-diabetic agents. The identification of adipose-derived endocrine factors has greatly increased our understanding of how adipose tissue influences whole body metabolism and pathological mechanisms that can lead to metabolic syndrome when adipokine levels change in obesity. This provides promising targets for pharmacological therapies and has resulted in better treatment of obesity and T2D. For example, leptin therapy in obese individuals has been shown to decrease voluntary food intake and increase voluntary exercise, thus reducing fat mass and leading to a significant decrease in BMI[21]. In general, it is accepted that a negative energy balance is desirable for obese and overweight individuals, though other metrics have also been used as indicators of efficacy in interventions[60,61]. A negative energy balance leads to decreased mass of the body's main energy stores, the WAT. This ameliorates over-capacity, malfunctioning WAT, thus improving the metabolic profile. The molecular mechanisms of a metabolic process of energy expenditure called adaptive thermogenesis has gained enormous attention in the last two decades as a potential target to promote a negative energy balance[62,63]. Adaptive thermogenesis increases energy expenditure in brown adipose tissue (BAT) through the production of heat in response cold or over-feeding.

1.3 ADAPTIVE THERMOGENESIS AS A THERAPERUTIC STRATEGY

BAT is a specialized adipose tissue that has been identified as a potential therapeutic target in obesity due to its ability to burn lipids in response to cold stress during adaptive thermogenesis. Thermogenesis is performed predominantly by the adipose tissues and maintains euthermia during exposure to low environmental temperatures. During short term exposure, skeletal muscle contributes to heat production via shivering thermogenesis, but adipose tissues are required for chronic acclimation to cold via adaptive thermogenesis[64,65].

Recently, functional BAT was discovered in healthy human adults. This tissue is particularly interesting in the context of energy metabolism because it is characterized by high rates of glucose uptake and lipid oxidation. BAT is the main site of adaptive thermogenesis in rodents, and while there are important differences between human and murine BAT, healthy adult humans also retain functional BAT later into life. The amount of BAT in humans is proportionally much smaller than the amounts seen in rodents, but the molecular mechanisms and basic function are very similar[66]. In the face of hypothermic stress, the hypothalamus receives sensory inputs from the skin indicating cold exposure and mounts a thermogenic response to ensure that body temperature is maintained within a tight range. This process is essential to maintain homeostasis in cold environments or during overfeeding and is called adaptive thermogenesis. The activity of human BAT is decreased with age[67] and in obesity[68], which suggests a that loss of BAT function may exacerbate or contribute to the development of obesity. As such, the BAT may hold promise in restoring energy balance in obese and overweight individuals by increasing energy expenditure using the thermogenic pathway.

Some adipocytes in WAT depots in humans and rodents are susceptible to physiological changes that cause them to behave more as energy expending brown adipocytes than energy storing white adipocytes. This includes a stark change in adipocyte morphology to multilocular lipid droplets, higher mitochondrial density, and increased thermogenic protein expression of uncoupling protein 1 (UCP1). A similar, though less dramatic, acclimatory process can be seen in brown adipocytes in response to cold exposure (Figure 1.2). This shift in metabolic function has been termed “browning” and occurs as a natural thermoregulatory mechanism in WAT of mice but its extent and physiological significance have not been thoroughly studied in humans. This intermediate type of adipocytes is called brown-in-white

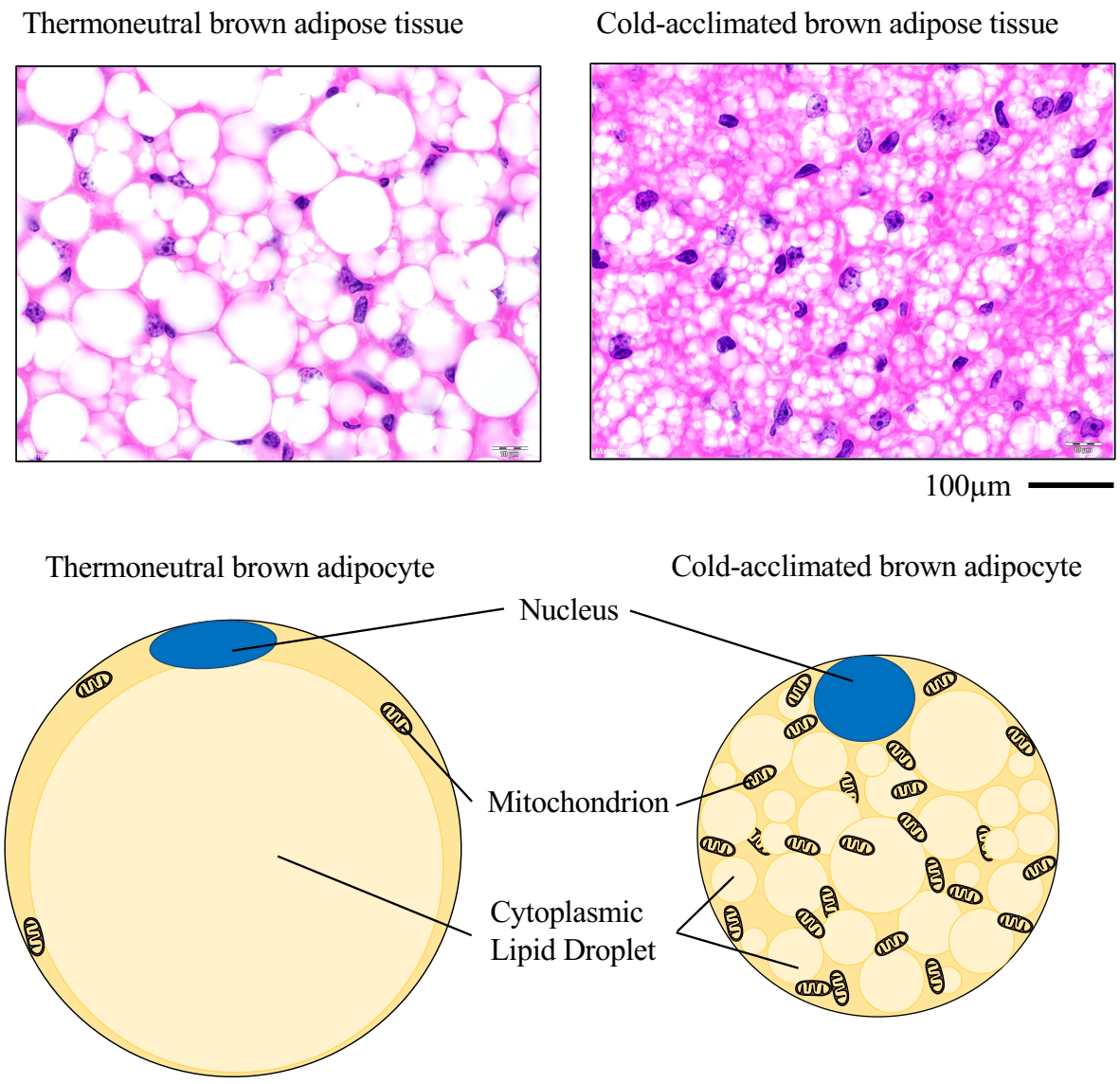

Figure 1.2. Representative histological adipose tissue sections and stylized representative adipocyte morphology to show the process of cold acclimation (browning) in murine brown adipose tissue. Thermoneutrality for mice is 30°C, while full cold acclimation is defined here as 4°C for 3.5 weeks. In the histological sections, nuclei are stained purple by hematoxylin, cytoplasm is stained pink by eosin, and lipid droplets appear as white empty space.

"brite", or "beige" and can be induced in the omental and, to a lesser extent, subcutaneous adipose tissue of humans[69-73]. Beige adipocytes are distinct in origin from brown adipocytes because they appear in WAT depots and their precursors lack myogenic factor 5 expression seen in brown adipocytes[74] and myocytes. Like white adipocytes, brown and beige adipocytes are targets of hypothalamus-controlled sympathetic nerve activation and induction of lipolysis. In contrast to white adipocytes, norepinephrine binding to thermogenic adipocytes additionally activates the inner mitochondrial membrane protein, uncoupling protein 1 (UCP1). This proton shuttle uncouples ATP production from mitochondrial respiration, releasing potential energy in the form of heat[64,65,75,76]. Since the proportion of WAT to body mass in humans is large, and the proportion of BAT is small, the process of browning has received attention as a potential target for substantially increasing metabolic rate in humans to induce negative energy balance and ameliorate obesity. As with many other processes related to energy expenditure, evidence suggests thermogenesis is largely under hypothalamic control, in coordination with other centres in the brain[77,78].

1.4 CENTRAL REGULATION OF HOMEOSTASIS INCLUDING THERMOGENESIS

A diverse array of stressors can disrupt energy metabolism, including psychological, physical, thermal, and nutrient stressors. Homeostasis requires that these complex signals be received and correctly interpreted by the central nervous system so that a coordinated response can be made to rebalance the body[79]. The peripheral nervous system detects stressors and relays information to the brain where the signal is integrated, and the appropriate physiological and behavioural changes are initiated. The hypothalamus and the brain stem are known for

managing nutrient imbalance by regulating food intake[80], and the hypothalamus is the main energy expenditure regulating centre[81] that can mediate responses such as feeding behavior, physical activity, metabolic rate and thermogenesis. The hypothalamus utilizes endocrine and nervous systems to communicate with effector organs in the periphery to achieve these outcomes. The key energy regulating pathways initiated by the hypothalamus are the hypothalamic-pituitary-adrenal axis (endocrine) and the autonomic nervous system (neuroendocrine). These axes are essential for survival.

Neurons in the hypothalamus respond to internal and external stimuli by secreting releasing hormones into the hypophyseal portal system of the pituitary stalk, which carries these endocrine factors the short distance from the base of the hypothalamus to the anterior pituitary[79]. In this way, neuroendocrine factors connect the CNS to the peripheral endocrine systems via the pituitary. The hypothalamic-pituitary-adrenal (HPA) pathway is initiated by the release of corticotropin releasing hormone (CRH) from the hypothalamus, which acts on corticotrophs of the anterior pituitary, which release adrenocorticotropic hormone (ACTH) into the blood and acts on cells of the adrenal cortex to stimulate the synthesis and release of cortisol[79].

The autonomic nervous system (ANS) is a key stress pathway under hypothalamic control that responds to physiological stressors without conscious thought. The autonomic nervous system is split into two branches: the sympathetic and parasympathetic nervous systems (SNS, PNS). The SNS is commonly known for the “fight or flight” response that is elicited by situations of physiological or psychological stress. This includes important roles of the SNS in maintaining body weight and temperature in the face of stressors such as nutrient excess and cold exposure, respectively. For example, when faced with hypothermia or overfeeding, the SNS induces energy expenditure through increased cellular metabolism,

burning energy and producing heat via adaptive thermogenesis. The PNS is traditionally thought of as the "rest and digest" arm of the ANS, but this paradigm has shifted to the understanding that both arms of the ANS work in concert to maintain a homeostatic balance. Hypothalamic energy regulation is further complicated by the incorporation of many endocrine factors that act on the brain or effector organs to modulate the energetic state.

1.5 PACAP: A NOVEL ENDOCRINE REGULATOR OF ENERGY METABOLISM

Miyata, et al. [82] were searching for peptides of the hypothalamus that stimulate a physiological response in the pituitary, which would implicate them in the HPA axis or other hypothalamic-pituitary-end organ axes. This led to their discovery of pituitary adenylate cyclase-activating polypeptide (PACAP) in 1989, which was named for its ability to stimulate adenylyl cyclase in the pituitary. PACAP has since been characterized as a high-level regulator of the stress response including the endocrine HPA axis and the SNS. The literature around this neuropeptide has exploded, gaining considerable attention for its pleiotropic regulatory activity and therapeutic potential.

PACAP belongs to the Glucagon/Secretin Superfamily of proteins and shares 68% amino acid sequence similarity with vasoactive intestinal peptide (VIP). VIP and PACAP share traits common to their Superfamily, such as C-terminal amidation, random N-terminal coils and C-terminal alpha-helices. PACAP is encoded by the ADCYAP1 gene and is translated as a 176aa precursor, which is then spliced into the mature PACAP peptide as one of two forms: PACAP38 and PACAP27. A suite of enzymes is responsible for the variable processing of preproPACAP, contributing to the diverse actions of PACAP[83]. The highly conserved biologically active 27 N-terminal residues of PACAP38 constitute PACAP27, though

biological activity for certain receptors differs slightly between the two forms. Investigations of PACAP's evolutionary history have shown conservation in amino acid sequence among taxa that diverged over 700 million years ago[84]. This strict conservation across diverse evolutionary groups aligns with a fundamental role in the maintenance of homeostasis.

PACAP is widely expressed in the CNS, PNS, and in many peripheral organs. In the CNS PACAP occurs in the brainstem nuclei, hypothalamic nuclei, amygdala, thalamic nuclei, cerebral cortex, medulla oblongata, posterior pituitary, thalamus, and nerves in cerebral blood vessels. PACAP is most highly expressed in the hypothalamus, specifically in the paraventricular, periventricular, ventromedial (VMH), suprachiasmatic, and supraoptic nuclei[85]. PACAP behaves as a hypothalamic releasing hormone and is actively transported to the anterior pituitary via the hypothalamic-hypophyseal portal system[86] to illicit secretions of the pituitary. In the autonomic nervous system, PACAP is best known for its expression in preganglionic neurons of the sympathetic and parasympathetic nervous systems. For example, PACAP is the primary neurotransmitter released from neurons at the sympathetic adrenomedullary synapse and required for sustained secretion of norepinephrine[87-89]. PACAP is widely distributed in the peripheral organs, occurring in (but not limited to) exocrine and endocrine glands, immune cells, gonads, pancreas, and the genitourinary tract.

PACAP mediates its effects through three distinct receptors, which are expressed in all major organ systems in the body and thus, PACAP regulates diverse physiological functions. Furthermore, the downstream activation of signaling pathways differs by cell/tissue type to allow fine-tuning of the physiological response in different contexts. The PACAP receptors have been cloned and are called PAC1R (495 amino acids)[90], VPAC1 (457aa)[91] and VPAC2 (438aa)[92], here collectively referred to as PACAP receptors. PAC1R mRNA is most abundant in the brain, pituitary, and adrenal gland and tissues expressing PAC1R have distinct profiles

of PAC1R splice variants. VPAC 1 and 2 are most abundant in the lung, liver, and testis[83]. All three are class B GPCRs. Since many clinically utilized pharmaceuticals target GPCRs, the PACAP receptors have received significant attention for their therapeutic potential.

Differential splicing of the receptors may increase the targeting ability of pharmaceuticals by taking advantage of differential binding affinities and physiological outcomes to reduce off-target effects. The PAC1R receptor is highly spliced, having at least 11 known isoforms in rodents and 9 in humans[93]. All PAC1R isoforms are selective for PACAP over VIP yet the affinity of the 27- and 38-amino acid version of PACAP differs based on PAC1R splice variant[83]. Splice sites occur at several points[93] within the receptor structure and mediate the removal of a 21aa segment in the extracellular domain and in some variants. Additionally, a set of cassettes called HIP (28aa), HOP1 (28aa) and HOP2 (27aa) can be independently inserted or absent (PAC1Rnull) in the third intracellular loop to create a variety of spice variants[94]. Each splice variant is functionally distinct in its binding affinity for certain ligands, its intracellular signaling components[94], and specific distribution[93]. For a list of the variants and their downstream signaling, see Dickson and Finlayson [84]. Maxadilan is an unrelated peptide isolated from the sandfly, *Lutzomyia longipalpis*, that has been characterized as a potent, specific PAC1R agonist[95] while a shortened version of Maxadilan, called M65, offers a selective antagonist for PAC1R[96]. Their specificity for PAC1R over VPAC1/2 illustrates the potential precision of pharmaceutical development in this area and these peptides provide an invaluable tool for studying the biological activity of PACAP receptors.

All three PACAP receptors are associated with stimulatory G-proteins (G_s and G_q) as well as inhibitory G-proteins (G_i). G_q leads to increased cytosolic Ca^{2+} through the activation of phospholipase C (PLC) and, subsequently, inositol triphosphate (IP_3). G_s causes the activation of adenylate cyclase, PACAP's namesake, whose activation has a number of

downstream effects. This includes activation of PKA, Rap guanine nucleotide exchange factor 4 (Rapgef4), and Rapgef2, which contribute to inhibition of the apoptotic pathway involving caspase 9 and 3, p38-mediated cell arrest, and neuritogenesis[97]. Rapgef4 also regulates cAMP response elements via cAMP response-element binding protein (CREBP)[83]. G_i has an inhibitory effect on adenylate cyclase and therefore decreases production of cAMP. Thus, differential activation of coupled G-proteins adds yet another level of control for downstream response to activation of PAC1R.

The extensive functions of PACAP in many tissues and cells types have been reviewed thoroughly elsewhere[83,84]. Thus, they will be only briefly highlighted here to showcase the diverse actions of this neuropeptide. In the nervous system, PACAP acts as a non-noradrenergic, non-cholinergic, mostly preganglionic neurotransmitter. In the central nervous system, PACAP acts as a neurotransmitter, neuromodulator, and neurotrophic factor and in the peripheral nervous system, as a neurotransmitter or neuromodulator regulating sensory stimuli and endocrine secretion[98]. In the circulatory system, PACAP is a potent vasodilator. In the endocrine system, it is an essential neurohormone with roles in regulation and production of other endocrine factors, such as catecholamines from chromaffin cells of the adrenal medulla and glucagon from pancreatic β-cells in response to hypoglycemia[88,99]. Coordination of these organ systems allows PACAP to contribute to neuroprotection, energy metabolism, catecholamine synthesis and release, nociception, circadian rhythms, headache pathology, stress-related pathologies, and neurological disorders.

PACAP's roles in disparate processes can be unified under the understanding that many of these processes are responses to different types of stress. Thus, we can view PACAP as an important regulator of adaptive and maladaptive responses to stress[100]. Stress can be defined

here as any internal or environmental threat to homeostasis and may include both physiological stressors and psychological stressors. For example, independent research performed by Lee Eiden and Victor May has demonstrated evidence that PACAP is involved in the response to emotional stress[101,102]. One such study showed that compared to wild-type controls, PACAP-null mice have significantly reduced activity in the hypothalamus and concomitantly lower plasma corticosterone[103], in response to physical restraint or light-induced stress. This result suggests that PACAP enhances the emotional stress response. In the context of physiological stressors such as cardiac injury, PACAP has displayed protective, anti-apoptotic effects on myocytes and increased the survival of mice following induced cardiac injury[104]. These and other studies have contributed to the conclusion that PACAP acts both centrally and peripherally to regulate the response to stressors of very different types.

1.6 THESIS SCOPE AND SIGNIFICANCE

Our research group is particularly interested in the role of PACAP in energy regulation in the brain, where it is most highly expressed in the hypothalamus and its expression has been demonstrated in a number of hypothalamic energy-regulating nuclei including the arcuate nucleus (ARH) and VMH[105,106]. As an energy regulating centre, the hypothalamus protects euthermia through the initiation of the thermogenic response, which burns fat to increase body temperature in the face of cold stress. Mouse pups lacking PACAP experience higher mortality due to hypothermia, even at room temperature (21°C) and adult mice lacking PACAP do not exhibit a full thermogenic response to norepinephrine stimulation of the BAT[107,108], which is the primary thermogenic organ in mice. Pharmacological studies have outlined a role for PACAP in the VMH as an activator of thermogenic signal, but these studies[109,110] used a single supraphysiological dose of PACAP or Maxadilan injected into the VMH in unreported

volumes and may not represent normal physiological action of this peptide in the hypothalamus. Thus, a targeted approach to genetic introduction of PACAP selectively into the VMH under control of an endogenous promoter is needed to understand the true physiological effect of PACAP action directly in the VMH. The development and verification of this genetic tool in the central nervous system will be the focus of Chapter 2.

To gain a more comprehensive understanding of the scope of PACAP's energy regulating actions, it will also be necessary to investigate the contribution of PACAP's peripheral activity. As mentioned above, adipose tissue is an important target of SNS outflow tracts that regulate responses to changes in energy status or thermogenic requirement. Sympathetic postganglionic nerves innervate the adipose tissues and act though GPCRs on adipocytes, stimulating responses including induction of lipolysis and thermogenic pathways. However, the role of PACAP-mediated thermogenesis by PACAP binding PAC1R directly at the level of the adipocyte has not yet been investigated. This may be, in part, due to the literature lacking comprehensive data about the expression of each of the receptors in adipose tissue of mouse and humans. In order to fully understand PACAP's regulation of the thermogenic response in brown and beige adipocytes, it is necessary to characterize the expression and function of PACAP and PACAP's receptors (PAC1R, VPAC1, and VPAC2) in thermogenic adipose tissues. Novel characterization of PACAP receptor expression and PACAP activity in the context of adipose tissues will be the focus of Chapter 3.

Worldwide obesity prevalence has reached unprecedented levels with its comorbidities in tow. This epidemic puts unmanageable demand on health care systems and introduces significant patient suffering. Physiological factors contribute to the development and maintenance of the obese state and provide promising therapeutic targets. To manage this disease, a stronger understanding of the central and peripheral mechanisms of energy

regulation must be achieved. This includes the study of adipose tissue in its role as a modulator of whole-animal energy status and the pathophysiological consequences of malfunctions in this tissue. Especially promising is the possibility of harnessing adaptive thermogenesis in adipose tissues to curb energy excess in overweight and obese individuals to restore energy homeostasis. Here I describe the study of a novel neuroendocrine factor PACAP in the context of its regulation of energy balance and explore the possibility that PACAP modulates energy expenditure peripherally by binding to adipose tissue.

Chapter Two: Developing an *in vivo* Model to Assess the Role of PACAP in VMH-Mediated Thermogenesis

2.1 INTRODUCTION

The hypothalamus is a key centre in the control of energy metabolism including appetite and energy expenditure such as thermogenesis. Therefore, the hypothalamus is an important brain region to consider when developing therapeutic approaches to obesity treatment. In terms of mass, the hypothalamus accounts for less than one third of one percent of the human brain[79]. Despite its small size, this brain region is critical for the maintenance of homeostasis in response to changes in the internal and external environment including the control of body energy stores through the regulation of satiety, physical activity and body temperature, and other dynamic processes such as blood pressure, reproduction, and growth. It is bilaterally organized and symmetrical, with each side a functional duplicate of the other[111]. The role of the hypothalamus in maintaining vital biological functions such as water balance points to the evolutionary advantage of such redundancy. Human patients with congenital or trauma-related lesions that affect both sides of the hypothalamus develop obesity in 25% of cases[112]. The regulation of energy balance by the hypothalamus is critical to basic biological functioning, but many of the neural circuits that underlie its functioning remain unmapped.

In the anterior/posterior axis, the hypothalamus can be divided broadly into three areas: the preoptic (anterior), tuberal (median), and posterior. Each area consists of distinct patterns of neural input, integration, and output. The preoptic area is an important integrator of thermoregulatory signals, reproductive behaviour, circadian rhythms, and electrolyte balance[113]. The tuberal region integrates satiety and feeding signals. Its outputs include mediators of reproductive behaviour, endocrine secretions, and other autonomic functions such as thermogenic activation, which will be the focus of this chapter. The posterior area's outputs include wakefulness, alertness and stress[113].

The hypothalamus is further subdivided into a diverse collection of semi-discrete units known as nuclei. In the CNS, the word *nucleus* refers to an organized group of neurons that work in concert to regulate metabolic, behavioural, and endocrine functions to ensure homeostatic balance. In the context of thermogenesis, the posterior hypothalamic nucleus is involved in the response to both hypothermia and hyperthermia. The medial, or tuberal region, includes the dorsomedial (DMH), ventromedial (VMH), paraventricular (PVH), and arcuate (ARH) nuclei (Figure 2.1) that collectively mediate thermogenesis, while lateral areas of the hypothalamus initiate heat dissipation mechanisms[111]. Significant progress has been made in attributing functional roles to nuclei in the hypothalamus[81]. However, a great deal of work remains to be done before a comprehensive functional map can be composed of this highly integrated, interconnected brain region[114]. This is partially due to the diverse and sometimes overlapping range of physiological roles that nuclei play as well as the pleiotropic activity of the genes they express[115]. In fact, the exact functions and boundaries of the hypothalamic nuclei in scientific literature are somewhat disputed[116]. In order to inform therapies targeted at energy regulation mechanisms such as adaptive thermogenesis, an increased understanding of the exact roles and boundaries of the DMH, VMH, ARH, and PVH in thermogenic activation are needed.

Increasing interest in energy regulating axes due to the rise in obesity, has spurred exciting work in the last 30 years that has delineated a complex pattern of cooperativity between the hypothalamic nuclei, in integrating and mediating neurochemical responses to homeostatic threats including nutrient and thermal stress. Despite the large body of literature describing orexigenic and anorexigenic signaling in the hypothalamus, only a small amount of this information will be described here as it pertains to energy regulation by a few of the tuberal nuclei and preoptic nuclei.

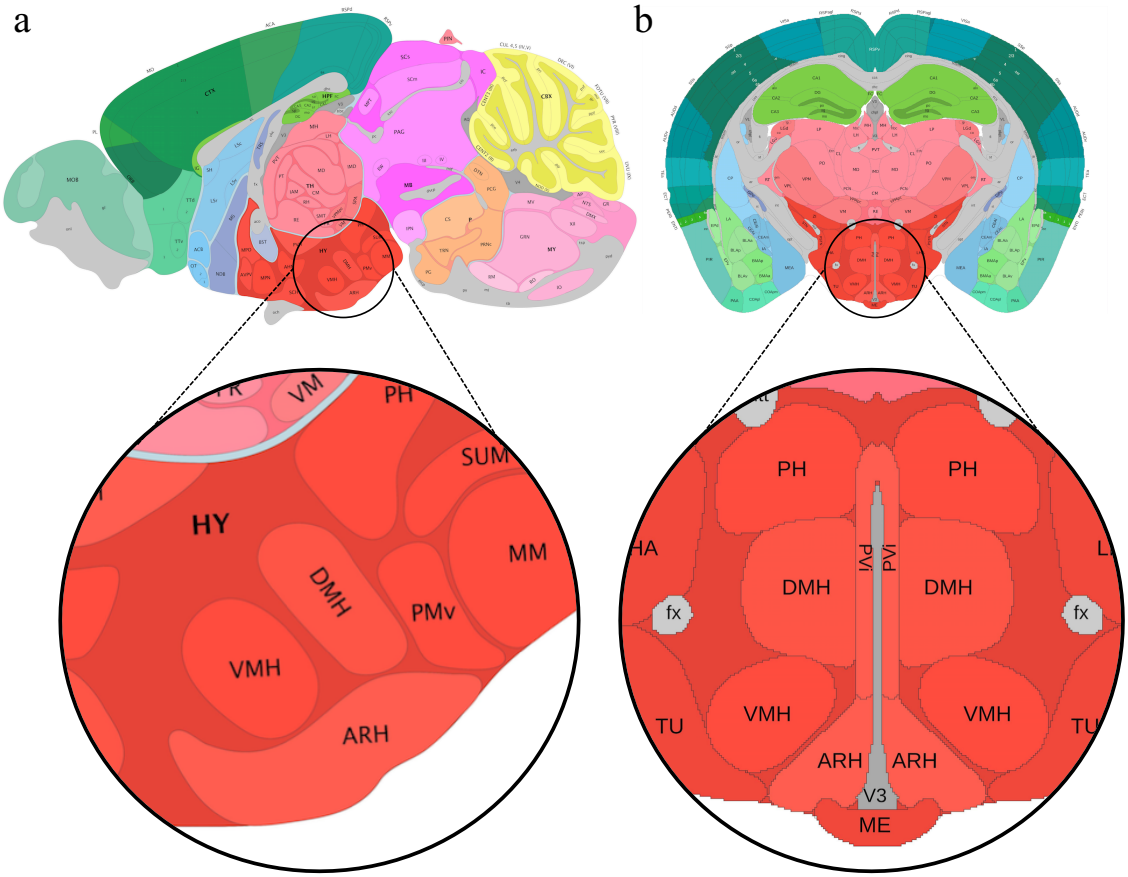

Figure 2.1. Cross-sectional images number 21 (a) and 72 (b) from the Allen Mouse Brain Reference Atlas (sagittal and coronal aspect, respectively) to show anatomical location of the hypothalami, coloured red. Inserts show enlargement of the medial hypothalamic region for spatial context and to show nuclei involved in thermogenesis, which include the dorsomedial (DMH), ventromedial (VMH), and arcuate (ARH) nuclei, but not the paraventricular (PVH) nuclei, which are positioned anterior of the others. Images collected from the following URLs with free, open access permission © Allen Institute.
(a) © [2004] Allen Institute for Brain Science. Allen Mouse Brain Reference Atlas, Sagittal. Available from: https://mouse.brain-map.org/experiment/thumbnails/100042147?image_type=atlas
(b) © [2004] Allen Institute for Brain Science. Allen Mouse Brain Reference Atlas, Coronal. Available from: https://mouse.brain-map.org/experiment/thumbnails/100048576?image_type=atlas

The study of neuropeptides over the last few decades has elucidated some of the molecular mechanisms that explain the results of older studies, which ascribed satiety and feeding mediation to the VMH. Reduced VMH function in rats has been associated with maladaptive eating habits for half a century[117,118]. Destruction of the VMH in rodents leads to intense hyperphagia, whereas destruction of the lateral hypothalamic nuclei leads to severe hypophagia and dangerous weight loss[111]. It is now known that leptin and brain-derived neurotropic factor (BDNF) are key hormonal mediators of energy balance in the VMH[111]. Recently, overeating behaviour resulting from VMH damage was attributed to loss of leptin signaling in this nucleus and an associated induction of leptin production from the adipose tissue[119], illustrating the importance of VMH leptin signaling in the control of energy balance. Injection of BDNF into the hypothalamus decreases food intake and causes gains in bodyweight irrespective of prior feeding or fasting[120]. BDNF supports neuron activity and cytogenesis into adulthood and has recently been associated with energy regulation due to genetic studies that described seven SNPs in and following the BDNF sequence that correlate with greater risk of obesity in humans[121,122]. The study of hormonal mediators of energy balance in the hypothalamus has thus provided promising targets and increased interest in hypothalamic regulatory peptides.

Other neuropeptides have been shown to regulate energy metabolism through the control of satiety. For example, PACAP action in the hypothalamus reduces food intake[109,123,124], perhaps by the induction of proopiomelanocortin (POMC) expression[109], reduction of orexigenic Agouti-related peptide (AgRP)[125] or regulation of anorexigenic neuropeptide Y (NPY) in neurons of the ARH[126], where PACAP, PAC1R, and VPAC2 are expressed[126,127]. PACAP mRNA expression is increased in the hypothalamus of mice fed high-fat diet compared to chow fed control mice, linking PACAP expression in the hypothalamus

to nutrient status and suggesting that PACAP could play a role in resisting maladaptive changes in body weight[106]. PACAP protein is expressed in the PVH, periventricular, VMH, suprachiasmatic, and supraoptic nuclei[85], further supporting its role in regulating energy metabolism including thermogenic activation in the hypothalamus. Thus, PACAP is surfacing as an important neuropeptide in the regulation of appetite in the hypothalamus.

The neuronal origins of the neurochemical signals for induction of adaptive thermogenesis in adipose tissue have also become clearer as techniques to study molecular structure and function have improved. The preoptic anterior region of the hypothalamus has temperature sensing neurons that can detect and initiate responses to minute changes in body temperature[128]. More recently, the importance of cold-sensing neurons in the brain has been called into question and some authors suggest that the activity of these cold-sensing neurons actually results from regulated input of signals from the preoptic warm-sensing neurons[116,129], which have been shown to co-express PACAP and BDNF[128]. Peripheral neuronal cold sensors, on the other hand, predominate over peripheral warm-sensing neurons and allow the detection of cold at the level of the skin and extremities[116]. Both cold and warm sensing peripheral neurons express transient receptor potential (TRP) ion channels, including vanilloid 1 (TRPV1) for hot and melastatin (TRPM8) for cold[130]. A number of other TRPs exist, with limited information available about their function. Once cold or warm-sensing inputs are passed through the preoptic area (anterior) of the hypothalamus, they are integrated by the tuberal (median) area of the hypothalamus, where illuminating functional data has been obtained through both pharmacological and electrical/chemical means using stereotaxic targeting strategies.

Stimulation of various nuclei of the hypothalamus including the DMN, VMH, PVN, and ARH through electrical or pharmaceutical means leads to increased sympathetic outflow

and induction of adaptive thermogenesis in the brown adipose tissue (BAT)[77,78,131,132]. Injection of PACAP into the VMH, but not the PVH, increases sympathetic output to BAT, and this effect is attenuated by prior treatment with PACAP receptor antagonists[110]. Viral tracing studies have shown that the sympathetic fibres, which innervate thermoeffector organs such as the BAT, originate in the sympathetic ganglia in the intermediolateral column of the spinal cord[116]. These receive input from the medulla, which in turn receives input from the hypothalamus[116]. Interestingly, viral tracing studies have failed to indicate the VMH as a direct source of thermogenic signaling via sympathetic innervation to the BAT[133-135] despite its well-established role in activating adaptive thermogenesis gleaned from functional data[77,131,136]. One important limitation of the retrograde viral tracing method is that its reach is restricted to approximately three neurons upstream[137]. Given the interconnected nature of the hypothalamic nuclei, it would be unsurprising were the thermogenic signal passed from the VMH onto other nuclei before leaving the brain through the brainstem, thereby positioning the VMH upstream from the maximum reach of the retrograde viral method.

Pharmacological injections into the VMH using PACAP have been successful in eliciting a thermogenic response at the BAT, but as mentioned in Chapter 1, these injections have a number of drawbacks. Volumes of the injections were not reported, supraphysiological doses were used, and single injections only provide acute effects, and thus long-term consequences could not be determined. It is clear that other experimental approaches are required to target the VMH and provide data to address these issues. Gene therapy has gained traction as a clinically relevant technique[138] and a useful tool in functional genomics, which introduces a functional copy of the gene to the host cells. Importantly, the expression of genes delivered by the virus can be controlled by endogenous host cellular machinery such as promoters. This benefit of this approach is twofold: endogenous cell- or tissue- specific

transcription factors induce the expression of genes at physiological levels, as well as restricting expression of the gene of interest to a target cell population thus reducing off-target effects.

Self-complimentary adeno-associated viruses (scAAVs) offer a promising solution to problems normally ascribed to gene therapy, including immune response, size restrictions of genes to be introduced, and disruption of the host genome upon viral gene insertion[138-140]. Biotechnological advances in viral packaging have allowed greater and greater plasmid size, meaning that genetic sequences over 5kb can transported reliably into host cells. AAVs induce a very low or undetectable immune response, which is essential to prevent lesioning in brain tissue following viral administration. Tissue-specific serotypes of AAVs, that preferentially infect particular tissue or cell types, further increase the accuracy of targeted gene delivery. AAV serotype 9 (AAV9) has been proven effective *in vivo* and *in vitro* for gene delivery[139,141] and favors neurons and glial cells. When injected into the CNS, there is little chance of the virus escaping the brain and delivering genes to unintended targets due to their unique inability to replicate independently without an accompanying adenovirus[140]. AAVs have an extrachromosomal mode of gene delivery that minimizes the risk of disrupting the host genome. Thus, the introduced genetic material acts as an auxiliary piece of genetic material that does not interact with the host genome. Preferential infection of AAVs to a specific tissue type, coupled with target-specific promoters allows for a high degree of expression specificity and has been successfully used to target gene expression in discrete populations of neurons in the CNS, including nuclei of the hypothalamus[142].

Stereotaxic intracerebral injection strategies for viral delivery of genetic material offer a very promising tool to study the functional role of PACAP in VMH-mediated thermogenesis, using the neurophilic AAV9 and a VMH-specific promoter. Direct injection into the target site

overcomes multiple difficulties that are encountered when trying to deliver viral particles to the brain via the blood with peripheral injections. To protect the brain from infection or damage, the blood-brain barrier prevents entry of a number of particles with therapeutic applications including viruses, greatly reducing pharmacological efficacy and demanding larger doses[140]. Therapies harnessing viral vectors can also suffer from undesirable accumulation of viral particles in the liver[140] that prevents their delivery to the brain and can increase gene delivery to hepatocytes and other cells of the liver at high local AAV conentration[143]. Stereotaxic intracerebral delivery provides a number of advantages over peripheral administration and coupled with a VMH-specific promoter could deliver PACAP to that nucleus with very high specificity and efficacy.

Steroidogenic Factor 1 promoter as a VMH-specific genetic tool

Steroidogenic factor 1 (SF1) is an exciting molecule for studying hypothalamic function because its expression is restricted to steroidogenic tissues such as neurons of the VMH, with little or no expression in other brain areas[144] and its expression is maintained throughout life as evidenced by multiple genetic models[105,145,146]. SF1, or nuclear receptor subfamily 5 group A member 1 (NR5A1), is a transcription factor that is essential in regulating reproductive development at all levels of the hypothalamic-pituitary-gonadal axis[136,146,147] including neurons of the VMH that regulate both metabolism and fertility[148]. SF1 and its promoter reside in the NR5A1 5' regulatory region[149] at LOC108489981 on chromosome 2, (NCBI: NG_051341.1). Evidence suggests that the promoter for SF1 is located at position 3701-3783[147], while SF1 itself is a 462 aa protein with a transcription start site at 3784. Genetic studies investigating the effects of SF-1 knockout have been performed at multiple levels of this axis in an attempt to isolate primary and secondary effects of SF1 loss, which produces a

complex phenotype of dysregulated endocrine functioning caused by absence of a developed VMH and adrenal glands, and greatly underdeveloped reproductive structures[150].

Mice with postnatal VMH-specific knockout have impairments in energy regulation, including hyperphagia, reduced thermogenesis, and decreased energy expenditure, leading to obesity[136,151]. This suggests that SF-1 is required for development of the VMH and steroid producing endocrine glands, and in adulthood is required for the maintenance of energy balance via the VMH. Pituitary gland-specific SF-1 knockout mice lack secondary sexual characteristics but have intact adrenal glands[146]. Leydig- or granulosa cell-specific knockout of SF-1 in either male and female mice, respectively, leads to sterility in both sexes and in males results in hypoplasia of testes and retention inside the body cavity[152], indicating the development of gonads relies on cell-specific SF-1 expression. Whole-animal and CNS-specific SF-1 knockdown studies show that SF-1 is important in the structural organization of the VMH[153] and its connections with surrounding nuclei[154]. To account for secondary effects of gonad-derived hormone secretion, an SF-1 knockout model was augmented with adrenal gland transplants to better understand the contribution of SF1 produced in the VMH. This model showed obesity and reduced leptin receptor expression in the VMH[136]. Thus, SF1 expression in the hypothalamus is key to energy balance including the activation of thermogenesis.

Rodent models of global PACAP knockout have been developed by Gray et al.[108] and others, allowing the characterization of a phenotype with impaired thermogenic capacity and nutrient metabolism. This model is complicated, however, as PACAP is ubiquitously expressed and global knockouts have multifaceted impairments in high-level regulation of stress circuits in the CNS including the hypothalamic-pituitary-adrenal (HPA) axis as well as being an important neurotransmitter and neuromodulator at the level of the effector organs such as the

pancreas and the adrenal medulla. Furthermore, overall neuron survival and function is likely reduced in this model due to the loss of PACAP's neuroprotective and neurogenerative effects in the CNS[155]. Genetic rescue of PACAP in specific nuclei of the hypothalamus in the context of a global PACAP knockout will help elucidate primary and secondary effects of PACAP in this complex phenotype.

This chapter has emphasized an integral role of PACAP in the thermogenic pathways, the importance of SF-1 in the development and thermogenic function of the VMH and has demonstrated a need for further study of the thermogenic nuclei. Thus, we propose that a genetic construct be developed to express PACAP specifically in the VMH under the control of the SF-1 promoter.

We hypothesize that genetic restoration of PACAP specifically in the VMH will rescue the impaired thermogenic phenotype observed in PACAP-/- mice.

The objectives of this chapter are the following:

AIM 1: Develop a protocol for stereotaxic intracerebral and intracerebroventricular injection surgery and perform injections of scAAV9 viral vectors into the third ventricle or VMH of mice, respectively.

AIM 2: To assess the performance of the scAAV9 viral vector carrying its genetic cargo, pscAAV9-SF1-GFP, in activating VMH-specific induction of EGFP expression *in vitro*.

This work will support development of an *in vivo* rodent model to study PACAP's role in the hypothalamic control of energy metabolism including feeding behaviour and thermogenesis. These insights will help inform treatment strategies in obesity by elucidating the complex interplay of hypothalamic nuclei in maintaining energy balance.

2.2 MATERIALS AND METHODS

Animals

Adult (12-week-old), male C57BL/6 mice were bred at the Northern Health Sciences Centre, UNBC. These mice were sourced from a PACAP-null mouse line previously generated by Gray, et al. [108] backcrossed to a C57BL/6 background, with $PACAP^{+/+}$ mice selected for the study. Mice were housed two per cage with sterile corncob bedding and placed on a 12-h light to 12-h dark cycle (lights on 0700–1900 h). Animals had unlimited access to water and standard rodent chow diet (LabDiet 5001, LabDiet, Inc., Brentwood, Leduc, AB, Canada; metabolizable energy 3.02 kcal/g). Body mass (g) was measured twice weekly to detect potential declines in mouse health. Care and treatment of mice was in accordance with the guidelines of the Canadian Council on Animal Care, and protocols for the study were approved by the University of Northern British Columbia's (UNBC) Animal Care and Use Committee (ACUC).

Construction of the pscAAV-SF1-GFP plasmid

The pAAV-CMV-GFP was developed and deposited at Addgene (Watertown, MA, USA) by Gray and Zolotukhin [156]. We obtained the plasmid (Addgene plasmid # 32396) in the form of an *Escherichia coli* agar stab, which was grown up and the plasmid isolated according to the supplied Addgene protocols as described in McMillan [157]. The putative SF1 promoter sequence, 3706 – 4095bp of NR5A1, was amplified, cloned into a pGEM-T Vector (Promega, Madison, WI), and sequenced (University of Northern British Columbia's Northern Analytical Laboratory Services).

The resulting pGEM-T-SF1 plasmid and the pscAAV-GFP plasmid containing CMV promoter were used to create the pscAAV-SF1-GFP plasmid (Figure 2.2) that was packaged into a self-complimentary AAV serotype 9 (scAAV9) viral vector (Vigene Biosciences, Rockville, MD, US).

The scAAV9 vector was chosen for its extra-chromosomal plasmid DNA delivery method, low stimulation of immune response, lack of self-replication, and long-term stability of the delivered DNA. Since this vector will not incorporate in the host DNA, there is very little chance of off-target effects resulting from the interruption of host genes.

Viral Dosage Calculations

Dosages for self-complementary AAV9 virus vary greatly in the literature. For example, some report injection volume without a viral titre[158], others report the number of viral particles[159], or viral genomes (vg) per kg of body mass[139], but many do not report volume, which is an important factor for ICV injections where small volumes are required to prevent changes in intercranial pressure. Meyer et al. (2015)[139] reported significant genetic rescue in a knockdown model for spinal muscular atrophy using 3.3e14 vg/kg as their highest viral dose. They found significant response at 1.8e14 vg/kg, though increased survival time due to restored gene delivery was approximately half. We received our virus (scAAV9-SF1-GFP) at a titre of 2.24e14 vg/mL, and thus for these initial studies testing expression and specificity of the virus, opted to inject 0.8-1 µl of undiluted virus per mouse, resulting in a dose of 7.7e12 vg/kg (ICV) or 8.6e12 vg/kg (VMH).

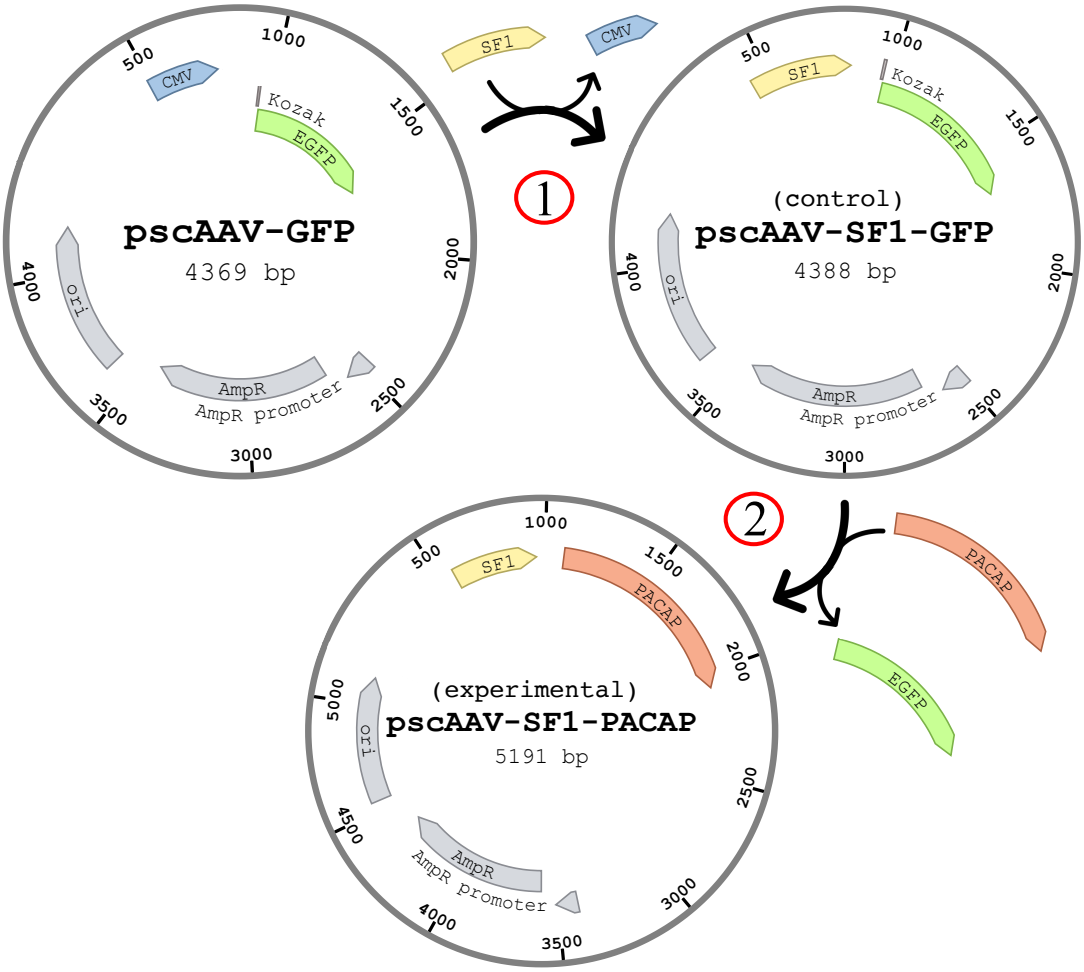

Figure 2.2. Simplified workflow process demonstrating the development of the pscAAV plasmids used in this chapter. Addgene Plasmid # 32396 (top left) contains the cytomegalovirus promoter (CMV) and EGFP. The pscAAV-SF1-GFP virus was developed by removal of CMV via restriction enzyme digest (1) followed by insertion of the steroidogenic factor 1 promoter (SF1). This control plasmid was created to facilitate characterization of in vivo viral vector expression following injection into the brain and should only be transcribed in neurons of the ventromedial nucleus of the hypothalamus, since SF1 expression in the brain is restricted to the VMH. The experimental virus was developed by restriction enzyme digest (2) of the control plasmid to remove EGFP and replace it with pituitary adenylate cyclase-activating polypeptide (PACAP). Plasmid maps were created in part using the online Benchling Plasmid tool (Benchling, Inc., San Francisco, CA, USA).

Stereotaxic Surgery and delivery of scAAV9-SF1-GFP

This procedure was adapted from the UNBC ACUC, Standard Operating Procedures, A3-4: Mouse Stereotaxic Surgery.

In preparation for surgery, mice were weighed and a 1 cm patch of fur was shaved from the scalp of the mouse. Mice were deeply anaesthetized with isoflurane (1 L/min O_2, 5% isoflurane) and placed in a stereotaxic ear bar apparatus. The left ear canal of the mouse was then placed over the left ear bar (set to 3.5 mm for C57BL/6), then the right ear bar was inserted into the right ear canal. The mouse was checked to ensure correct positioning by lightly pushing on the left and right side of the mouse's snout to ensure no lateral movement. If the mouse was secure, the right and left ear bars were alternately adjusted in the y-axis to ensure that the measurements of each ear bar were equal (Figure 2.3a). Once centered, the incisor bar was locked carefully in place and the anesthetic mask positioned to cover the snout to restore isoflurane anesthesia at a surgical plane (1 L/min O_2, 2% isoflurane).

After 2 minutes, anesthesia level was assessed by toe pinch and a rectal probe was inserted to track body temperature and control the automatically adjusting safe heat pad to maintain body temperature during the surgery. The surgical site was cleaned three times (70% isopropyl alcohol swabs) and mice were given Ringer's lactate solution (0.3 mL) subcutaneously. A line block was injected subcutaneously at the incision site (bupivacaine hydrochloride USP (2.5 mg/mL in Ringer's Lactate solution (100 μL)), 10 min prior to making a 0.5 cm incision exposing lambda and bregma (Figure 2.3b).

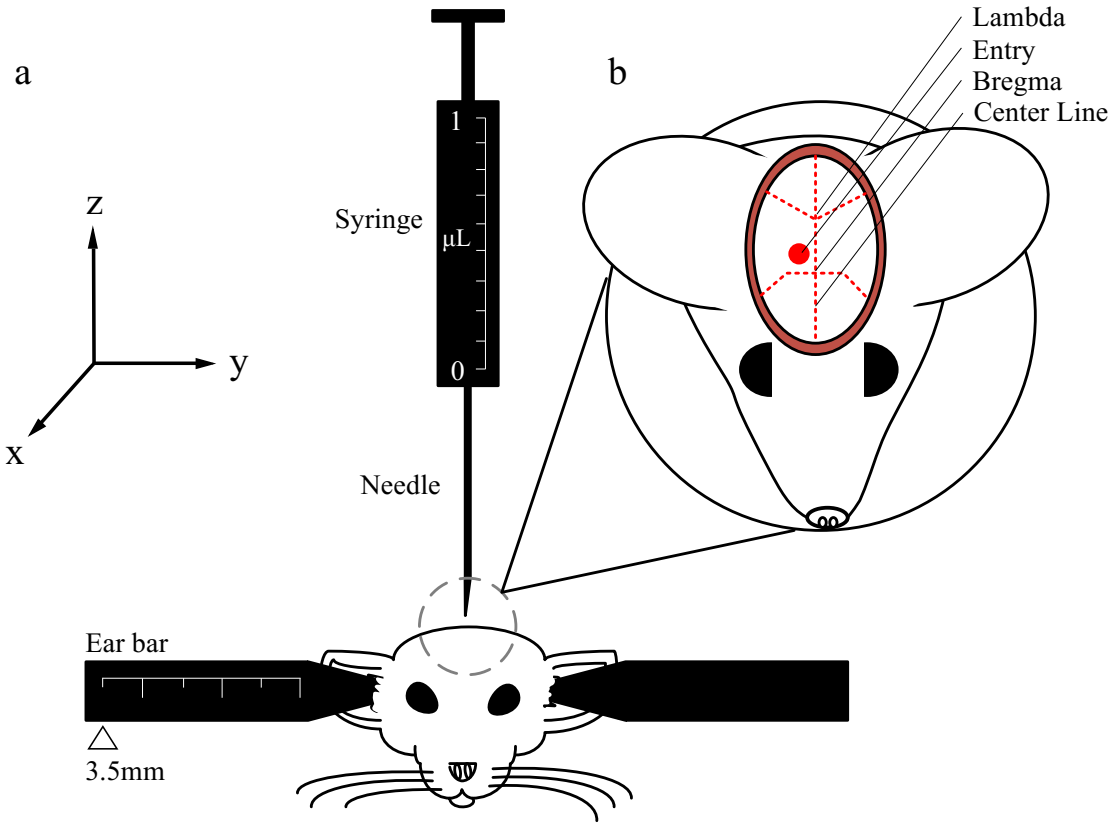

Figure 2.3. Stylized diagram of stereotaxic surgery setup (a) and dorsal view of mouse skull suture lines, shown as red dashed lines (b), used as landmarks for intracranial injection of AAV9 viral vector bearing pscAAV9-SF1-GFP. The entry point shown as a red dot approximates the location of drilling and needle insertion for the ventromedial nucleus of the hypothalamus (VMH)-targeted injection strategy. Diagram not to scale.

Using the micropositioner arm of the stereotaxic stand, the height (z) of bregma and lambda were equalized by adjusting the incisor bar appropriately. A trephination through the skull was carefully made using a drill bit (1 mm diameter ball mill carbide) at pre-planned coordinates targeting the ventromedial nucleus of the hypothalamus (1.46 mm posterior of bregma and 0.39 mm lateral to the midline) ensuring no damage to the underlying tissue. Coordinates for the third ventricle were the same except directly at the midline, not 0.39 mm lateral to it.

The drill was replaced on the stereotaxic micropositioner arm with the zero dead volume Hamilton Syringe 7000 model 1 μL syringe and 69.9 mm-long needle with 0.515 mm outer diameter. To account for differences in size and lateral position of the drill holder and the syringe holder, the syringe needle was lowered until it touched the surface of the brain in the trephination and this became the starting point for the vertical coordinate (-5.7 mm in the z-axis). The injection assembly was lowered at a rate of 1 mm per minute until the planned coordinates were reached and 0.8-1 μl of undiluted (2.24e14 vg/mL) AAV9 viral particles carrying psc-AAV9-SF1-GFP was injected over 30 seconds and not withdrawn until 5 min after the injection to ensure adsorption of the fluid. The trephination was flushed with saline and excess saline removed with a sterile cotton swab. The incision was sutured (5-0 polyglactin 910 braided suture on an RB-1 17 mm needle) under a sterile drape.

Following suturing, isoflurane was set to 0 and oxygen left at 1 L/min for approx. 10 min. While the animal recovered from the anesthetic, lidocaine cream (2.5% w/v) was applied to the incision site, ear bars were removed and ear canals checked for damage, monitoring equipment was removed and the mouse was placed in a warmed cage with low light until normal behaviors, such as coordinated walking and grooming, returned (approx. 45 min). Long-term recovery and monitoring procedures were performed as outlined in UNBC

ACUC's, Standard Operating Procedures A3-4: Mouse Stereotaxic Surgery and SOP A-40: Anaesthetic Depth and Monitoring.

Mice were "incubated" (meaning injected with virus then returned to normal housing) with the virus for 2.5 weeks before brain collection and analysis because the manufacturer (Vigene) reports that this timeline provides the maximal level of viral genome expression, which is expected to decrease over time. To assess the potential for long-term acclimation or developmental studies, a long-term incubation of 6 months was performed. This timeline encompasses the time of development from weaning until mid-adulthood and reveals whether this model is suitable for developmental studies to elucidate long-term effects of genetic rescue.

AAV9-EGFP Brain collection and Imaging Protocol

Mice were anesthetized with 2.5% isoflurane delivered at 1 L/min oxygen. Surgical plane anesthesia was confirmed by lack of withdrawal from toe-pinch and absent palpebral reflex. An incision in the skin was made from the pelvis to the chin, then through the visceral peritoneum and up through the diaphragm and right side of the rib cage to the neck, exposing the heart. A 25 g needle attached to a syringe containing phosphate buffered saline was inserted into the left ventricle of heart. A 3 mm incision was made in the right atrium of the heart then the 10 mL of saline was injected over 4 min to flush the capillaries of autofluorescent erythrocytes. Following saline perfusion, isoflurane anesthetic was stopped. The empty syringe was replaced with one containing 10 mL 4% (w/v) formaldehyde, and the entire volume injected over 4 min. Fixation tremors and blanching of internal organs and brain were used as indicators of successful fixation. The brain and adrenal glands were collected and fixed in 4% formaldehyde for 8 hr and prepared for cryoprotection by placing them in 15% sucrose until

they sank, then switching to 30% sucrose before cryosectioning, mounting, and DAPI staining (Wax-It Histology, Vancouver, B.C., CAN).

Brain sections were mounted two or three per slide and the best-quality section was imaged on each slide. Sections with visible mounting artifacts were not imaged when it could be avoided. Images were acquired using AxioObserver.Z1/7 with Axiocam 503 camera with 10X/0.30 M27 lens. For imaging on the DAPI channel, the following settings were used: LED-Module at 385 nm, 28.40% intensity, 353 nm excitation, 465 nm emission, and 500 ms exposure. For the imaging on the FITC channel, the following settings were used: LED-Module at 470 nm, 100% intensity, 488 nm exitation, 509 nm emission, and 1.1 s exposure.

2.3 RESULTS

Two injection strategies were used in this study (Table 2.1): one intracerebral injection targeting the VMH, and one intracerebroventricular (ICV) targeting the third ventricle. For each strategy, a mouse was incubated with the virus for 2.5 weeks following the surgery, then brains were collected and analyzed for expression of enhanced green fluorescent protein (EGFP). An additional mouse was injected using the VMH-targeted strategy and incubated for 6 months.

ICV

The ICV injection strategy did not yield EGFP expression in any part of the brains after 2.5 weeks, including the hypothalamus (Figure 2.4a).

Table 2.1. Stereotaxic injection strategies used for intracerebral injections of scAAV9 viral particles containing pscAAV9-SF1-GFP plasmid. Injections were targeted at either the ventromedial nucleus of the hypothalamus (VMH) or the third ventricle (V3) in volumes of less than 1 μL and the virus allowed to incubate for 2.5 weeks or 24 months before collection of brains to assess injection efficacy and longevity of the introduced plasmid gene expression. Mice were male C57BL/6, except VMH-24wk, which was from a line of SVJ mice 10x backcrossed to C57BL/6.

Study ID	Injection target	Dose (vg/kg)	Time (weeks)	Age (d)	UNBC ID	Sex	Mass (g)
V3-2.5wk	V3	7.7e12	2.5	86	650	M	29
VMH-2.5wk	VMH	8.6e12	2.5	80	662	M	21
VMH-24wk	VMH	8.6e12	24	84	S772	M	26

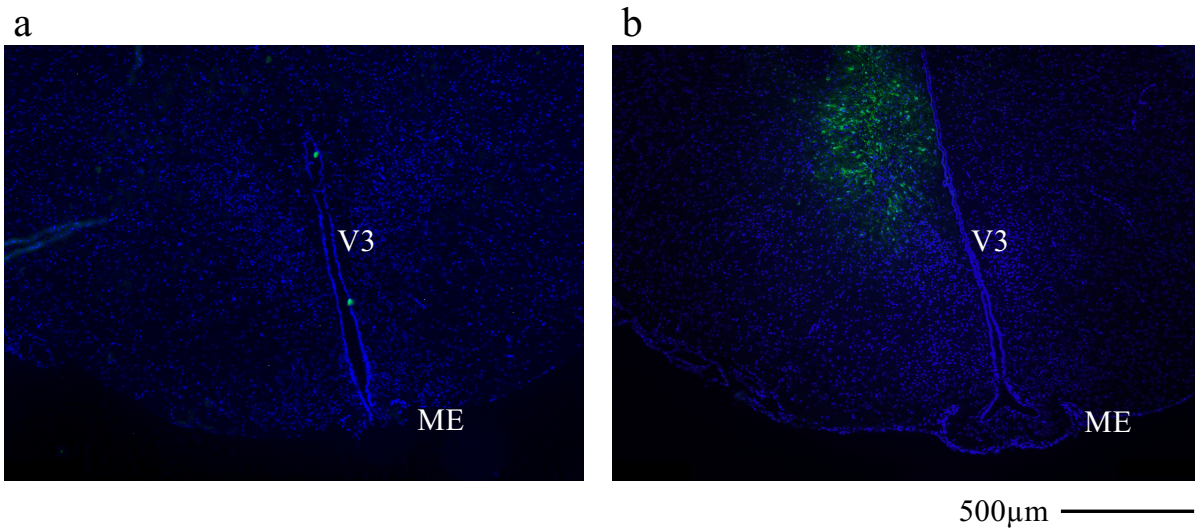

Figure 2.4. Representative images (100x mag.) of coronal-aspect hypothalamic cryosections from adult (3-month-old) male C57BL/6 mice 2.5 weeks following a single intracranial injection containing 10^{13} vg/kg (viral genomes per kg body mass) of pscAAV9-SF1-GFP packaged in scAAV9 virus (Vigene Biosciences) to show efficacy of injection strategies in inducing EGFP protein expression. Injections were targeted at (a) the third ventricle (1.46 mm posterior to bregma, 5.7 mm inferior to the top of the brain) or (b) the ventromedial nucleus of the hypothalamus (1.46 mm posterior to bregma, 0.39 mm lateral to the midline, 5.7 mm inferior to the top of the brain). The third ventricle (V3) and median eminence (ME) are included as hypothalamic landmarks. Nuclei were stained with DAPI in mounting media and EGFP autofluorescence was imaged on the FITC channel.

VMH

Conversely, the VMH-targeted injection yielded high EGFP expression lateral to the third ventricle in the area of the hypothalamus, approximately 750 μm superior to the median eminence (ME) (b). In the VMH-targeted injection strategy, EGFP expression was present at the injection site in an ovoid area but also projected superiorly towards the trephination site, following the path that the needle would have taken. This strip of EGFP expression continued outside the hypothalamus and halfway to the dentate gyrus (Figure 2.5). Other areas of the brain were EGFP-negative. The path of the needle did not leave damage that was visible after 2.5 weeks, with the exception of a 120 μm by 40 μm lesion-like area at the site of the injection.

The hypothalamic EGFP expression pattern observed in this study was compared with the coronal-aspect Allen Mouse Brain Reference Atlas (Figure 2.6 a,b). The VMH-targeted injection of scAAV9 virus containing EGFP plasmid (psc-AAV9-SF1-GFP) shows that the EGFP expressing area begins at approximately 850 μm superior to the bottom of the brain and extends for 750 μm (c), which does not overlap with the area outlined as the VMH in the Allen Mouse Brain Atlas (b). *In situ* hybridization data included in the Allan Brain Atlas shows SF1 mRNA occupies a region beginning 200 μm superior to the median eminence and extending for 700 μm (Figure 2.6d), which corresponds to the VMH as demarcated by the reference atlas (b) but does not correspond to the EGFP-expressing area that resulted from our VMH-targeted injection (c).

Micrographs reveal that the EGFP expression and DAPI staining were not co-dependent (Figure 2.7). In representative micrographs, EGFP expression occurred in the cytoplasm (solid arrows) around nuclei and extended out in thin projections of variable length (open arrows), with some over 100 μm long (Figure 2.7a,b,c). Panel (d) shows multiple adjacent EGFP-positive filaments in parallel.

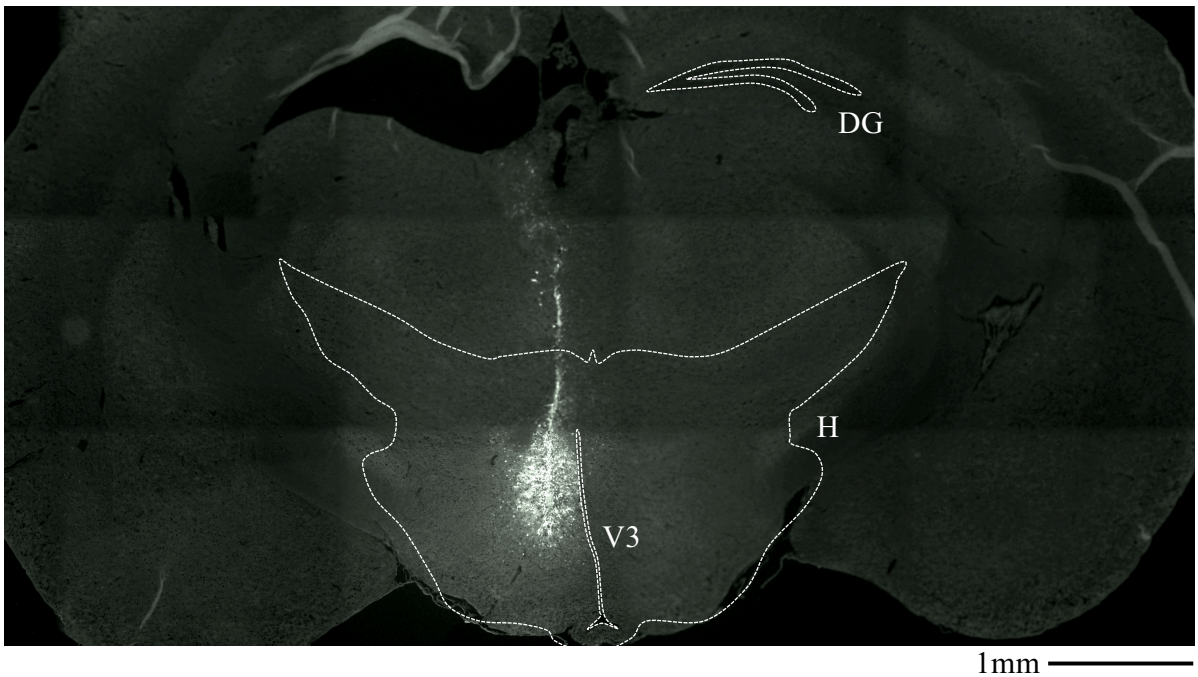

Figure 2.5. Representative twelve-image (100x mag. each) stitch taken on the FITC channel of a coronal-aspect whole brain cryosection from a male C57BL/6 mouse 2.5 weeks following a single intracranial injection containing 10^{13} vg/kg (viral genomes per kg body mass) of pscAAV9-SF1-GFP packaged in AAV9 virus (Vigene Biosciences) to show anatomical distribution of autofluorescent EGFP expression and evaluate injection accuracy. The dentate gyrus (DG), hypothalamus (H), and third ventricle (V3) are outlined as anatomical landmarks. The injection was targeted at the ventromedial nucleus of the hypothalamus (1.46 mm posterior to bregma, 0.39 mm lateral to the midline, 5.7 mm inferior to the top of the brain).

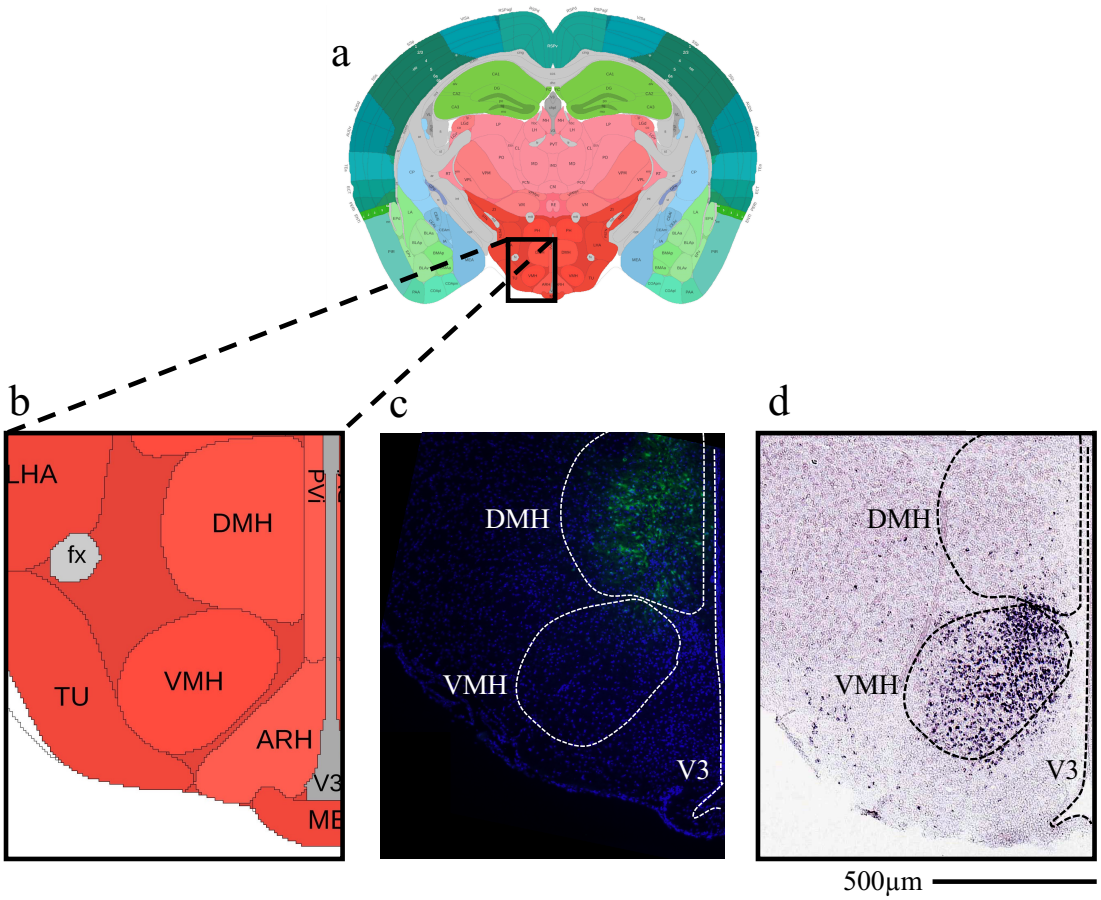

Figure 2.6. Panels showing coronal aspect of brain sections from male C57BL/6 mice to evaluate specificity and efficacy of EGFP expression. Image 72 (a) was taken from the Allen Mouse Brain Reference Atlas (coronal aspect) and included for spatial context then enlarged to show hypothalamic nuclei (b), coloured red. The corresponding brain section area (c) from an adult male mouse 2.5 weeks following a VMH-targeted injection of scAAV9 virus containing pscAAV-SF1-GFP plasmid at a concentration of 10^{13} vg/kg (viral genomes per kg body mass) shows the distribution of plasmid-encoded EGFP expression. Hypothalamic anatomical landmarks include the dorsomedial nucleus (DMH), ventromedial nucleus (VMH) and third ventricle (V3). Nuclei were stained with DAPI in the mounting media and EGFP was detected through autofluorescence on the FITC channel. Image 24 (d) was taken from Allen Mouse Brain ISH Atlas for the nuclear receptor (Nr5a1), aka SF1. This image shows the corresponding area stained with an in situ antisense RNA probe and was included to compare the anatomical area of EGFP expression following intracranial injection (c) to wild-type SF1 expression in the hypothalamus (d). Images (a) and (d) collected from the following URL with free, open access permission © Allen Institute.
© [2004] Allen Institute for Brain Science. Allen Mouse Brain ISH Atlas, Coronal. Available from: https://mouse.brain-map.org/search/index.

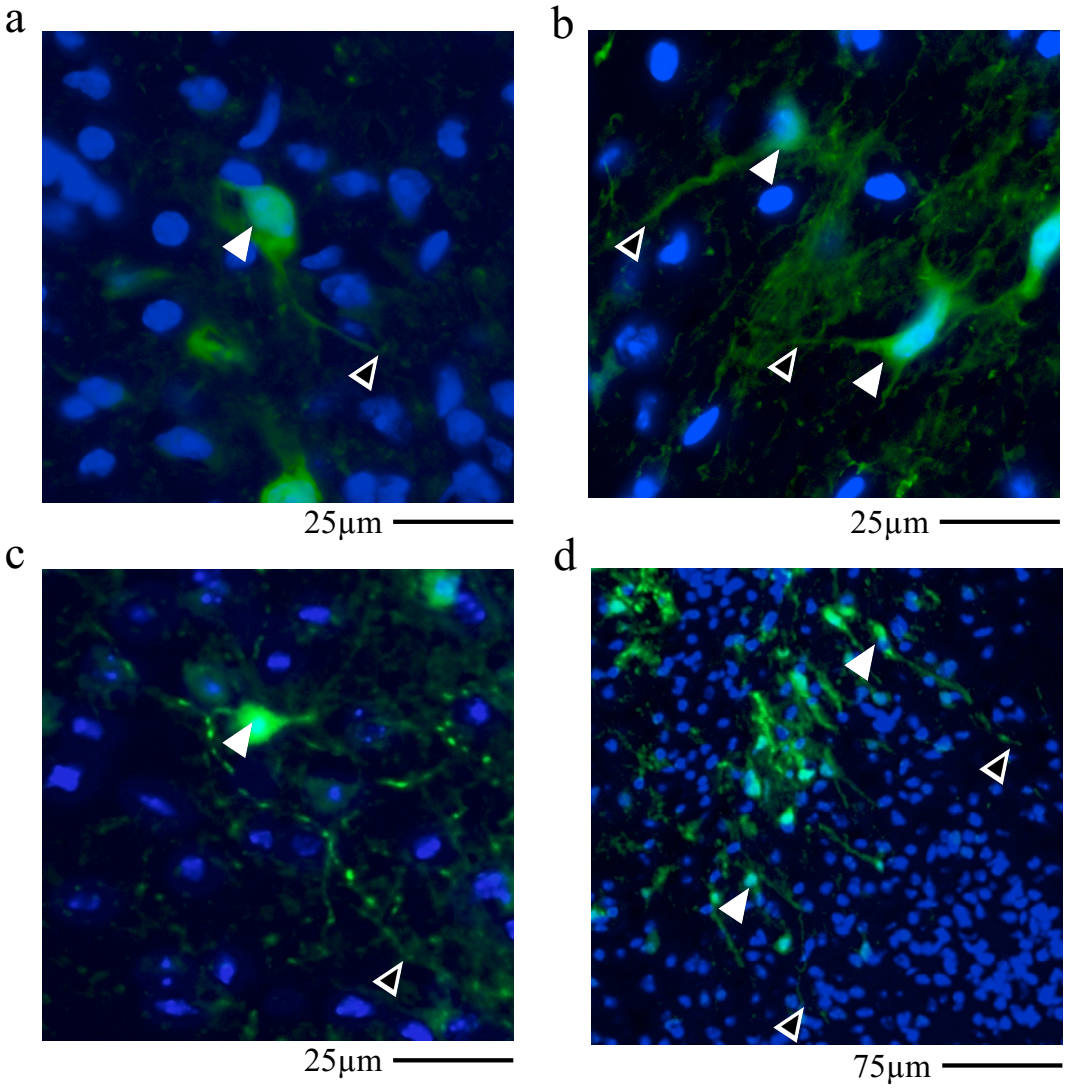

Figure 2.7. Representative images of DAPI-stained hypothalamic coronal-aspect cryosections from male C57BL/6 mice 2.5 weeks following a single intracranial injection containing 10^{13} vg/kg (viral genomes per kg body mass) of pscAAV9-SF1-GFP packaged in AAV9 virus (Vigene Biosciences) to show cellular localization of EGFP expression and cell morphology of EGFP-positive cells. EGFP-positive cell bodies and indicated solid arrowheads and their EGFP positive projections are indicated by open arrowheads. Nuclei were stained with DAPI in mounting media and EGFP was detected through autofluorescence on the FITC channel. Field of view indicated for each micrograph, which were taken at 400x (a,b,c) or 100x magnification (d).

2.4 DISCUSSION

The results presented in this Chapter are an essential step towards the generation of a transgenic animal expressing PACAP in the VMH on a PACAP-null background to study the effect of PACAP in the VMH on the regulation of thermogenesis. This work contributes to the validation of using an AAV9 vector expressing the VMH-specific SF1 promotor in combination with VMH-targeted injection. The control virus expressing EGFP (psc-AAV9-SF1-GFP) is an excellent tool to characterize the efficacy and distribution of the viral genome in the host tissue, as EGFP can be visualized without an additional step of antibody chemistry. This would be much more difficult to do with PACAP, which is not autofluorescent and would thus require the development of an *in situ* hybridization protocol to detect mRNA or antibody-based approach to detect the protein. PACAP is part of the glucagon/secretin superfamily of proteins and therefore shares sequence and structural similarity with a number of other proteins, making the development of PACAP-specific probes and antibodies difficult. If the AAV9 vector and SF1 promoter cause a very high level of protein expression, there is also the possibility of off-target effects, providing another important reason to first test expression patterns of AAV9 with EGFP, which does not have bioactive properties in mammalian cells. Thus, the development and characterization of the control virus is described in this Chapter to guide future stereotaxic injections, ensuring that the stereotaxic intracerebral injection technique, viral vector, and plasmid are all optimized before implementing the PACAP-expressing virus.

The first major success provided here is that the virus and plasmid we developed were effective in gaining access to the host cells, introducing their plasmid pscAAV-SF1-GFP, and that the plasmid EGFP gene was successfully translated into functional protein by the host cells. Of the two strategies presented here, injection of AAV9-SF1-GFP directly into the

hypothalamic nucleus was more effective in inducing the desired cellular infiltration by the virus and expression of EGFP by host cell machinery. The ICV injection strategy used to deliver AAV9-SF1-GFP in this study was not successful in inducing detectable EGFP expression in the hypothalamus, or any other part of the brain (Figure 2.4a), while the VMH-targeted strategy was able to induce high levels of EGFP expression in an area approximately equal to the size of the VMH (Figure 2.4b). These preliminary observations suggest that hypothalamic nucleus injections are superior when using a small injection volume (0.8-1 μL). The lack of EGFP expression seen in the brain sections from mice with ICV injections of AAV9-SF1-GFP is likely due to the large dilution factor provided by the cerebrospinal fluid in the third and lateral ventricles, which are connected and may have caused the virus to disperse so thinly that few (if any) cells of the hypothalamus were successfully infected. The total volume of the ventricles in the C57BL/6 mouse brain is 50 μL[160] and thus the virus may have been diluted by up to 50x in the ICV-targeted injection strategy.

A zero dead volume needle and syringe were specifically used in this study to prevent leaking and give as localized delivery as possible. The needle was also left in place for 5 min following the injection to allow the injected fluid to disperse. Despite this, significant EGFP expression was detected along the track of the needle (Figure 2.5), suggesting that there was some leakage of the virus as the needle entered the brain or that injected fluid followed the needle as it was retracted. Future injections should increase the amount of time that the needle is left in place at the injection site post-injection from 5 to 10 min, and the withdrawal should be performed over 5min instead of 1min to discourage spreading injected fluid away from the injection site.

In comparison to the Allen Mouse Brain Reference Atlas[161] in Figure 2.6 (a) and (b), the EGFP expression in the hypothalamus (c) was mostly outside of the VMH's area, and thus

occurred largely within the area of the DMH, suggesting that this injection was proximately 250 μm anatomically superior to the target location of the VMH. Comparing this area to the expression of SF1 nuclear receptor reveals that the EGFP expression (c) is also outside of the SF1-positive area (d), suggesting that the SF1 promoter is not functioning as specifically as expected. This could be due to SF1 promoter leakiness, meaning that it promotes expression in the absence of its inducer. Most promoters are leaky to some degree[162]. While this seems unlikely given the very low abundance of SF1 elsewhere in the brain, promoter leakiness increases at very high plasmid concentrations[163]. It should also be taken into consideration that the CMV promoter may still be present in some copies of the plasmid, though this would be surprising since the pGEM-SF1 plasmid was sequenced[157] before being sent to Vigene. Therefore, the most probable explanation for SF1-promoter-driven EGFP expression outside of SF1-expressing tissue of the VMH is the very high local concentration of plasmid causing excessive leakiness of the promoter.

A closer look at cellular morphology and localization shows that EGFP expression is not confined to the area surrounding the cellular nuclei (Figure 2.7a-d), and thus the protein persists long enough to be actively transported or diffuse throughout the cell, including along cell projections (d). Since no neuronal marker was used in this study, it is difficult to decisively conclude which cell types are expressing EGFP. AAV9 vectors are capable of infecting both glial cells and neurons with relatively comparable efficiency (~50% *in vitro* expression of EGFP driven by CMV promoter)[141]. However, some preliminary observations of EGFP-positive cell morphology presented here suggest that at least some glial cells and some neurons are EFGP-positive. The indicated cells in panels (a) and (b) may show glial cells since the projections are relatively short (Figure 2.7). Conversely, panels (c) and (d) likely show neurons based on the cellular projections, which are many times the length of the cell body. The

organized nature of the EGFP-expressing projections in panel (d) is suggestive that these are axons of neurons. From these data it is highly probable that at least some neurons are expressing EGFP. One limitation of this study is that there were no neuronal markers included in the histological analysis, prohibiting strong conclusions about the type and number of cells that were EGFP-positive.

The data reported here show promising evidence that the EGFP plasmid will be a useful tool to study the potency and specificity of gene expression driven by the SF1 promoter, but a number of important experiments must be performed to confidently understand the functioning of this genetic tool before strong conclusions can be made. Below I have outlined some suggested experiments that aim to improve the functionality of this technique.

Future directions

To achieve the desired localization and specificity of expression, the viral titre should be reduced. Further, the injection depth should be increased from 5.7 mm to 5.725 mm to ensure that the virus is directly introduced to the VMH since the data presented here show that a 5.7 mm injection depth leads to an injection 250 μm superior to the VMH, corresponding to the DMH. From the micrograph in Figure 2.6c, it is tempting to suggest that perhaps the injections should also be targeted slightly more lateral, but due to the lateral distortion introduced during the slide mounting process, it is challenging to make conclusions about the lateral accuracy of the injection performed here.

Once the location of the injection is confirmed to be in the VMH, and off-target expression has been reduced as much as possible through reduced titre, it will be essential to conclusively show whether neurons are EGFP-positive, potentially by using a neuron-specific antibody such as Abcam's Anti-Neurofilament heavy polypeptide antibody (Cat. No. ab8135).

This antibody has been shown to be effective in PFA-fixed mouse neurons[164] and is selective for neurons over glial and other contaminating cell types. Microscopic analysis could then be used to determine colocalization EGFP (green) and neuropeptide heavy chain (red) to confirm neuronal expression of EGFP with a high degree of confidence.

The inclusion of the SF1 promoter in the plasmid was an important step in trying to prevent off-target vector-derived protein expression. To ensure that the promoter is effective in targeting SF1 neurons, an anti-SF-1 antibody such as the rabbit anti-NR5A1 Polyclonal Primary Antibody (MyBioSource cat. No. MBS9205805). This antibody has been shown independently by a separate research group to be effective in histological analysis of SF1 in mouse cell lines[165]. The injection and slide preparation could be performed similar to the methods detailed in the above paragraph, followed by counterstaining with anti-SF1 antibody and a fluorophore-bearing conjugated secondary antibody. Ideally, the fluorophore on the secondary antibody would be orange (i.e. BD Horizon™ PE-CF594) to allow for the potential of using it in conjunction with the neuronal marker described above. This experiment would provide a qualitative measure of off-target EGFP expression.

A quantitative measure of the efficacy of the promoter would require counting the percentage of SF1-positive and SF-negative cells that express EGFP. This could be accomplished by microscopy or flow cytometry. The manufacturer of the anti-SF1 antibody above has provided results showing that it is suitable for use in flow cytometry as well. Thus, the hypothalamus could be excised from the brain of a euthanized VMH-injected mouse either before or after fixation[166], then single neurons could be isolated from the hypothalamus tissue by digestion. Given the small amount of starting material, it would probably be best to perform the neuron isolation before the fixation step since digestion of unfixed tissues tends to give higher yields of intact cells. DAPI and SF-1 staining could then be performed, followed by

quantitative analysis by flow cytometry. Flow cytometry analysis of mouse neurons has been performed previously[167] on neurons isolated using the Neural Tissue Dissociation Kit (P) (Miltenyi Biotec) and thus would be a good place to start. Intact, single neurons could be identified using DAPI fluorescence and standard singlet gating, and in the same analysis experiment, cells could be separated based on fluorescence on the FITC and PE-CF594 channels to identify four populations of cells: SF1(-)/EGFP(-), SF1(+)/EGFP(-), SF1(-)/EGFP(+), and SF1(+)/EGFP(+). A high proportion of SF1(+)/EGFP(+) neurons would indicate specificity of the SF1 promoter.

2.5 CONCLUSION

In conclusion, significant progress has been made in the development of a method for the stereotaxic intracerebral injection of AAV9 viral particles containing pscAAV9-SF1-GFP plasmid. The results show that the injection was within 250 μm of the target site, the AAV9 successfully incorporated its genome into the host brain tissue, injected mice were free of malaise, and that the pscAAV9-SF1-GFP plasmid EGFP gene was successfully expressed by host cellular machinery *in vivo*. Improvements to this protocol will include site targeting based on coordinates optimized for our mice, reduced non-VMH neuron expression of EGFP, and better characterization of EGFP expressing cell types. The resulting method will provide evidence for an effective gene delivery strategy and will support the implementation of a virus carrying the PACAP gene driven by the SF-1 promoter. This study will allow us to characterize the contribution of VMH-derived PACAP to energy regulation including adaptive thermogenesis and will therefore provide a more comprehensive understanding of central body

mass regulation that will contribute to efficacious and safe treatment of obesity as new therapeutics are developed.

Chapter Three: Investigating a Role for PACAP in Adipocyte-Mediated Activation of Thermogenesis

Preface
Content from this Chapter was, in part, published previously[168].

3.1 INTRODUCTION

Adipose tissue is central to the regulation of energy metabolism. This role is highlighted by the debilitating effects of perturbations to adipose tissue functioning seen in metabolic disease. Despite this, adipose tissue biology is not well represented in the literature. In recent years this has begun to change, leading to a better understanding of adipose tissue physiology and the identification of potential therapeutic targets for the treatment of body mass-related metabolic disease. The pathology of obese adipose tissue has been characterized, revealing the importance of both physical and metabolic processes in maintaining adipose tissue function[19,35,38,51,68]. These include limits of physical remodeling of adipose tissue through hyperplasia and hypertrophy[169,170], and decreased adipocyte lipid turnover[47,53]. Finally, a long-known process called adaptive thermogenesis is now being rigorously examined as a mechanism to burn lipids in adipose tissue and thus may be a promising therapeutic target to increase energy expenditure[171,172]. By studying the mechanisms by which adipose tissue maintains energy balance, or how cellular mechanisms can malfunction in adipose tissue, we hope to enhance the understanding of the pathophysiology of obesity.

Accumulation of lipid in adipose tissues past their normal range in obesity drives a number of such pathological consequences. This defines an upper limit of storage capacity that when exceeded results in metabolic decompensation as observed in the Metabolic Syndrome. Exceeded adipose capacity manifests as excessive adipocyte hypertrophy and results in pathophysiological changes in lipid metabolism within the adipose tissue and negative effects on the endocrine function of the tissue[31,169]. In obese individuals, decreasing adipose lipid content and increasing energy expenditure would improve energy balance, outcomes that could

be simultaneously achieved through induction of adaptive thermogenesis. Thus, renewed interest in the search for novel strategies to induce adaptive thermogenesis has focused on the physiology of a specialized adipose tissue called brown adipose tissue (BAT). This energy-burning fat produces heat using lipids in response to cold or overnutrition. Augmenting BAT function or programming white adipose tissue (WAT) to act like BAT would shift the overall adipose tissue function from energy storing organs into energy burning ones. As proof of concept, remarkable improvements in glucose homeostasis have been shown simply through the implantation of exogenous BAT into mice[173]. The understanding of the biochemical and physiological regulation of adaptive thermogenesis has increased greatly since its identification as a potential therapeutic target.

Adipose tissues and their capacity for thermogenesis

Adaptive thermogenesis is regulated by the secretion of norepinephrine from sympathetic nerve terminals that synapse onto thermogenic adipocytes. Brown adipocytes are very responsive to β-adrenergic stimulation due to their high membrane concentrations of beta-3 adrenergic receptor (β_3-AR)[64,174,175]. Brown adipocytes have a high density of mitochondria that facilitate the high rates of β-oxidation of fatty acids required for heat production via uncoupling protein 1 (UCP1)[176-178,179]. Indeed, the abundance of mitochondria is what makes BAT brown in colour. The stored lipid in BAT is used to fuel thermogenesis and is reduced in cold-acclimated BAT from the interscapular depot[180,181]. BAT has also been shown to undergo hyperplasia with exposure to cold[176] to increase thermogenic capacity of the tissue and meet thermogenic demands to maintain homeostasis.

Not all adipose tissues contain thermogenic adipocytes. Energy expenditure can be controlled differentially in each adipose depot by the selective stimulation of sympathetic

output tracts to one or more adipose depots. The functional significance of β-adrenergic stimulation depends on the intracellular machinery at the target adipocyte, and thus the physiological response differs by depot. For example, β_3-AR stimulation of the thermogenic BAT depot will stimulate both lipolysis and thermogenesis, while this same signal in most WAT results only in an increase in mobilization of lipids with no accompanying increase in thermogenic recruitment[32].

White adipose tissues can be broadly divided into two groups with respect to thermogenesis. While classical white adipocytes do not express significant amounts of UCP1 to allow for heat production, some white adipose tissues possess the ability to "brown" by developing cells with significant UCP1 expression. In mice, the inguinal white adipose tissue (ingWAT) is a subcutaneous depot known to undergo this process[182]. If housed at thermoneutrality (30°C), mice need not perform thermogenesis to maintain euthermia. In this state, the ingWAT adipocytes are uniform in size, having a large single lipid droplet, few mitochondria relative to BAT or muscle, and low expression of UCP1[72]. Conversely, when mice are housed at 4°C, high rates of thermogenesis are required to maintain an internal temperature of 37°C. This thermogenic requirement drives remodeling of subcutaneous adipose tissues such as ingWAT including the appearance of thermogenic adipocytes[178]. These adipocytes are not true brown adipocytes, since they are derived from a different lineage of progenitors and express lower levels of UCP1 compared to brown adipocytes. Due to their intermediary morphology between brown and white adipocytes, they have been called "beige" or brown-in-white "brite" adipocytes owing to their anatomical location. Understanding the mechanisms of browning in white adipose tissue depots may have therapeutic potential to enhance energy expenditure in obesity[63,70,172,183,184].

Classical murine visceral white adipose such as gonadal adipose tissue (gWAT) does not undergo adaptive thermogenesis in response to cold exposure, at least in part due to genetic inhibition of browning, which when experimentally removed, allows browning in gWAT[185]. In response to cold exposure the lipid stores of this depot are depleted, but this does not correlate to an increase in UCP1 expression.

Sympathetic activation of thermogenesis and genetic control

Thermogenesis is inseparable from β-oxidation of fatty acids[186,187] but glycolysis is dispensable[188] for thermogenesis, despite the fact that glycolysis is capable of producing reducing equivalents for the electron transport chain. Exogenous free fatty acid (oleate) administration alone can increase thermogenesis as measured by oxygen consumption in primary brown adipocytes independent of β-adrenergic stimulation[189]. As such, β_3-ARs are densely expressed on thermogenic adipocytes and their activation increases lipolysis, thermogenesis, and genes controlling expression of UCP1. In BAT, protein kinase A (PKA) activation leads to the phosphorylation of cAMP response element-binding protein (CREBP), which is an essential transcription factor driving thermogenic capacity of adipocytes. CREBP drives the expression of another transcription factor peroxisome proliferator-activated receptor gamma (PPAR-γ), ultimately resulting in increased UCP1[190] expression. In contrast, cold-exposed WAT does not have the same increases in genes known to drive UCP1 expression, providing a potential mechanism to explain the lack of browning of certain white adipose tissues[191]. Thermogenic vs non-thermogenic adipocyte status is maintained by differences in transcriptional control[50,192-194], epigenetic modifications[192], and sympathetic innervation[32,195].

Thus, while sympathetic stimulation of BAT and some WAT drives browning, some WAT depots are destined to be non-thermogenic.

Endocrine control of thermogenesis

As discussed, sympathetic stimulation of thermogenic adipocytes by norepinephrine is the key regulator of thermogenesis. Other endocrine factors can increase the thermogenic capacity of brown adipocytes or increase the receptivity of the adipocytes to adrenergic stimulation by the sympathetic nervous system. One such factor is bone morphogenic protein-8b (BMP8B), which is expressed in BAT. Treatment with this protein increases the differentiation and thermogenic response of brown adipocytes to norepinephrine[196]. BMP8B is also implicated in central regulation of thermogenesis, being expressed in the ventromedial nucleus (VMH) of the hypothalamus. Mice lacking BMP8B have decreased sympathetic output to BAT[196] and intracerebroventricular (ICV) injection of BMP8B increases the rate of BAT thermogenesis and significantly enhances thermogenic gene expression in BAT[196]. Another autocrine/paracrine factor that has been shown to modulate thermogenesis is fibroblast growth factor-21 (FGF21), which upregulated in BAT of mice during cold stress[197]. Treatment of brown or white adipose tissues with FGF-21 increases the expression of thermogenic genes[198], including UCP1. Vascular endothelial growth factor A (VEGFA) is secreted by BAT to increase vascularization and increase the expression of UCP1 with cold stress[199]. Coupling of these processes by VEGFA results in increased thermogenesis in BAT, as well as increased export of heat form this tissue via the blood. Ablation of VEGFA in mice impairs the cold acclimation response[200]. Another potent activator of the thermogenic program is the thyroid gland-derived hormone, thyroxine (also known as tetraiodothyronine), which reaches the BAT through the bloodstream and seems to be required for the full induction of UCP1 in this tissue

in the face of cold exposure[201]. These findings and others have increased interest in understanding the endocrine regulation of BAT in the hopes of specifically targeting thermogenic activation for therapeutic use.

In this chapter we will investigate the possibility that pituitary adenylate cyclase-activating polypeptide (PACAP) may act in an endocrine manner to stimulate thermogenesis or increase the capacity of brown adipocytes to perform thermogenesis. Peripheral expression of PACAP is confined to immune cells, gonads and pre-ganglionic sympathetic and parasympathetic neurons, including those innervating exocrine and endocrine glands such as the pancreas[202], genitourinary tract, and the adrenal medulla, where it is the primary neurotransmitter. The expression and significance of PACAP and its receptors in adipose tissue depots of mice or humans has not yet been fully explored. In mice, only scattered reports exist of PAC1R in rat adipocyte cell lines and VPAC2 expression in cultured primary rat adipocytes[203]. In humans, only a single report of genetic expression of PAC1R in adipose tissue exists, and this report neglects to report the depot from which the cDNA were isolated[204]. No evidence of PAC1R expression in brown adipocytes has yet been reported.

The possibility that PACAP may be present in the neurons innervating the adipose tissue is supported by the fact that PACAP is expressed in nerve terminals innervating other important energy regulatory functions, such as the adrenal medulla. PACAP is produced and secreted by the preganglionic sympathetic nerves of the adrenomedullary synapse[88]. It is important to note, however that the adipose tissues are innervated by postganglionic neurons, and thus our expression data will not detect PACAP if it is acting further upstream, at the preganglionic synapse.

We hypothesize that PACAP acts directly at the adipocyte to regulate thermogenesis in BAT.

The objectives of this chapter are as follows:

AIM 1: Produce a robust mouse model of maximal activation of thermogenesis and characterize genetic changes in PACAP and its receptors in response to cold acclimation.

AIM 2: Determine whether PACAP or its receptors are expressed specifically by mouse adipocytes.

AIM 3: To assess the functional significance of PACAP binding to PAC1R at the adipocyte with respect to thermogenesis and lipolysis *in vitro*.

This work will increase our understanding of the endocrine regulation of energy metabolism in adipose tissues. These insights will help inform treatment of obesity and better management of the comorbidities associated with the disease, many of which are a consequence of adipose tissue pathophysiology.

3.2 MATERIALS AND METHODS

Animals

Adult (12-week-old), male, wild-type C57BL/6 mice were obtained from Charles River Laboratories (Sherbrooke, QC, Canada) and housed two per cage with sterile corncob bedding on a 12-h light to 12-h dark cycle (lights on 0700–1900 h). Water and standard rodent chow diet were freely available (LabDiet 5001, LabDiet, Inc., Brentwood, Leduc, AB, Canada; metabolizable energy 3.02 kcal/g). For PACAP receptor expression analysis, mice (n = 8/treatment) were housed at thermoneutrality (30 °C) (Solace Zone, Alternative design,

Siloam Springs, AR, USA) or cold (4 °C) conditions for 3.5 weeks to achieve full cold acclimation[64]. Mice utilized for cell culture were housed at 24°C until 10 weeks of age. Body mass (g) for all mice was measured twice weekly to detect potential declines in mouse health. Measurements of fat, fluid, and lean mass (g) were collected weekly by time-domain nuclear magnetic resonance (TD-NMR) using a minispec LF50 (Bruker, Billerica, MA, USA). Mice were unrestrained during the 2-min measurement period. Care and treatment of mice was in accordance with the guidelines of the Canadian Council on Animal Care, and protocols for the study were approved by the University of Northern British Columbia's Animal Care and Use Committee.

Postmortem Analysis and Tissue Processing

Non-fasted mice were anesthetized with isoflurane and sacrificed by cardiac puncture followed by cervical dislocation. Interscapular brown adipose tissue (iBAT), inguinal subcutaneous white adipose tissue (ingWAT), and gonadal white adipose tissue (gWAT) were collected by dissection, weighed and flash-frozen in liquid nitrogen and stored at −80 °C for RNA analysis or fixed in 10% formalin then stored in 70% ethanol for histological analysis. These adipose tissue depots were selected as they represent the classic thermogenic brown fat (iBAT), an inducible thermogenic white fat depot that contains beige adipocytes (ingWAT), and a non-thermogenic intraperitoneal white fat depot (gWAT), thus encompassing the physiologically distinct roles of fat with respect to thermogenesis [205].

Histological Analysis of Adipose Tissue

Adipose tissues (iBAT, ingWAT and gWAT) were fixed in 10% formalin for 36 h and then stored in 70% ethanol for 2-3 months. Samples were embedded in paraffin, sectioned (5

μm) and stained with hematoxylin and eosin (Wax-it Histological Services, Vancouver, BC, Canada). Images were captured, processed, and measured using cellSens Dimension software controlling a BX61 microscope and attached DP72 camera (Olympus Richmond Hill, ON, Canada).

For iBAT, ten regions of interest (ROI) at 20X magnification were examined across four sections for each tissue from each mouse (n = 4 per treatment). Slides with visibly damaged adipocytes or with contaminating epithelial tissue were excluded from image analysis. Micrographs were processed manually by selecting and deleting areas with contaminating tissue that was not representative of adipocyte morphology, such as blood vessels, erythrocytes, and macrophages and therefore were mathematically excluded in downstream analysis of area calculations. Photographs of the ROIs were captured, converted to grayscale and contrast was digitally maximized. White areas in these micrographs represent lipid droplets, which appear transparent-white due to lack of staining of these regions, and coloured areas represent cytoplasm (pink) or nuclei (purple). The images were computationally binarized to black and white. Non-lipid area was calculated by cellSens software as black areas in the ROI, and this area was then subtracted from the total area to give the lipid area (white area), which was then divided by total area to give lipid area as a percentage of the total ROI area.

To assess cell size, the number of cells per ROI were determined by manually counting the number of nuclei per ROI. Each ROI was split into four panels and the panels counted individually, then summed to increase accuracy of the counts. To mitigate bias, all photographs and calculations were performed by the same individual who was blind to the treatment of each sample.

For ingWAT and gWAT, histological sections were prepared as described above and representative micrographs (20x) taken to assess the anatomical changes associated with cold acclimation.

Adipose Tissue Fractionation

Adipose tissue was fractionated into the pelleted stromal vascular fraction (SVF) and the buoyant mature adipocyte fraction for gene expression analysis in each fraction. Non-fasted, male C57BL/6 mice (n = 6) were sacrificed and BAT, ingWAT and gWAT adipose tissue depots were dissected and trimmed on ice visually aided by an SZX7 Olympus dissecting microscope to remove contaminating material: muscle and white fat from the iBAT, lymph nodes from the ingWAT, and reproductive tissues from the gWAT. Adipose tissues from six mice were pooled by depot and minced into 1–2 mm pieces and digested in 10 mL Hank's Balanced Salt Solution with 2% Bovine Serum Albumin (Sigma Aldrich, St. Louis, MO, USA), 150 U/mL Type II Collagenase (Sigma Aldrich), and 5 mM CaCl2 at 37°C, at 200 rpm in a two-directional shaker for 1h. Tubes were inverted every 15min to ensure even distribution of the collagenase. Tissue slurries were strained (300μm) and fractionated by centrifugation at 350 rcf for 5 min at 4 °C. Buoyant cells were collected carefully from the floating layer, supernatant was discarded, and the pelleted SVF was collected. The mature fraction was washed twice with phosphate-buffered saline (PBS). The collected fractions were flash-frozen in liquid nitrogen and stored at −80 °C.

Primary Tissue Culture

To assess PACAP receptor expression in pre-adipocytes or mature adipocytes without contaminating vasculature, neural innervation or immune cells, adipocytes were grown in primary culture, and half the wells were collected at confluence while the other half were

differentiated to become mature adipocytes before being collected. Fourteen-week-old, male C57BL/6 mice (n = 24) were sacrificed and adipose tissues collected by dissection, digested and fractionated as above. Debris and undigested material were removed using a tissue strainer (100 μm) and red blood cells removed using Red Cell Lysis Buffer (Sigma Aldrich, St. Louis, MO, USA) according to the manufacturer's protocol. The cells were washed by centrifugation and resuspension in Dulbecco's Modified Eagle's Medium/Nutrient Mixture F-12 Ham (DMEM/F12) three times, with the mature layer being discarded following the first centrifugation, then the resuspended SVF containing pre-adipocytes was plated and cultured at 37 °C, 5% CO_2 in a 6-well plate until confluent. Growth media contained DMEM/F12, 0.01 M HEPES buffer, 10% fetal bovine serum (FBS), and 1% v/v antibiotic (penicillin/streptomycin) (Sigma Aldrich). One day post-confluence, half the wells for each tissue type were collected for RNA extraction (n = 3) and the other half (n = 3) were differentiated for 6 days in media containing 1.5 nM tetraiodothyronine, 4 nM insulin, and 126 μM/mL sodium L-ascorbate. Full differentiation was assessed in primary adipocytes by the presence of large lipid droplets in 70% of cells. For primary brown adipocyte cultures, maturation was confirmed post hoc by measuring induction of UCP1 mRNA expression.

RNA Extraction and cDNA Generation

All equipment and reagents were acquired from Thermo Fisher Scientific (Waltham, MA, USA) unless otherwise stated. Samples (n = 8 per treatment) of iBAT, ingWAT, and gWAT from the acclimated mice (thermoneutrality (30 °C) or cold (4 °C)) were homogenized completely using a PowerGen 125 power homogenizer according to tissue and treatment type. Cells were lysed, RNA extracted and purified using Trizol Reagent and subsequently ethanol

precipitated as per the manufacturer's protocol with the following modifications: the extra centrifugation step for high fat samples was utilized and RNA precipitation was conducted for 1h at −20 °C, then 10 min at −80 °C. RNA purity was assessed by spectrophotometry (NanoDrop 1000). Integrity of the RNA was assessed by the quality of 18S and 28S bands on a native 1.5% agarose gel stained with 0.5% ethidium bromide. DNA contamination was removed by treating extracted RNA with TURBO-DNase as per the manufacturer's protocol. RNA was reverse transcribed to cDNA using iScript Reverse Transcription Supermix for RT-qPCR (Bio-Rad; Hercules, CA, USA) containing a blend of oligo(dT) and random primers to prevent bias during cDNA synthesis. Additionally, no-template and no-RT negative controls were performed to test for contaminating genomic DNA. RNA extractions from primary cell culture and fat fractionation experiments were performed using RLT lysis buffer and RNeasy Mini and RNeasy Micro kits, respectively (QIAGEN, Hilden, Germany). Furthermore, RNA integrity from fat fractions was assessed using the Experion (Bio-Rad) automated electrophoresis system using RNA StdSens kits according to the manufacturer's instructions.

Real-time quantitative PCR (qPCR)

Melt curves were visually assessed and amplification efficiency was determined for all primers in Table 3.1 (Integrated DNA technologies (IDT), Coralville, CA, USA) to detect non-specific products and primer-dimer formation, respectively. Homogeneity of reference gene expression was indicated by an M-value lower than 0.5 for each primer pair (geNorm, qBase+ software, Biogazelle, Zwijnaarde, Belgium). Primers and PrimeTime (IDT) hydrolysis probes were designed using the NCBI online PrimerBLAST tool. SYBR Green chemistry (SYBR Green Supermix for iQ5, Bio-Rad) was used to measure mRNA expression of UCP1, β_3-AR, homeobox protein Hox-C9 (HOXC9), hormone-sensitive (HSL), PAC1R, VPAC1, and VIP.

Table 3.1. Primer and probe sequences used for real-time quantitative PCR. All primers developed using the National Center for Biotechnology (NCBI) online Primer Blast tool with the Accession numbers provided.

Target Genes	NCBI Accession #	Forward Primer (5'-3')	Reverse Primer (5'-3')	Annealing T (ºC)
HOXC9	NM_008272.3	GCAGCAAGCACAAAGAGGA	CGTCTGGTACTTGGTGTAGGG	58
HSL	NM_010719.5	GGAGCACTACAAACGCAACGA	TCGGCCACCGGTAAAGAG	55
PAC1R	NM_007407.4	TTGATGACTATGAGCCCGAGT	ACAAGATGACCATGGCAGTG	57
PACAP	NM_009625.3	ATCCAGCGGACAGGAGAGAT	TCCGAGTGGCGTTTGGTAAG	55
UCP1	NM_007407.4	CCTGGCAGATATCATCAC	TCACCTTGGATCTGAAGG	52
VIP	NM_011702.3	CAGGAACCGGGAACAGACT	TATCAGGAATGCCAGGAACT	57
VPAC1	NM_011703.4	AAGTCATTGTAGAGGCAGAT	AATATGTCAAGACGGAATCAG	59
VPAC2	NM_009511.2	AGAGCCATCTCTGTGCTGGTCAA	AGGTAGGCCAGGAAGCAC	57
β3-AR	NM_013462.3	CAACCCGGTCATCTACTG	ACCGTAGCTACACAGAAG	50
Hydrolysis Probes (5'-3')				
VPAC2	NM_009511.2	56FAM/CAGGTAGAG/ZEN/ACCCTCCACCAGAAGCCAGTAG/3IABkFQ		63
PACAP	NM_009625.3	56FAM/TCGCCCACG/ZEN/AAATCCTTAACGAAGCCTATCGAA/3IABkFQ		62
Reference Genes				
β-actin	NM_013462.3	GCTCTGGCTCCTAGCACCAT	GCCACCGATCCACACAGAGT	55
GAPDH	NM_001289726.1	TGCACCACCAACTGCTTAG	GGATGCAGGGATGATGTTC	55
RPL19	NM_009078.2	CCATGAGTATGCTCAGGCTACAG	CTGATCTGCTGACGGGAGTTG	57.5
TBP	NM_013684.3	CACCAATGACTCCTATGA	CCAAGATTCACGGTAGATA	53
18S	NR_003278.3	CGGCTACCACATCCAAGGAA	GCTGGAATTACCGCGGCT	55

Amplification conditions were as follows: 95 °C/180 s, 95 °C/10 s, and then (annealing T)/30 s (repeat 40 times) (annealing temperatures in Table 3.1). Melt curves were performed by 55 °C/10 s + 0.5 °C per repeat up to 95 °C to ensure that a single peak, corresponding to a single qPCR product, was obtained for each reaction. mRNA expression for each gene was analyzed using the comparative CT method. MIQE guidelines[206] were considered in the design and optimization of primers and probes, as well as the determination of relative expression for all of the above genes.

RNA sequencing

To determine which PAC1R splice variants were most prevalent in iBAT samples of thermoneutral and cold-acclimated mice, mRNA (1 μg) was sequenced at a depth of 25 million paired-end reads on a NextSeq 500 sequencing system (Illumina, San Diego, CA, USA) at the Biomedical Research Centre (UBC, Vancouver, BC, Canada). Samples (n = 3/treatment) were chosen based on RNA-Quality Index values obtained from Experion electrophoresis following TURBO DNase treatment. cDNA libraries were prepared using the TruSeq Stranded mRNA Library Prep Kit and analysis of the resulting paired-end sequence data was performed in the BaseSpace Sequence Hub (Illumina) as follows. TopHat[207] was utilized for alignment to the Mus musculus UCSC mm10 reference genome. Indexing and variant calls were determined using Strelka Variant caller[208]. Fragments per kilobase million (FKPM) calculation and differential expression, including statistical analysis, was performed using Cufflinks[207].

Significance level was determined by use of q-value (Cufflinks), which is a p-value that is adjusted for false-discovery rate.

Lipolysis Assay in Primary Adipocytes

Rates of lipolysis were determined by measuring free fatty acids (n = 4) and free glycerol (n = 2) in tissue culture media following acute stimulation of β_3-AR and/or PACAP receptors in differentiated primary cultures of murine adipocytes. All reagents were obtained from Thermo Fisher Scientific (Waltham, MA, USA) and used in accordance with the manufacturer's instructions unless otherwise stated. Preadipocytes isolated from iBAT and ingWAT, cultured to 90% confluence, and differentiated into mature adipocytes as stated in the above primary culture methods. On day 5 post-confluence, cells were gently washed three times with 37 °C PBS to remove differentiation media containing newborn calf serum (serum Cat. No. N4637), which may contain hormones that stimulate lipolysis. Following washing, 37 °C DMEM/F12 (Cat. No. 12634028) was added to each well and plates were incubated for 4 h without media supplementation to establish a baseline state were lipolytic pathways are not extrinsically activated in cultured adipocytes.

During the stimulatory phase of the assay, a Krebs-Ringer-HEPES assay buffer (120 mM NaCl, 5 mM KCl, 1.2 mM MgSO, 10 mM NaHCO, 1.3 mM CaCl, 1.2 mM KHPO, 20 mM HEPES) was prepared with 0.5 mM glucose, 4% bovine serum albumin (BSA) at pH 7.4 and supplemented with the β_3-AR agonist CL316,243, which is a potent stimulant of lipolysis[209,210] and/or mixtures of PACAP receptor agonists. All agonists and their concentrations can be found in Table 3.2. Maxadilan is a potent and specific agonist of PAC1R[95], PACAP is an agonist for all three PACAP receptors (PAC1R, VPAC1 and VPAC2), and M65 is a potent, specific antagonist of the PAC1R receptor[96]. M65 was used in combination with PACAP to prevent stimulation of PAC1R while allowing stimulation of VPAC1 and VPAC2, for which specific agonists are not currently available.

Table 3.2. Treatment scheme for free fatty acid and glycerol quantification assay. Final concentrations of agonists and antagonists in the media are shown. Agonism strength is denoted by (+), antagonism strength by (-), as described in the literature. Reagents obtained from Thermo Fisher Scientific (Waltham, MA, USA). Phosphate buffered saline (PBS) was used as the diluent for all reagents.

Media supplements		Receptor agonism (+) or antagonism (-)			
Reagent	Concentration (μM)	β_3-AR	PAC1R	VPAC1	VPAC2
PBS	1X				
CL316,243	1	+ + +			
Maxadilan	0.5		+ + +		
PACAP	0.1		+ +	+	+
M65	1.5		- - -		

Cells were incubated with supplemented media described above at 37 °C for 2 h and then immediately placed on ice to stop metabolic processes while assay media (300 μL) were collected and flash-frozen in liquid nitrogen. Media aliquots were later thawed on ice and diluted in Assay Buffer (1:5). Free fatty acid content in the media were quantified using a free fatty acid kit (Abcam, Burlingame, CA, USA) as per the manufacturer's protocol. Fluorometric readings (excitation/emission = 535/587 nm) were measured using a Varioscan LUX Multimode Microplate Reader (Thermo).

Cellular Oxygen consumption

To assess potential cooperativity of PACAP and adrenergic receptors in activating thermogenesis, in-well oxygen consumption of mature primary adipocyte cultures was measured using a Seahorse Analyzer (Agilent, Santa Clara, CA, USA) after acute stimulation of the β_3-AR and PAC1R. Male C57BL/6 mice (n = 20) were housed at the animal unit in the Pharmaceutical Sciences Building at UBC, Vancouver, until 14 weeks of age (Charles River, Sherbrooke, QC, Canada). Mice were euthanized using CO_2, followed by cervical dislocation. ingWAT and iBAT depots were collected by dissection and preadipocytes were isolated and grown in primary culture as described previously, except with the following modifications: erythrocytes were not lysed prior to plating, and Collagenase Type I (StemCell Technologies, catalog # 07416) was substituted because Type II collagenase from Sigma was no longer available. Care and treatment of mice were in accordance with the guidelines of the Canadian Council on Animal Care, and protocols for the study were approved by the University of British Columbia's Animal Care Committee.

Following adipose tissue digestion and centrifugation, SVFs were pooled by tissue type (hereafter called iBAT and ingWAT) and then plated into 50 wells of a 96-well plate. Cell density was assessed visually three days post-plating, each well was photographed prior to the induction of differentiation to record plating density, and final percent maturity visually assessed immediately prior to the oxygen consumption assay. Two wells of iBAT adipocyte cultures and four wells of the ingWAT adipocyte cultures had significantly fewer mature cells than the other wells at the time of the assay and were therefore excluded from the analysis.

The purposes of each treatment group were described below. Saline was a vehicle control to show unmodified response to stimulation of oxygen consumption by carbonyl cyanide-4 (trifluoromethoxy) phenylhydrazone (FCCP). CL316,243, a β_3-AR agonist, was a positive control for adrenergic-stimulated oxygen consumption because it is known to stimulate lipolysis and mitochondrial activity [174] in adipocytes. Maxadilan, a PAC1R agonist, was used to assess stimulation of PAC1R only. PACAP was used as a non-specific agonist to stimulate PAC1R, VPAC1, and VPAC2. PACAP was used in combination with M65 to selectively stimulate VPAC1 and VPAC2 while preventing stimulation of PAC1R.

To measure oxygen consumption of mitochondrial origin the Seahorse XF Mito Stress Kit assay (Agilent Technologies, Santa Clara, CA USA) was performed according to manufacturer's instructions (Figure 3.1) with some modifications (see Table 3.2) following stimulation of cells with the agonists listed above.

The main modification of the assay was the addition of an extra injection step to accommodate the addition of β_3-AR and/or PACAP receptor agonists prior to the addition of FCCP. Therefore, the assay protocol (total 1 h, 48 min) for both differentiated brown adipocytes and differentiated white adipocytes consisted of five phases in the following order: Baseline

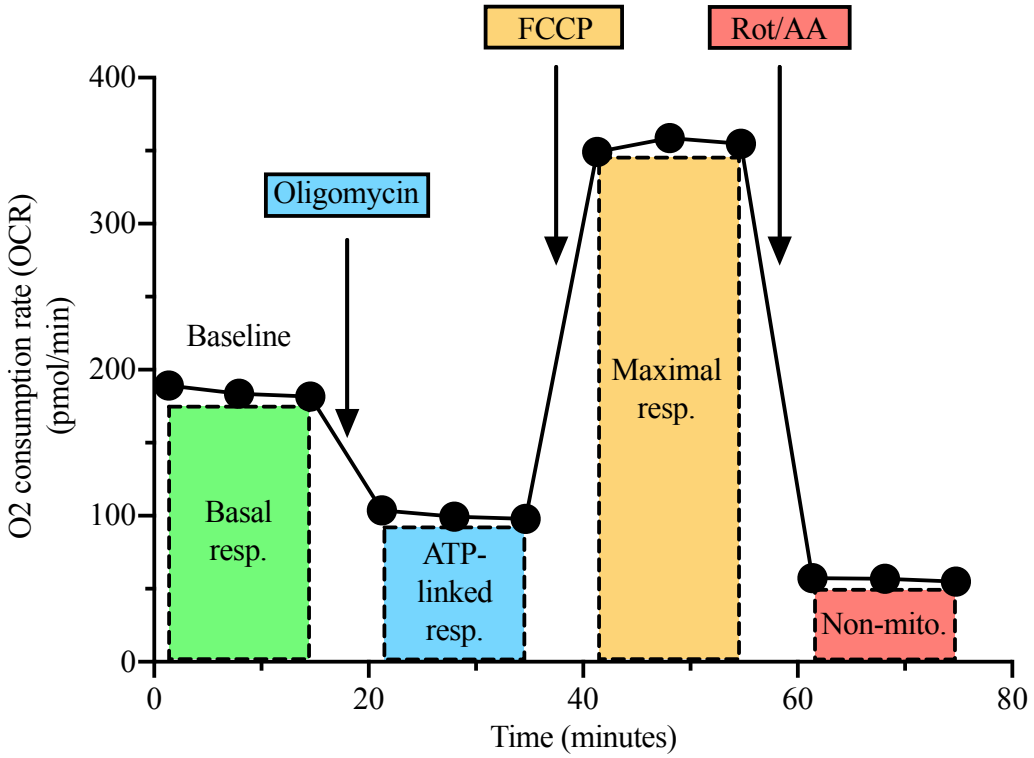

Figure 3.1. Manufacturer protocol for the Agilent Seahorse Mitochondrial Stress Test kit to show expected effects of kit reagents on oxygen consumption in cultured adipocytes. Image created from data in this Chapter.

(equilibration- no injection), Phase 2- Oligomycin (2 μM), Phase 3- Experimental Agent(s) (Table 3.2) Phase 4- FCCP (μM) and Phase 5- Rotenone/Antimycin A (1 μM). The effect of four of these Phases on oxygen consumption can be seen in Figure 3.1. Each 18-min phase, excluding the 24-min Baseline, consisted of an injection of agonists followed by three cycles of the following: 3 min of automated mixing (to ensure even distribution of the experimental agent), 3 min measurement of in-well dissolved oxygen and pH. In the Baseline phase, no injection was performed and there were four cycles. This allows the cells to equilibrate to the assay conditions and facilitates the establishment of baseline metabolism for comparison against the subsequent treatments.

3.3 RESULTS

Animal and organ morphology

At the start of the acclimation period, (a) overall body mass, (b) lean mass, and (c) fat mass were not significantly different between treatment groups (Figure 3.2). Following housing for 3.5 weeks at 4 °C (cold-acclimated) or 30 °C (thermoneutral), overall body mass and fat mass, but not lean mass, were significantly lower in the cold-acclimated group. The masses of the white adipose depots (ingWAT and gWAT) were significantly lower in the cold-acclimated mice compared to the thermoneutral mice. iBAT mass did not differ significantly between treatments (Figure 3.2d).

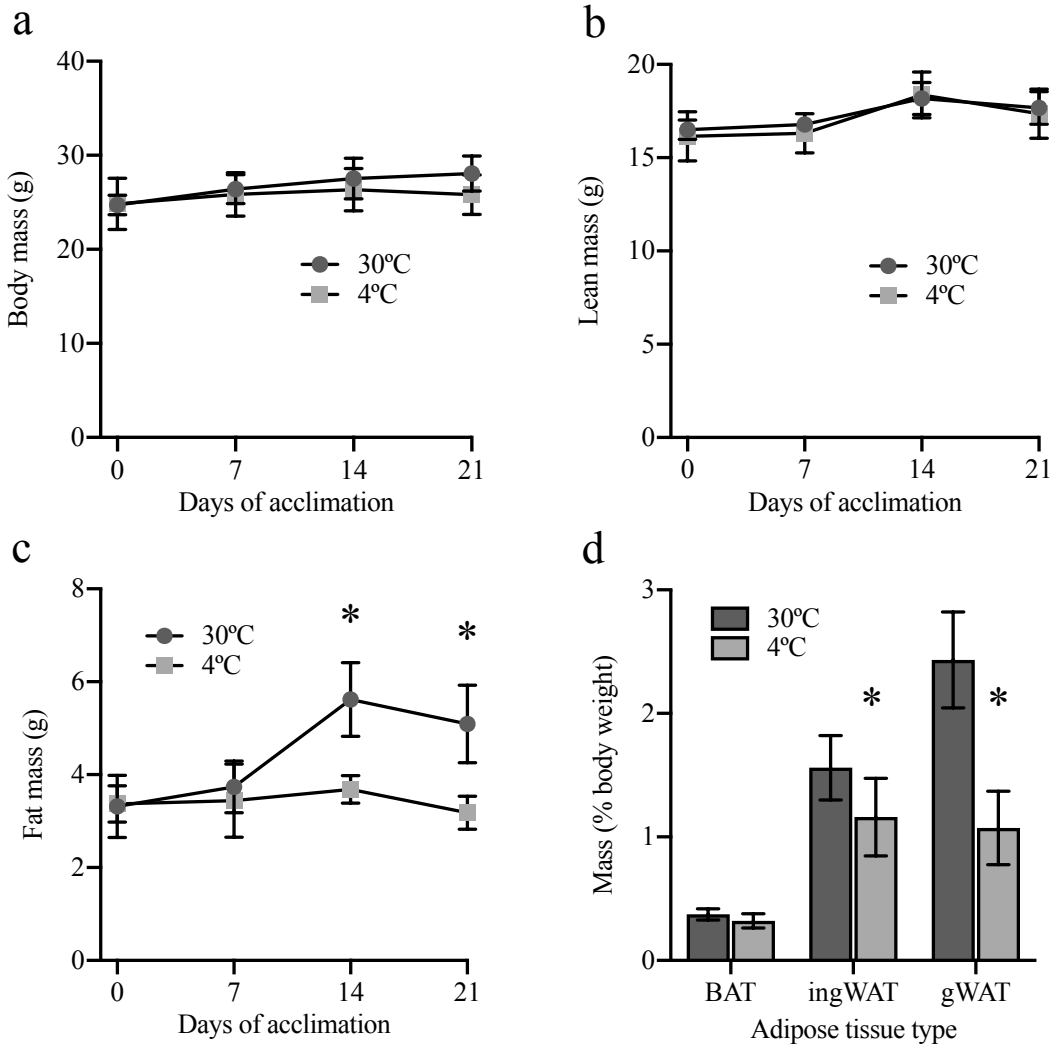

Figure 3.2. Whole body mass, composition, and post-mortem adipose tissue mass measured over 3.5 weeks of cold acclimation (housing at 4 °C) in male C57BL/6 mice compared to thermoneutral-housed (30 °C) control mice. Body mass (a), lean mass (b), and total fat mass (c) were measured by non-invasive time-domain nuclear magnetic resonance (Bruker minispec LF50) (n = 8 for days 0 and 21, n = 4 for days 7 and 14). Sample size differs due to technical problems. Adipose depot mass (d) of interscapular brown adipose tissue (BAT) subcutaneous inguinal while adipose tissue (ingWAT), and visceral gonadal adipose tissue (gWAT) determined by dissection measured post-mortem at 3.5 weeks (n = 8). Data are expressed as mean ± SD and asterisks denote a significant temperature effect at $\alpha = 0.05$ (30 °C vs. 4 °C).

Histological analysis

Hematoxylin and eosin stained sections of iBAT from cold-acclimated mice appeared visually darker and with a higher degree of adipocyte multilocularity than iBAT sections from thermoneutral controls (Figure 3.3a,b). Darker-staining cells with multilocular lipid droplets, indicative of thermogenic adipocytes, appeared in sections of cold-acclimated ingWAT (Figure 3.4a,b) but not cold-acclimated gWAT (Figure 3.5a,b). In contrast, multilocular cells (thermogenic adipocytes) were not detected in ingWAT nor gWAT sections of mice kept at 30 °C for 3.5 weeks. Analysis of iBAT sections showed decreased mean lipid area (Figure 3.3c) and increased cell number (Figure 3.3d) in sections from cold-acclimated mice.

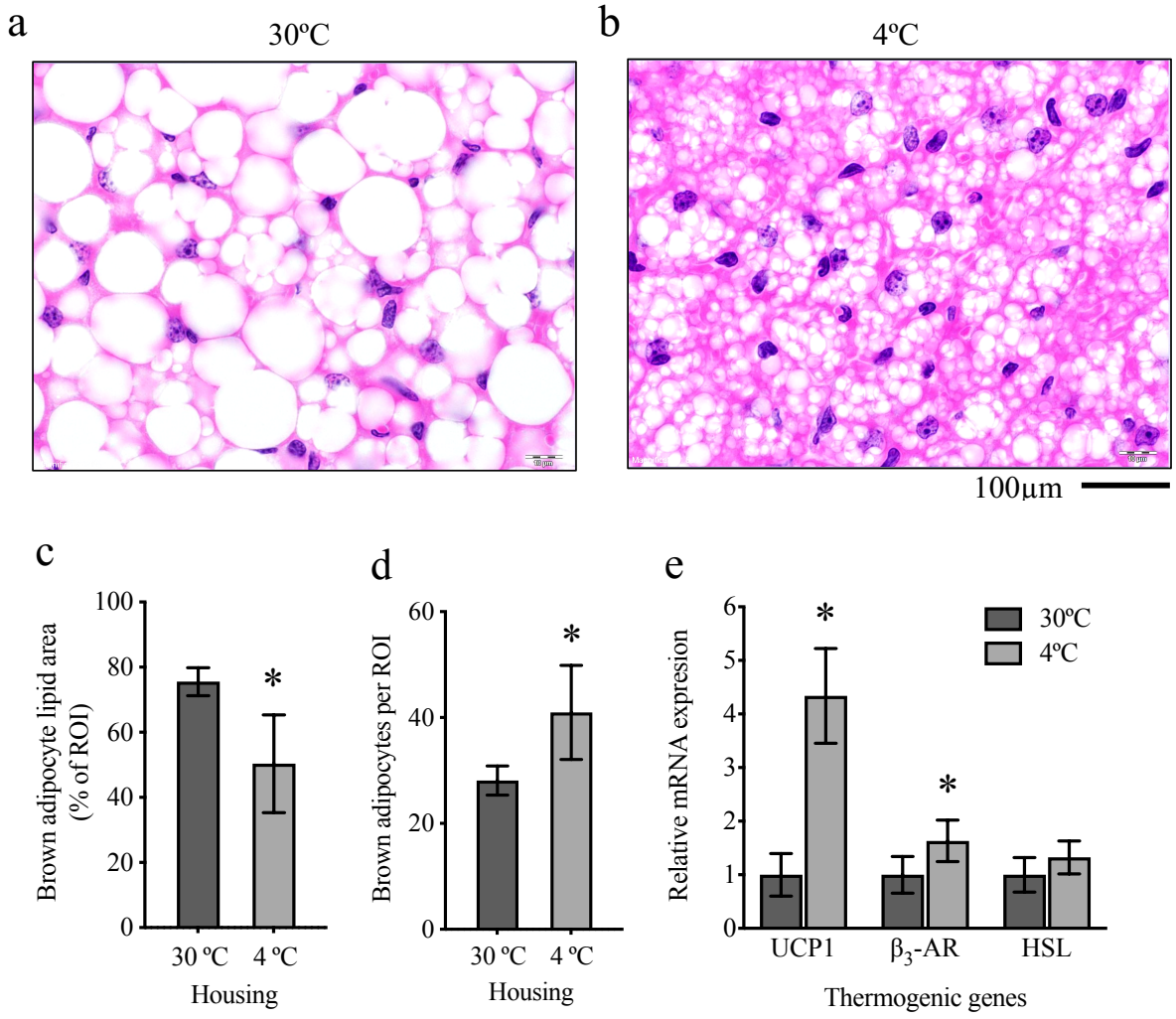

Figure 3.3. Cold acclimation of interscapular brown adipose tissue (iBAT) after 3.5 weeks of cold exposure (4 °C housing) in male C57BL/6 mice compared to thermoneutral-housed (30 °C) control mice. Representative bright field images (a and b) of Hematoxylin- and Eosin-stained sections of dissected iBAT taken at 600x magnification. Histological analysis of iBAT from cold-acclimated mice showing lipid area (c) as a percentage of the total region of interest (ROI) area and the number of brown adipocytes (d) per ROI (n = 4) as determined by nuclei count. Micrograph acquisition, and image processing for lipid area quantification were performed using Olympus CellSens software, while nuclei counts were performed manually from visual analysis of the images. Relative mRNA expression (e) of genes related to iBAT thermogenesis: uncoupling protein 1 (UCP1), β_3 adrenergic receptor (β_3-AR), and hormone-sensitive lipase (HSL) (n = 8/group). Expression was normalized to the endogenous controls TATA binding protein (TBP) and ribosomal protein (RP)-L19. Data are expressed as mean ± SD and asterisks denote a significant temperature effect at $\alpha = 0.05$ (30 °C vs. 4 °C).

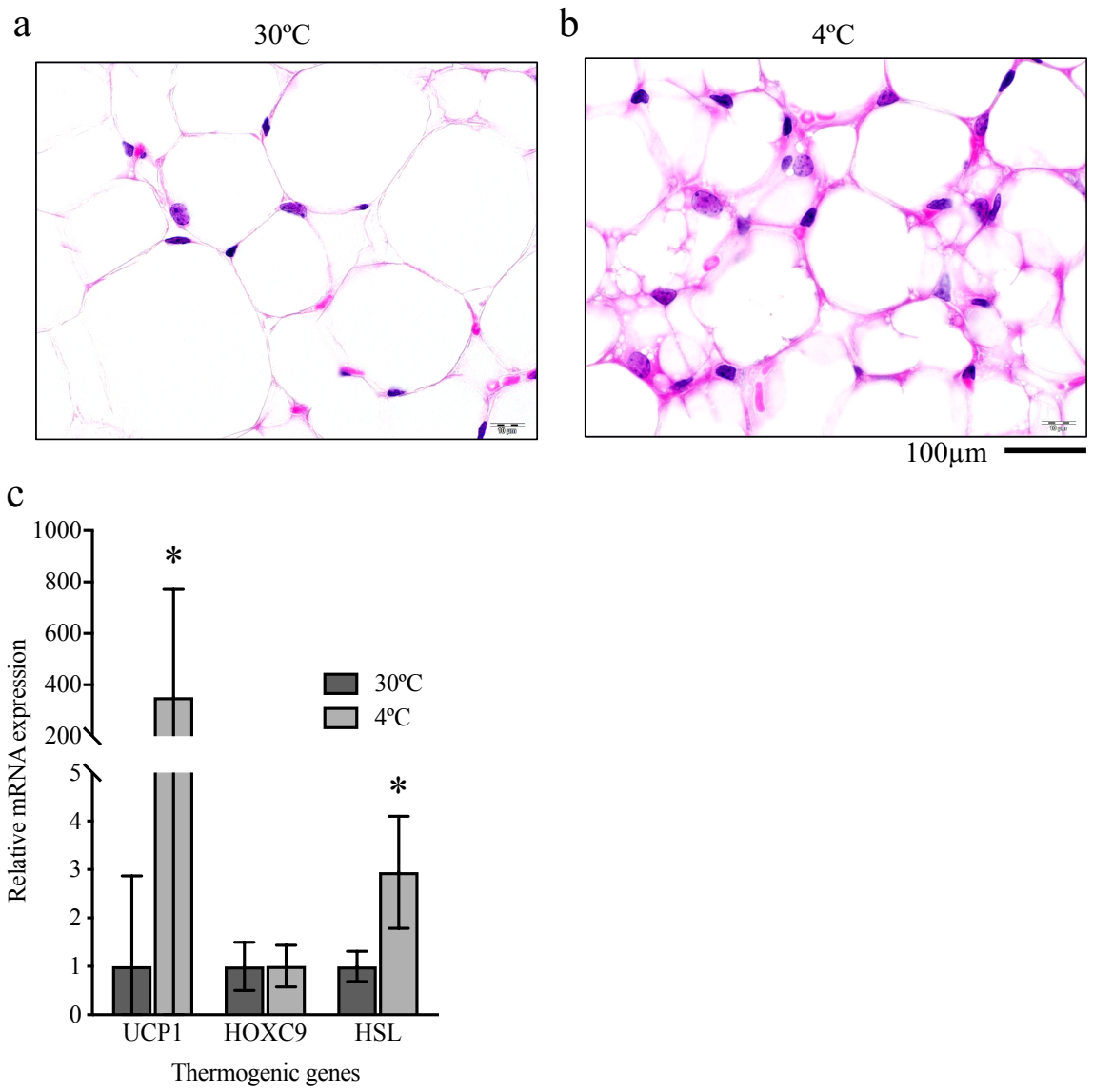

Figure 3.4. Cold acclimation of inguinal white adipose tissue (ingWAT) after 3.5 weeks of cold exposure (4 °C housing) in male C57BL/6 mice compared to thermoneutral-housed (3 0°C) control mice. Representative bright field images (a and b) of Hematoxylin- and Eosin-stained sections of dissected ingWAT taken at 600x magnification. Relative mRNA expression (c) of genes related to thermogenesis in ingWAT: uncoupling protein 1 (UCP1), homeobox protein (HOX)-C9, and hormone-sensitive lipase HSL (n = 8/group). Expression was normalized to endogenous controls: ribosomal 18S rRNA, beta-actin, and glyceraldehyde-3 phosphate dehydrogenase. All data are expressed as mean ± SD unless not detected (n.d.) and asterisks denote a significant temperature effect at $\alpha = 0.05$ (30 °C vs. 4 °C).

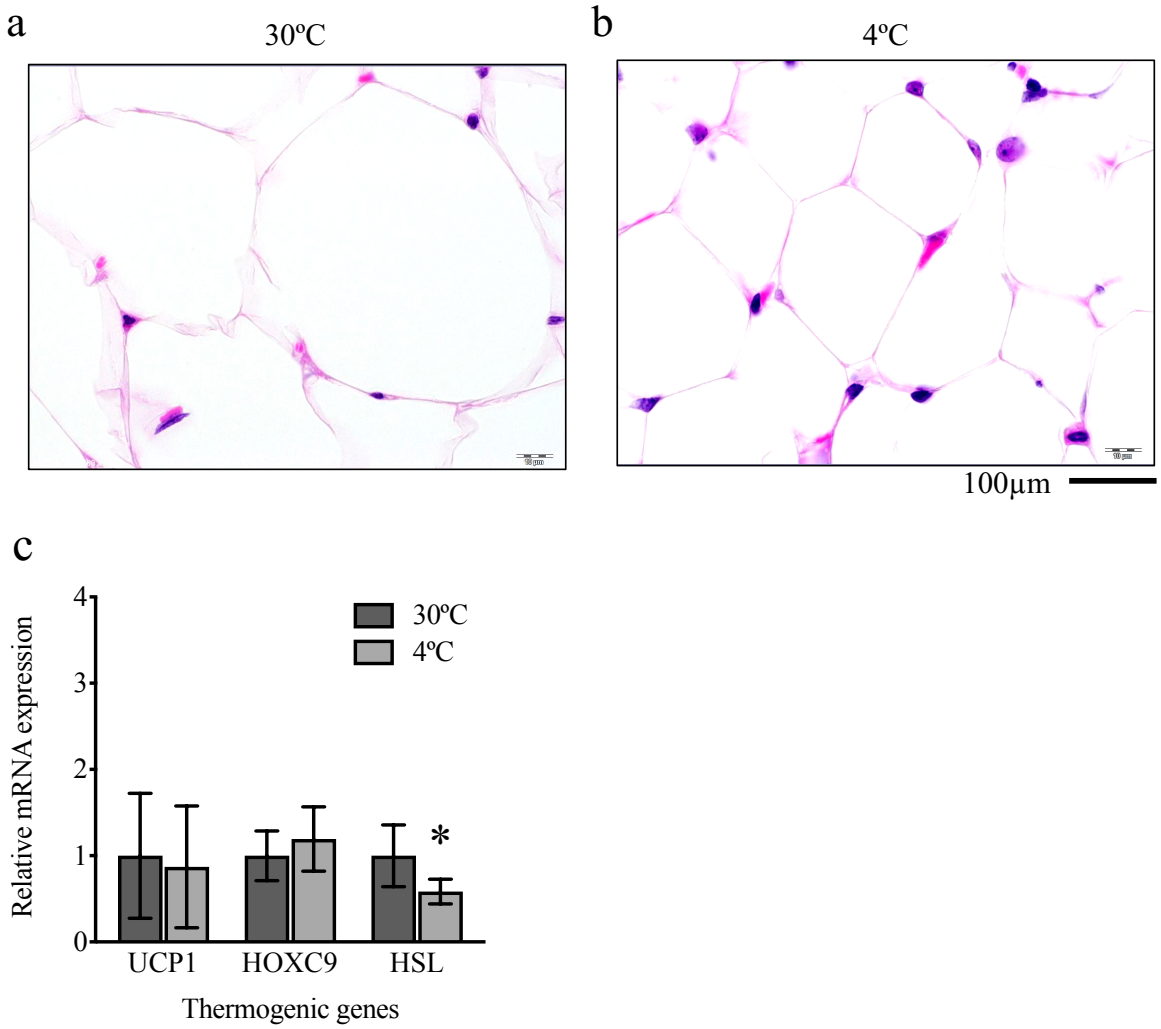

Figure 3.5. Cold acclimation of gonadal white adipose tissue (gWAT) after 3.5 weeks of cold acclimation (4 °C housing) in male C57BL/6 mice compared to thermoneutral-housed (30 °C) control mice. Representative bright field images (a and b) of Hematoxylin- and Eosin-stained sections of dissected gWAT were taken at 600x magnification. Relative mRNA expression (c) of genes related to thermogenesis: uncoupling protein 1 (UCP1), homeobox protein (HOX)-C9, and hormone-sensitive lipase (HSL) (n = 8/group). For UCP1, n = 6 in the cold treatment group as two mice with extremely high relative fold mRNA expression (24 and 1450) were excluded. Expression was normalized to the endogenous controls (ribosomal 18S rRNA, beta-actin and glyceraldehyde-3 phosphate dehydrogenase. All data are expressed as mean ± SD unless not detected (n.d.) and asterisks denote a significant temperature effect at $\alpha = 0.05$ (30 °C vs. 4 °C).

mRNA-Seq and real-time PCR analysis

Expression of β_3-AR and UCP1 mRNA were significantly higher in iBAT of cold-acclimated mice compared to iBAT from thermoneutral control mice (Figure 3.3e). VIP, PAC1R, VPAC1, and VPAC2 mRNA were detected in iBAT tissue by qPCR (Figure 3.6a). Expression of VIP appeared to be higher in the cold-acclimated group, though not significantly so. PAC1R mRNA expression was significantly lower in the cold-acclimated group compared to the thermoneutral condition. As measured independently with RNA-Seq, the cold-acclimated group had significantly higher expression of β_3-AR, UCP1, and hormone-sensitive lipase (HSL) in iBAT than thermoneutral control iBAT samples (Table 3.3). PAC1R mRNA expression was detected and confirmed to be lower in the cold-acclimated group. VPAC1, VPAC2, VIP, and PACAP mRNA expression was not detected in iBAT of either treatment, contrary to real-time qPCR results.

Review of qPCR melt curves revealed PAC1R and VPAC1 expression in both the SVF and mature adipocyte fractions isolated from iBAT samples from both the thermoneutral and col-acclimated mice. Because pooled samples were used for this experiment, standard error could not be reported, and consequently, we cannot make conclusions about the relative expression of receptor mRNA between the SVF and mature fractions.

In primary iBAT-derived adipocytes, PAC1R and VPAC1 were expressed in preadipocytes (Figure 3.6b) before differentiation was induced (i.e., with no visible lipid droplets), as well as after differentiation (i.e., 70% mature cells with lipid droplets). VPAC1 expression was significantly increased in mature adipocytes compared preadipocytes.

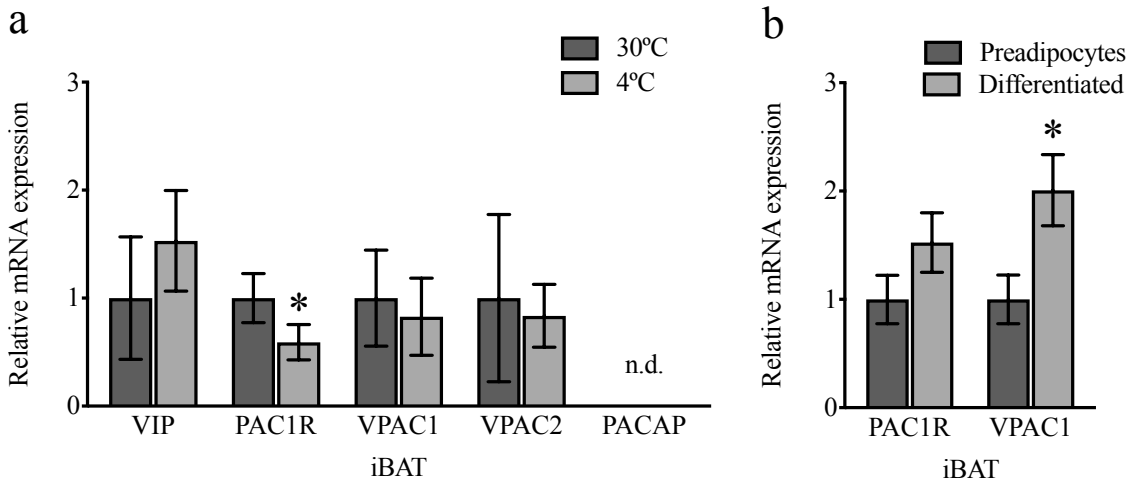

Figure 3.6. Expression of genes related to pituitary adenylate cyclase-activating polypeptide (PACAP) signaling in cold-acclimated interscapular brown adipose tissue (iBAT) (a) and cultured primary brown adipocytes (b), including vasoactive intestinal peptide (VIP), PACAP receptor 1 (PAC1R), and VIP/PACAP receptor 1 and 2 (VPAC1/2). iBAT (a) was dissected from male C57BL/6 mice acclimated to cold (4 °C) for 3.5 weeks (n = 8/group) to mice housed at thermoneutrality (30 °C). Primary brown adipocytes (b) were collected from iBAT of non-acclimated (24 °C) mice and adipocytes were pooled from 4 mice for each well (n = 3/group). Expression was normalized to the endogenous controls TATA binding protein, and ribosomal protein L-19. All data are expressed as mean ± SD unless not detected (n.d.) and asterisks denote a significant temperature effect at $\alpha = 0.05$ (30 °C vs. 4 °C) for iBAT (a), and significant differentiation effect for primary cultures (b)

Table 3.3. Interscapular brown adipose tissue mRNA sequenced to a 24 million read depth. Log fold change in fragments per kilobase million (FKPM) from expression in thermoneutral controls (TN, 30 °C n = 3) compared to cold-acclimated animals (C, 4 °C, n = 3). Positive values in green denote higher FKPM in the cold-acclimated group, red shows the inverse. Rows 1-7 were chosen as indicators of adaptive thermogenesis and/or lipolysis, while expression of experimental genes in rows 8-12 represent PACAP, VIP and the three PACAP receptors.

Gene	Locus	q Value	Significance	Log fold change (C:TN)
β3-AR	chr8:27225775-27229588	4.00E-04	***	0.93
UCP1	chr8:83290347-83298456	4.00E-04	***	2
HSL	chr7:25376818-25566417	2.26E-02	*	0.57
DIO2	chr12:90724551-90738438	4.00E-04	***	1.49
PGC-1α	chr5:51454248-51553921	7.40E-04	***	0.66
PGC-1β	chr18:61298135-61400431	6.82E-01	n.s.	0.11
COX	chr11:90638183-90687601	4.00E-04	***	1.02
PAC1R	chr6:55451977-55501455	4.00E-04	***	-1.78
PACAP	chr17:93199017-93206537	n.d.	n/a	n/a
VPAC1	chr9:121642716-121672954	n.d.	n/a	n/a
VPAC2	chr12:116077726-116159604	n.d.	n/a	n/a
VIP	chr10:5639139-5647617	n.d.	n/a	n/a

ingWAT from the cold-acclimated group had significantly higher mRNA expression of UCP1 and hormone-sensitive lipase (gene name LIPE) compared to the thermoneutral ingWAT (Figure 3.5). Two PACAP receptors, PAC1R and VPAC1, were expressed in this depot, with PAC1R expression significantly increased in response to cold exposure (Figure 3.7a). In contrast, VPAC2 and PACAP mRNA were detected in only a few ingWAT samples and in all samples exceeded or approached the limit of detection (≥35 CT). Therefore, it was not possible to assess the expression levels between groups with any degree of confidence and these genes were considered to be undetectable (n.d.) with our reaction conditions. PAC1R and VPAC1 were expressed in preadipocytes isolated from ingWAT and in differentiated cultures (Figure 3.7b), but the expression level did not differ pre- and post-differentiation.

UCP1 mRNA was not induced in gWAT isolated from cold-acclimated mice (Figure 3.5c) and was the only adipose tissue with a significant decrease in the expression of HSL in the cold-acclimated group. In gWAT from the cold-acclimated group compared to thermoneutral gWAT, PAC1R, VIP, and VPAC1 mRNA were expressed and PAC1R mRNA expression was significantly decreased (Figure 3.8a). Similar to ingWAT, VPAC2 and PACAP mRNA were not detected in all samples and when detected, were approaching the limit of detection (≥35 CT). PAC1R and VPAC1 were expressed in primary preadipocytes and differentiated adipocytes (Figure 3.8b) and PAC1R expression was significantly higher in differentiated cultures (≥70% cells containing large lipid droplets).

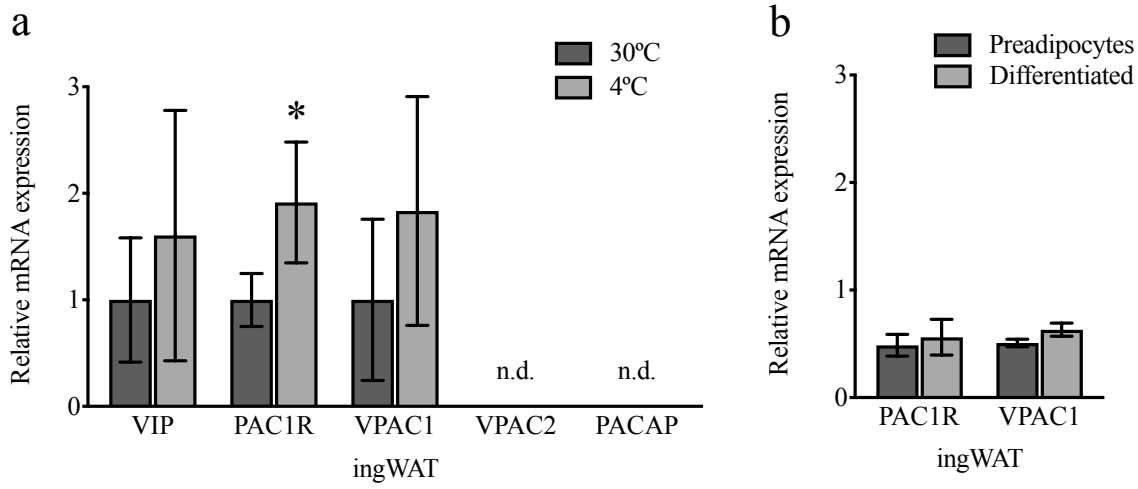

Figure 3.7. Expression of genes related to pituitary adenylate cyclase-activating polypeptide (PACAP) signaling in cold-acclimated inguinal white adipose tissue (ingWAT) (a) and cultured primary white adipocytes (b) from ingWAT, including vasoactive intestinal peptide (VIP), PACAP receptor 1 (PAC1R), and VIP/PACAP receptor 1 and 2 (VPAC1/2). ingWAT (a) was dissected from male C57BL/6 mice acclimated to cold (4 °C) for 3.5 weeks (n = 8/group) to mice housed at thermoneutrality (30 °C). VPAC2 was detected (at levels nearing the limit of detection (Ct > 35)) only in some ingWAT samples from both treatment groups and was therefore considered to be not detected. Primary white adipocytes (b) were collected from ingWAT of non-acclimated (24 °C) mice and adipocytes were pooled from 4 mice for each well (n = 3/group). Expression was normalized to endogenous controls: ribosomal 18S rRNA, beta-actin, and glyceraldehyde-3 phosphate dehydrogenase. All data are expressed as mean ± SD unless not detected (n.d.) and asterisks denote a significant temperature effect at $\alpha = 0.05$ (30 °C vs. 4 °C) for acclimated ingWAT (a), and significant differentiation effect for primary cultures (b).

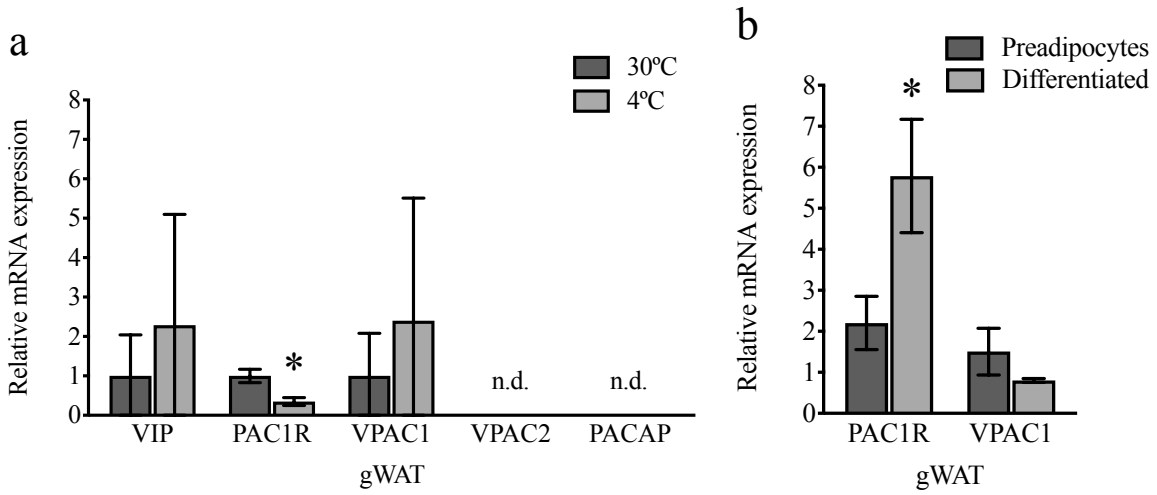

Figure 3.8. Expression of genes related to pituitary adenylate cyclase-activating polypeptide (PACAP) signaling in cold-acclimated gonadal white adipose tissue (gWAT) (a) and cultured primary white adipocytes (b) from ingWAT, including vasoactive intestinal peptide (VIP), PACAP receptor 1 (PAC1R), and VIP/PACAP receptor 1 and 2 (VPAC1/2). gWAT (a) was dissected from male C57BL/6 mice acclimated to cold (4 °C) for 3.5 weeks (n = 8/group) to mice housed at thermoneutrality (30 °C). VPAC2 was detected (at levels nearing the limit of detection (Ct > 35)) only in some ingWAT samples from both treatment groups and was therefore considered to be not detected. Primary white adipocytes (b) were collected from gWAT of non-acclimated (24 °C) mice and adipocytes were pooled from 4 mice for each well (n = 3/group). Expression was normalized to endogenous controls: ribosomal 18S rRNA, beta-actin, and glyceraldehyde-3 phosphate dehydrogenase. All data are expressed as mean ± SD unless not detected (n.d.) and asterisks denote a significant temperature effect at α = 0.05 (30 °C vs. 4 °C) for acclimated gWAT (a), and significant differentiation effect for primary cultures (b).

Lipolysis

Acute treatment of differentiated brown adipocytes with Maxadilan, a PAC1R-specific agonist or with PACAP, which stimulates all three PACAP receptors, did not alter FFA or glycerol release compared to saline treated control adipocytes (Figure 3.9).

Selective stimulation of the VPAC1 and VPAC2 receptors with PACAP while blocking stimulation of PAC1R with M65 did not increase either measure of lipolysis but did increase the variance of measurements of glycerol and free fatty acid in the media of brown primary adipocyte cultures (Figure 3.9). In differentiated preadipocytes of either iBAT or ingWAT, FFA release and glycerol release were significantly increased in the presence of the β_3-AR specific agonist, CL316,243 (Figure 3.10), but addition of PACAP receptor agonists with CL316,243 did not enhance the levels of lipolysis seen in response to CL316,243 alone.

Acute treatment of white adipocytes with Maxadilan did not alter FFA or glycerol release compared to controls (Figure 3.11). FFA release and glycerol release were significantly increased in the presence of the β_3-AR specific agonist, CL316,243, but this effect was not enhanced by PACAP receptor agonism in differentiated preadipocytes of ingWAT (Figure 3.12).

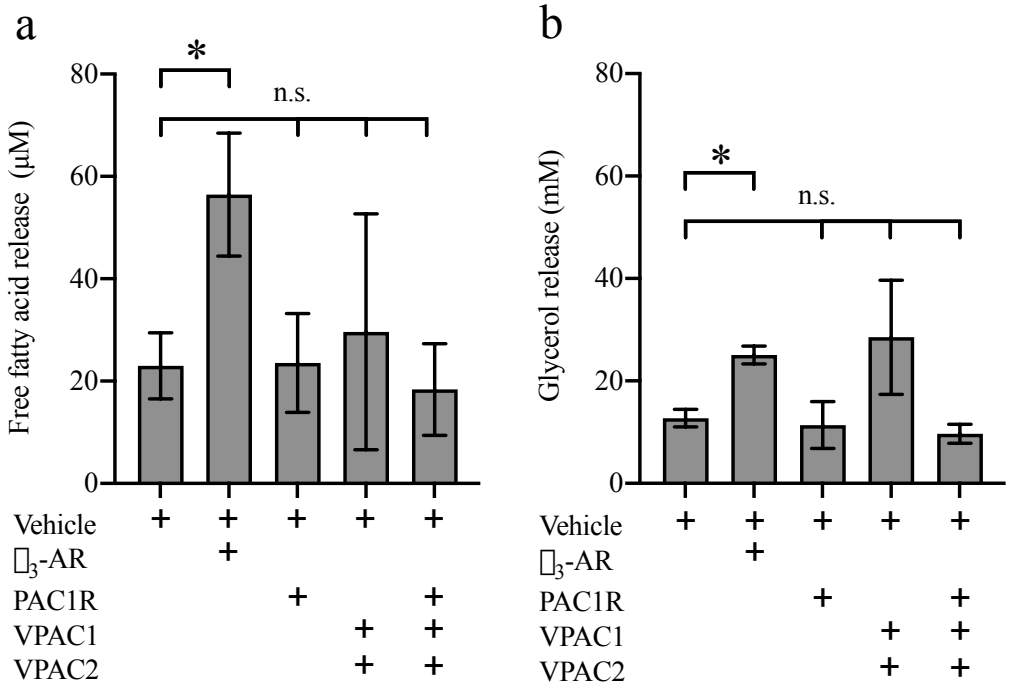

Figure 3.9. Lipolysis in primary brown adipocyte cultures following 2-hour stimulation of pituitary adenylate cyclase-activating polypeptide (PACAP) receptors. Free fatty acid (a) and glycerol (b) release were measured in media of differentiated primary cultures from interscapular brown adipose tissue of male C57BL/6 mice (n = 2 wells/treatment). Patterns of receptor agonism (+) were achieved using CL316,243 to stimulate β_3 adrenergic receptor (β_3-AR) as a positive control, pituitary adenylate cyclase-activating polypeptide (PACAP) for non-specific simultaneous stimulation of VPAC1, VPAC2, and PAC1R, Maxadilan for PAC1R-specific activation, and M65 (PAC1R-specific antagonist) plus PACAP to stimulate only VPAC1 and 2 but not PAC1R. Data are expressed as mean ± SD and asterisks denote a significant effect of treatment at $\alpha = 0.05$ (stimulated vs. saline vehicle control).

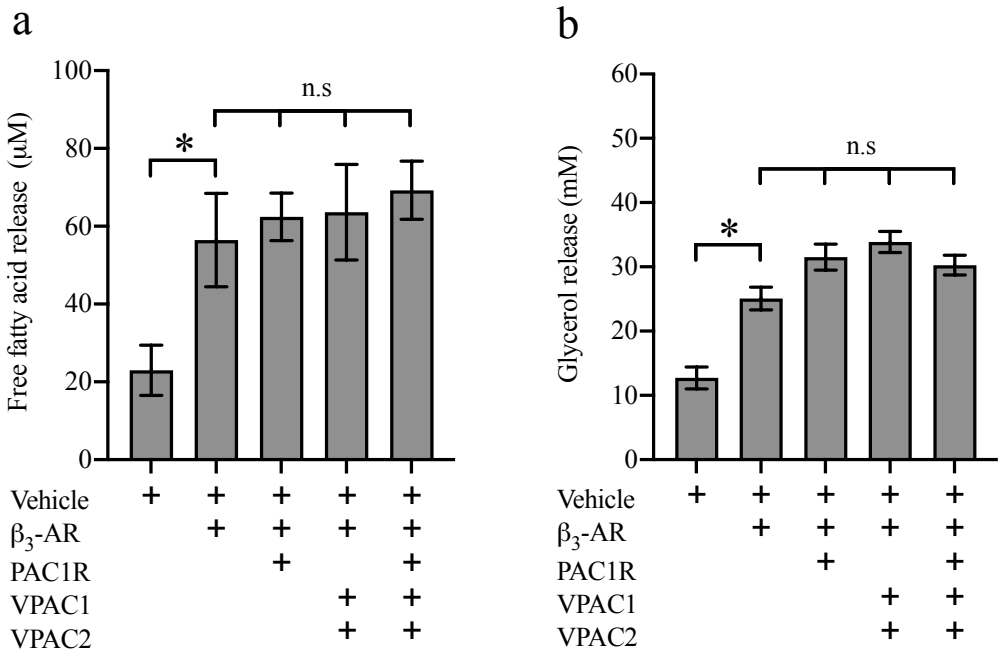

Figure 3.10. Lipolysis in primary brown adipocyte cultures following 2-hour stimulation of pituitary adenylate cyclase-activating polypeptide (PACAP) receptors in combination with β_3 adrenergic receptor (β_3-AR). Free fatty acid (a) and glycerol (b) release were measured in media of differentiated primary cultures from interscapular brown adipose tissue of male C57BL/6 mice (n = 2 wells/treatment). Patterns of receptor agonism (+) were achieved using CL316,243 to stimulate β_3 adrenergic receptor (β_3-AR), pituitary adenylate cyclase-activating polypeptide (PACAP) for non-specific simultaneous stimulation of VPAC1, VPAC2, and PAC1R, Maxadilan for PAC1R-specific activation, and M65 (PAC1R-specific antagonist) plus PACAP to stimulate VPAC1 and 2 but not PAC1R. Data are expressed as mean ± SD and asterisks denote a significant effect of treatment at $\alpha = 0.05$ (stimulated vs. saline vehicle control).

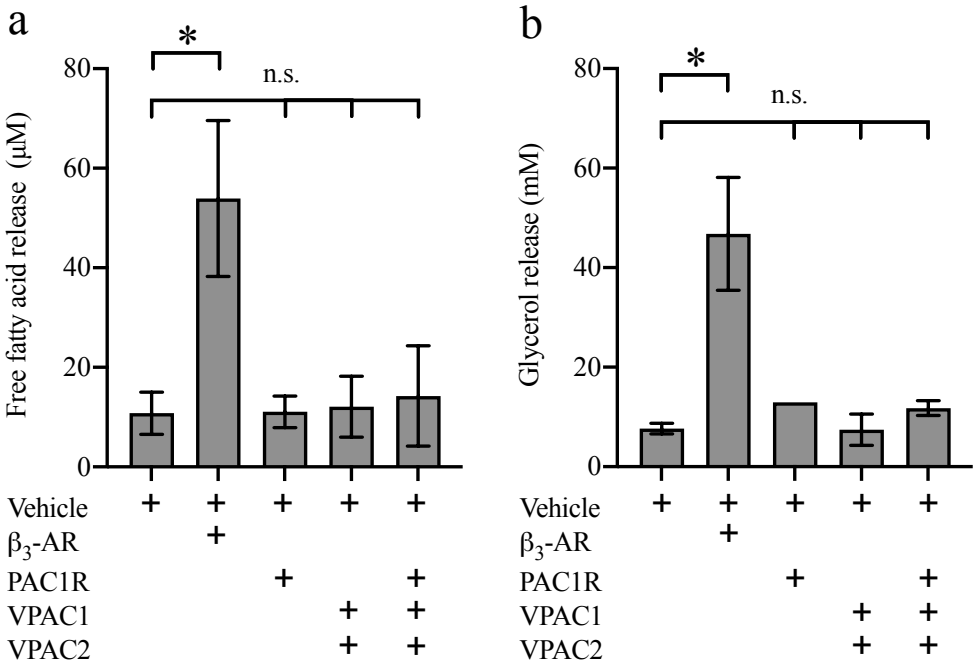

Figure 3.11. Lipolysis in primary white adipocyte cultures following 2-hour stimulation of pituitary adenylate cyclase-activating polypeptide (PACAP) receptors. Free fatty acid (a) and glycerol (b) release were measured in media of differentiated primary cultures from inguinal white adipose tissue of male C57BL/6 mice (n = 2 wells/treatment). Patterns of receptor agonism (+) were achieved using CL316,243 to stimulate β_3 adrenergic receptor (β_3-AR) as a positive control, pituitary adenylate cyclase-activating polypeptide (PACAP) for non-specific simultaneous stimulation of VPAC1, VPAC2, and PAC1R, Maxadilan for PAC1R-specific activation, and M65 (PAC1R-specific antagonist) plus PACAP to stimulate only VPAC1 and 2 but not PAC1R. Data are expressed as mean ± SD and asterisks denote a significant effect of treatment at $\alpha = 0.05$ (stimulated vs. saline vehicle control).

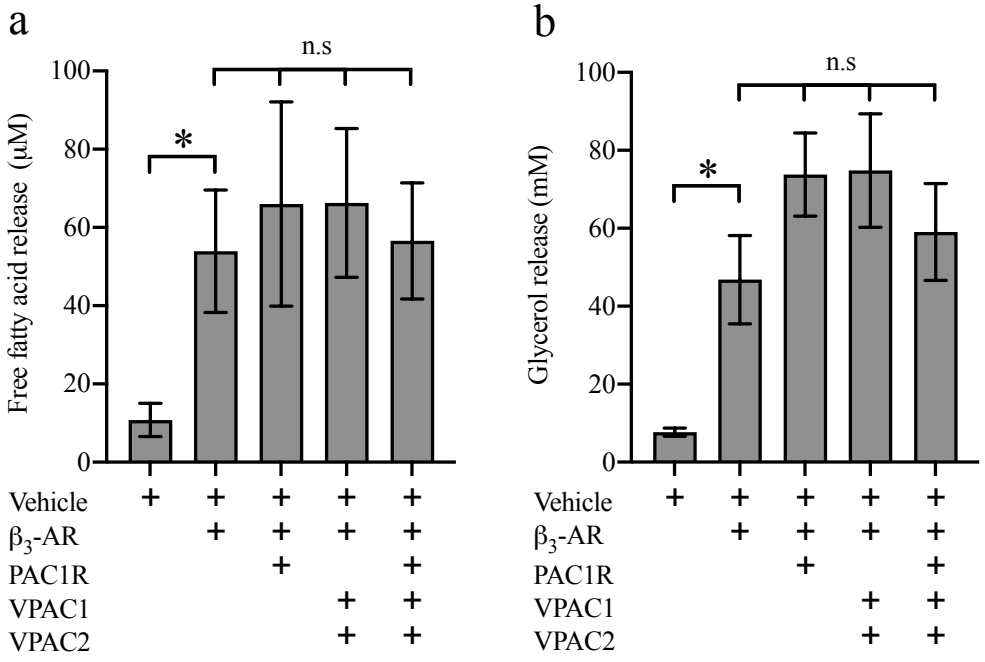

Figure 3.12. Lipolysis in white adipocyte cultures following 2-hour stimulation of pituitary adenylate cyclase-activating polypeptide (PACAP) receptors in combination with β_3 adrenergic receptors (β_3-ARs). Free fatty acid (a) and glycerol (b) release were measured in media of differentiated primary cultures from inguinal white adipose tissue of male C57BL/6 mice (n = 2 wells/treatment). Patterns of receptor agonism (+) were achieved using CL316,243 to stimulate β_3 adrenergic receptor (β_3-AR), pituitary adenylate cyclase-activating polypeptide (PACAP) for non-specific simultaneous stimulation of VPAC1, VPAC2, and PAC1R, Maxadilan for PAC1R-specific activation, and M65 (PAC1R-specific antagonist) plus PACAP to stimulate VPAC1 and 2 but not PAC1R. Data are expressed as mean ± SD. and asterisks denote a significant effect of treatment at $\alpha = 0.05$ (stimulated vs. saline vehicle control).

Oxygen consumption measurements

Acute treatment of differentiated brown adipocytes with PACAP receptor agonists *in vitro* did not alter the rate of oxygen consumption compared to saline controls (Figure 3.13). Oxygen consumption rate was significantly increased by CL316,243. Addition of PACAP receptor agonists along with CL316,243 did not enhance the rate of oxygen consumption compared to the response to CL316,243 alone in differentiated primary adipocytes of iBAT. In our modified version of the Mito Stress Kit assay, 10 mM CL316,243 stimulated brown adipocyte oxygen consumption as significantly as 3 μM FCCP (Figure 3.14).

Acute treatment of differentiated white adipocytes with PACAP receptor agonists *in vitro* also did not alter oxygen consumption compared to controls (Figure 3.15). Oxygen consumption rate was significantly increased by CL316,243, but not enhanced in combination with PACAP receptor agonists compared to CL316,243 alone. In our modified version of the Mito Stress Kit assay, 10 mM CL316,243 significantly increased oxygen consumption in differentiated primary white adipocytes, and subsequent addition of FCCP increased oxygen consumption significantly further (Figure 3.16).

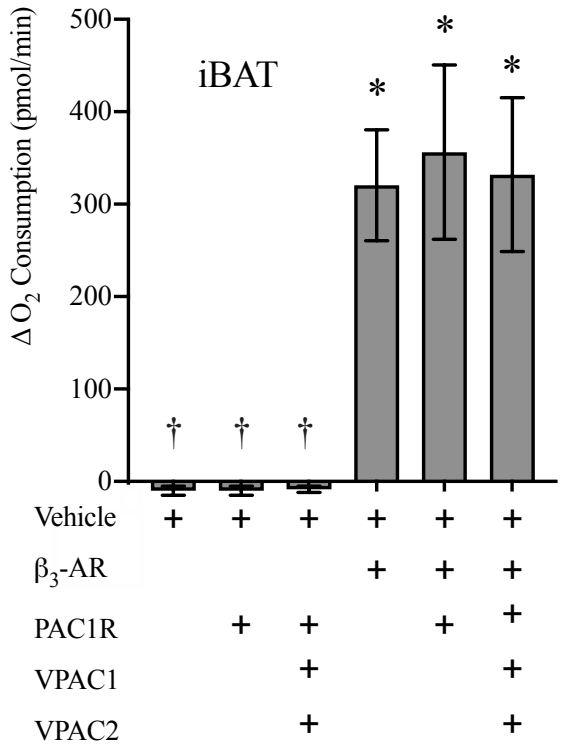

Figure 3.13. Activation of thermogenesis in primary brown adipocyte cultures following acute stimulation of pituitary adenylate cyclase-activating polypeptide (PACAP) receptors alone or in combination with β_3 adrenergic receptor (β_3-AR). Oxygen consumption rate was measured in media of primary cultures of adipocytes from interscapular brown adipose tissue from male C57BL/6 mice (n = 7 wells per treatment). Mitochondrial respiration was brought to a minimum using Oligomycin, receptors were selectively stimulated, and then the difference (Δ) in oxygen consumption calculated. Patterns receptor agonism (+) were achieved using CL316,243 to stimulate β_3 adrenergic receptor (β_3-AR), pituitary adenylate cyclase-activating polypeptide (PACAP) for non-specific simultaneous stimulation of VPAC1, VPAC2, and PAC1R, and Maxadilan for PAC1R-specific activation. Data are expressed as mean ± SD and asterisks (*) denote a significant effect ($\alpha = 0.05$) of treatment compared to vehicle (-) control, while daggers (†) denote a significant effect of treatment compared to β_3-AR stimulated (+) control.

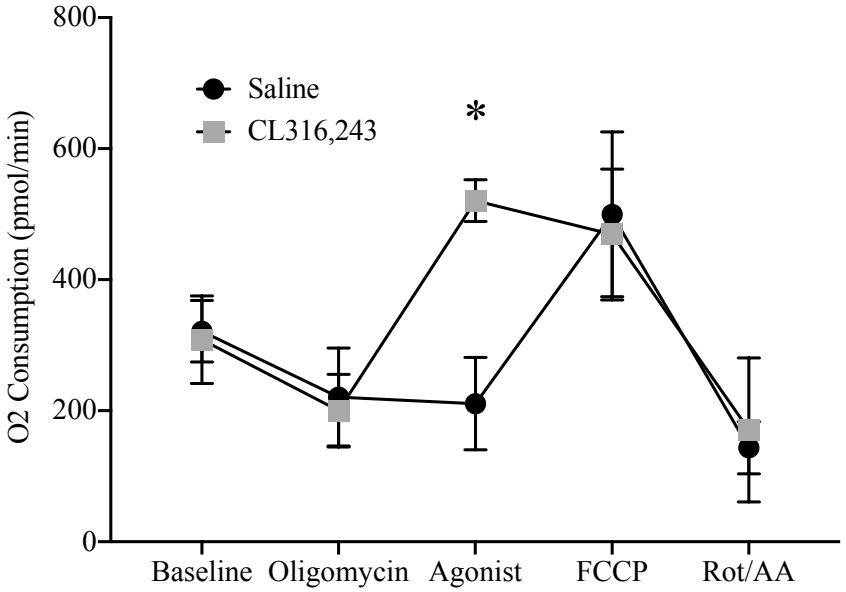

Figure 3.14. Oxygen consumption profile of differentiated primary brown adipocytes of interscapular origin (a) and differentiated primary white adipocytes of inguinal origin (b) from C57BL/6 mice (n = 7/treatment) during the Mitochondrial Stress Test Kit assay (Agilent, Santa Clara, CA, USA). During the Agonist stage, either saline vehicle (black dots) or CL316,243, a specific β_3-AR agonist (gray boxes) was added. Data are expressed as mean ± SD and asterisks denote a significant effect of treatment at $\alpha = 0.05$ (stimulated vs. PBS vehicle control).

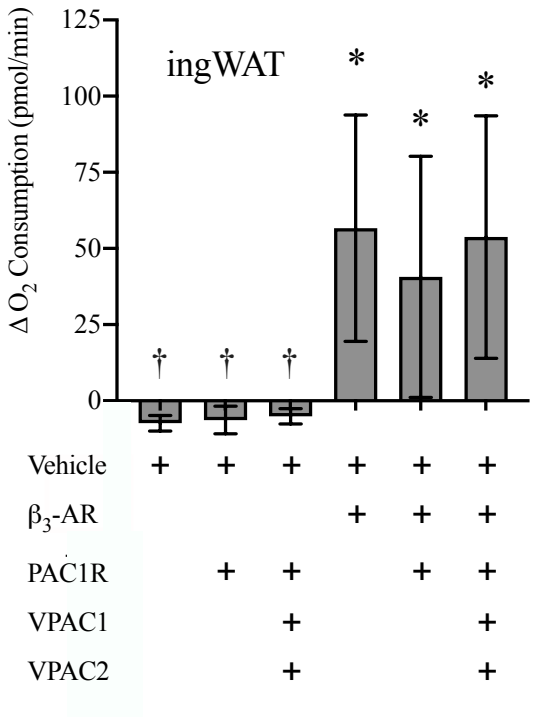

Figure 3.15. Activation of thermogenesis in primary white adipocyte cultures following acute stimulation of pituitary adenylate cyclase-activating polypeptide (PACAP) receptors alone or in combination with β_3 adrenergic receptor (β_3-AR). Oxygen consumption rate was measured in media of primary cultures of adipocytes from inguinal white adipose tissue from male C57BL/6 mice (n = 7 wells per treatment). Mitochondrial respiration was brought to a minimum using Oligomycin, receptors were selectively stimulated, and then the difference (Δ) in oxygen consumption calculated. Patterns receptor agonism (+) were achieved using CL316,243 to stimulate β_3 adrenergic receptor (β_3-AR), pituitary adenylate cyclase-activating polypeptide (PACAP) for non-specific simultaneous stimulation of VPAC1, VPAC2, and PAC1R, and Maxadilan for PAC1R-specific activation. Data are expressed as mean ± SD and asterisks (*) denote a significant effect ($\alpha = 0.05$) of treatment compared to vehicle (-) control, while daggers (†) denote a significant effect of treatment compared to β_3-AR stimulated (+) control.

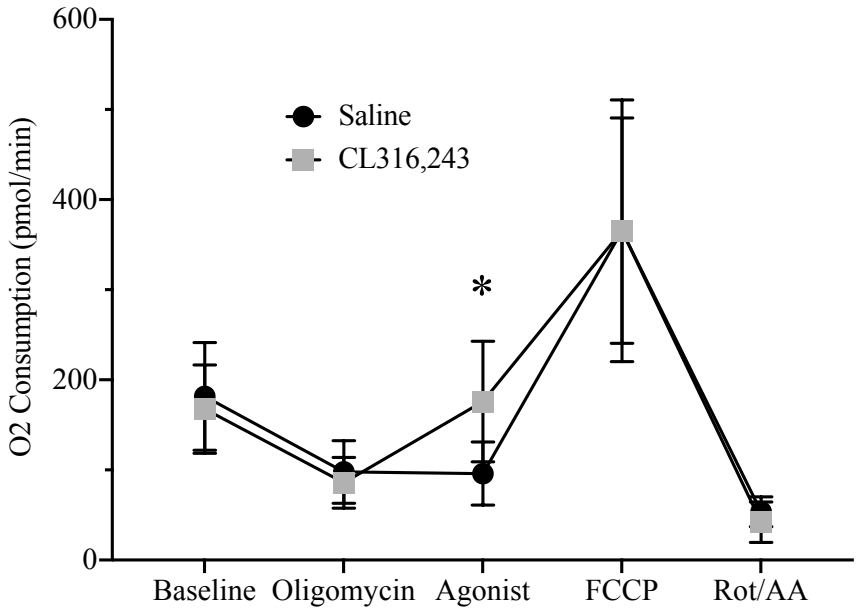

Figure 3.16. Oxygen consumption profile of differentiated primary brown adipocytes of interscapular origin (a) and differentiated primary white adipocytes of inguinal origin (b) from C57BL/6 mice (n = 7/treatment) during the Mitochondrial Stress Test Kit assay (Agilent, Santa Clara, CA, USA). During the Agonist stage, either saline vehicle (black dots) or CL316,243, a specific β_3-AR agonist (gray boxes) was added. Data are expressed as mean ± SD and asterisks denote a significant effect of treatment at $\alpha = 0.05$ (stimulated vs. PBS vehicle control).

3.4 DISCUSSION

Whole-animal and organ-level acclimation

As expected, mice in the cold-acclimated group had significantly lower body mass compared to the thermoneutral group due to the greater energetic requirements required to maintain an internal body temperature of 37 °C in the face of an external temperature of 4 °C (Figure 3.2a). The fat mass of cold-acclimated mice was significantly lower than the fat mass of mice housed at thermoneutrality by 2 weeks of acclimation (Figure 3.2c), as mice depleted lipid stores within adipose tissue to fuel shivering in muscle and adaptive thermogenesis in the BAT. Lean mass was not significantly different between the groups after 3.5 weeks, which shows that the differences in body mass and fat composition were not due to reduced growth or malaise (Figure 3.2b). Adipose tissues examined-post dissection revealed that gWAT and ingWAT depots from cold-acclimated mice weighed significantly less than the same adipose tissue depots from mice housed at thermoneutrality, while BAT mass did not differ between groups (Figure 3.2d). The loss of white adipose tissue mass results from mobilization of lipid stores to fuel thermogenesis and is a well-documented outcome of cold acclimation[182]. While some groups report increased BAT mass following cold exposure as brown adipocytes undergo hyperplasia during cold exposure[177], the increase in adaptive thermogenesis requires utilization of intracellular lipid stores and thus these two processes compete such that overall iBAT mass is increased, decreased, or unchanged after cold exposure depending on the strain of mouse and species examined [64,182,211].

As expected, iBAT from cold acclimated mice showed morphological and molecular characteristics of increased thermogenic activity, including increased mitochondria as determined from the darker pink eosin staining (a non-specific protein stain) (Figure 3.3a,b) and a darker brown colour upon dissection indicative of increased mitochondrial content[190].

Histological analysis of sections revealed smaller cells with lower lipid content (Figure 3.3c,d) and gene expression analysis reveal increased thermogenic gene expression (UCP1) and sympathetic sensitivity (β_3-AR) in iBAT from cold acclimated mice (Figures 3.3e). These data outline a complete morphological, histological, and genetic acclimation to cold.

In this robust model of thermogenic activation, PAC1R was significantly down-regulated in cold-acclimated iBAT, suggesting that contrary to our hypothesis, PACAP action directly at the adipocyte is not an important activator of the thermogenic response in this tissue (Figure 3.6a). Since PACAP mRNA could not be detected in this tissue in either group, PACAP is not an adipokine involved in thermogenesis. The discovery of PAC1R in this tissue and its downregulation after cold-acclimation were nonetheless interesting and we therefore set out identify the cell types within adipose tissue that were expressing PAC1R. PACAP receptors are known to be expressed in immune cells, such as macrophages[212], that have been isolated from adipose tissues. Therefore, we measured the expression of these receptors in cultures of adipocytes that are free from contaminating tissues. Interestingly, adipocytes isolated from iBAT express the PAC1R, with a trend of increased expression in differentiated adipocytes compared to preadipocytes (Figure 3.6b), although this result was not statistically significant. This shows, for the first time, that adipocytes themselves express PAC1R and that the detection of its mRNA in whole adipose tissue was not solely derived from macrophage, endothelial, and/or nerve cell expression.

Sequencing of mRNA from iBAT samples supported the real-time data for PAC1R but, interestingly, sequence reads encoding VIP and the VPAC receptors were not detected despite the mRNA having been sequenced to a depth of 24 million reads or more (Table 3.3). It is generally accepted that mRNA-Seq is a more sensitive method than real-time qPCR. The discrepancy between the qPCR results and the sequencing results is unusual, but both datasets

agree that PAC1R is expressed in iBAT of both cold-acclimated as well as thermoneutral mice, and that PAC1R expression is significantly lower in the cold-acclimated samples. Of note, UCP1 was the only other gene from this study with a higher degree of change than PAC1R. This suggests that a large reduction of PAC1R mRNA may be important in iBAT's response to cold acclimation, although the functional significance of this is not yet known.

As expected, ingWAT showed signs of browning with cold acclimation confirming that sufficient cold exposure had occurred to initiate patchwork thermogenic programing in this adaptable tissue. Brite adipocytes are quite unlike neighbouring white adipocytes as can be seen in the ingWAT of cold-acclimated mice (Figure 3.4a) but not their thermoneutral counterparts (b).

The thermogenically competent adipose depots of ingWAT also experienced an expected and significant upregulation of UCP1 mRNA in the cold-acclimated group (Figure 3.4c), which is known to correlate with greater thermogenic capacity of the adipocytes (reviewed in Nedergaard, et al. [179]). While the cold-induced upregulation of UCP1 mRNA in ingWAT was higher than that seen in iBAT, previous studies show that the thermogenic capacity of iBAT is still higher[73,178]. This paradox is due to the very low basal UCP1 mRNA expression in thermoneutral ingWAT, which mathematically inflates the calculated fold induction in cold-acclimated ingWAT since the expression is calculated as a relative induction.

Studies have shown that HOXC9 is a WAT-specific marker whose expression is retained through the browning process[213]. As expected, we found no significant upregulation of HOXC9 mRNA in ingWAT in response to cold acclimation (Figure 3.4c). These findings show that the ingWAT underwent normal physiological browning with an increase in UCP1 mRNA and retention of genetic markers of WAT despite the activation of the thermogenic program.

As we had hypothesized, PACAP receptors were significantly increased in cold-acclimated ingWAT (Figure 3.7a), but without a corresponding cold-induced increase in iBAT, lack of PACAP mRNA expression in adipocytes, and lack of PAC1R mRNA upregulation in differentiated primary adipocytes compared to preadipocytes from ingWAT (Figure 3.7b), it is unlikely that this is indicative of a direct effect on the regulation of thermogenic genes. Therefore, these results initially suggest a role for PACAP in thermogenic activation of ingWAT, but not all lines of evidence corroborate this finding. Further study will be required to define the role of PACAP in ingWAT acclimation to cold.

Adipose tissue from the gWAT depot showed an expected lack of thermogenic enhancement with cold acclimation, including the absence of brite cells and retention of cells dominated by a single, unilocular lipid droplet (Figure 3.5a,b). UCP1 expression did not differ between gWAT samples from thermoneutral and cold-acclimated mice (Figure 3.5c). Similar to ingWAT results, gWAT retained expression of HOXC9, showing normal levels of WAT-specific genetic markers throughout the process of acclimation to cold.

PAC1R was shown for the first time to be expressed in gWAT and was significantly down-regulated in cold-acclimated gWAT tissue compared to gWAT isolated from mice housed at thermoneutrality (Figure 3.8a). Furthermore, PAC1R expression was significantly higher in differentiated gWAT adipocytes than gWAT preadipocytes (Figure 3.8b). Taken together these results show that PAC1R expression is regulated in gWAT, and future studies including cultures of adipocytes from gWAT with genetic deletion of PAC1R could be utilized to interrogate PACAP's role in metabolic pathways of gWAT adipocytes.

PACAP itself was not detected using qPCR in any of the adipose tissues tested (Figures 3.6-3.8). This was somewhat surprising given previous reports of PACAP mRNA expression in human visceral adipose tissue[214]. Thus, our results suggest that mouse adipose tissues do not

express PACAP and that is not an important murine adipokine regulating adipose tissue function during cold acclimation. Additionally, the pattern of PAC1R gene expression in cold-acclimated BAT and WAT does not clearly suggest PACAP signalling to be a key regulator of adaptive thermogenesis in cold-acclimated adipocytes.

PACAP does not participate in β_3-AR-stimulated lipolysis or thermogenesis

The expression and genetic control of PAC1R mRNA in response to cold stress across all three adipose tissues calls to question its functional significance in adipocyte biology. PACAP acting centrally[109,110], and norepinephrine acting peripherally[215], are both important modulators of the thermogenic response of BAT[107]. There is currently no evidence in the literature indicating PACAP can bind PACAP receptors expressed on adipocytes to peripherally affect energy expenditure. In fact, the first evidence of PAC1R expression in brown adipocytes was published by the Gray lab last year[168]. To assess a functional role for PACAP in adipocytes, we measured the effect of PACAP agonism on lipolysis and oxygen consumption. These were selected because the liberation of free fatty acids and increased oxygen consumption at the inner mitochondrial membrane are hallmarks of increased thermogenic activation by beige and brown adipocytes[64,177]. Stimulation of the β_3-AR in adipocytes results in the well-characterized activation of heterotrimeric G proteins, downstream adenylyl cyclase activation, adipocyte lipolysis and, finally, oxygen consumption in thermogenic adipocytes. Free fatty acids provide fuel for thermogenesis and acutely activate UCP1, thereby uncoupling ATP production and dissipating stored energy in lipids as heat. Increased oxygen consumption results in part from utilization in the β-oxidation process but mainly from O_2 utilization by Complex IV of the mitochondrial electron transport chain where oxygen acts as the final electron acceptor during cellular aerobic respiration. PACAP receptors

are known to modulate energy balance in the hypothalamus[216] and to activate adenylate cyclase[82] and so we were interested in the idea that PACAP could independently activate lipolysis and thermogenesis peripherally in adipocytes or act to modulate the effect of adipocyte β_3-AR stimulation by the β3-specific agonist CL316,243, through the interaction of signalling pathways.

Previous work measuring lipolytic rates following β_3-AR agonism *in vivo* suggests that white adipocytes excrete free fatty acids at greater rates than brown adipocytes[217]. This may result from the primary role of white adipose tissue in the storage and release of lipids in times of energetic need. Higher lipolytic rates were therefore expected for ingWAT cultures compared to iBAT. Contrary to those expectations, release of FFA to the media was similar between brown and white adipocytes cultures (Figures 3.9a and 3.11a) and ingWAT cultures had roughly 2 times higher glycerol release than iBAT (Figure 3.9b and 3.11b). Previous reports have shown increases in oxygen consumption by stimulating intact culture brown adipocytes[218] as well as isolated mitochondria[178] with CL316,243. Our methods provided similar results, with oxygen consumption rate increasing significantly in differentiated brown preadipocytes upon CL316,243 treatment (Figure 3.13). Adipocytes isolated from iBAT have higher mitochondrial content than white adipose tissues, and a greater relative concentration of carrier proteins in the mitochondria[178]. Therefore, we were not surprised to see that cultures of ingWAT adipocytes provided a lower induction of oxygen consumption upon CL316,243 stimulation (Figure 3.15). In summary, these data suggest successful differentiation of preadipocyte cultures to give mature adipocytes that respond appropriately to adrenergic stimuli.

We hypothesized that PAC1R stimulation is capable of initiating lipolysis and acute thermogenic activity in cultured brown adipocytes. Thus, we expected the addition of the

synthetic agonist Maxadilan (PAC1R) or the natural ligand PACAP (stimulates PAC1R, VPAC1 and VPAC2) would increase the release of glycerol, release of free fatty acids, and consumption of oxygen in the media. Alternatively, we hypothesized that simultaneously stimulating β_3-ARs and PACAP receptors would increase lipolysis and oxygen consumption above the level of β_3-AR stimulation alone. This latter hypothesis would indicate that PACAP was capable of potentiating the stimulatory effects of β_3-AR. Contrary to our expectations, stimulating PACAP receptors alone in the adipocyte cultures did not elicit any change in FFA, glycerol, or oxygen measurements for brown (Figures 3.9 and 3.13) or white (Figures 3.11 and 3.15) cultures. Furthermore, addition of PACAP with CL316,243 did not potentiate stimulation of iBAT (Figure 3.10) or ingWAT (Figure 3.12) above the level of CL316,243 stimulation alone . Collectively, these data suggest that PACAP does not independently activate lipolysis or thermogenesis or potentiate the adrenergic response at the level of the adipocyte in ingWAT or iBAT. This was surprising considering unpublished results from single-cell sequencing data from human adipocytes, which show a strong correlation between the expression level of PAC1R and lipolysis-related genes (personal communication with Arthe Raajendiran[219]).

It is possible that the ability of PACAP to augment adrenergic-stimulated lipolysis and oxygen consumption may have been masked by the high levels of CL316,243 used. If β_3-AR stimulation was intense enough that mitochondrial respiration was maximally activated, this could have saturated pathways responsible for the physiological measurements that we used in this study. Figure 3.14 shows that CL316,243-stimulated brown adipocyte cultures displayed oxygen consumption levels similar to FCCP, which is the theoretical maximum. This indicates that even if a higher concentration of CL316,243 had been added, there would not have been an increase in oxygen consumption above that level. To the best of our knowledge, there are no pharmacological stimuli capable of enhancing adipocyte oxygen consumption higher than

FCCP. To better characterize the response to CL316,243, a titration curve should be run to determine a half-maximal stimulation. In this half-maximally stimulated state, addition of Maxadilan may reveal a modulatory effect.

Future prospects

Since these findings show that PAC1R mRNA expression is significantly regulated in adipose tissues *in vivo* in response to cold stress, but is not associated with any *acute* effect on lipolysis or thermogenesis in the main thermogenic adipose tissue iBAT, or the thermogenically inducible adipose tissue ingWAT, future work in this field should interrogate the alternative hypothesis that PACAP is important in stimulating adaptive processes for long-term acclimation to cold. To test this hypothesis, I would perform two experiments. First, I would assess the effect of PACAP on the differentiation of primary brown adipocytes in culture to determine whether PACAP enhances differentiation of thermogenic adipocytes thus increasing the functional capacity of BAT to perform thermogenesis. Secondly, I would assess genetic markers of thermogenesis in cultured adipocytes differentiated in the presence or absence of PACAP and/or isoproterenol to determine if PACAP can augment adrenergic-induced differentiation. Lastly, it is also possible that PAC1R mRNA expression are only transiently expressed in the acclimation to cold or differentiation, as many other factors are[72,220] and thus we missed a short period of PAC1R mRNA induction in iBAT. To test this, adipose tissues should be collected from mice at different time points in the acclimation process and qPCR used to test for PAC1R expression.

3.5 CONCLUSION

Current evidence in the literature suggests that PACAP is an important central regulator of the thermogenic response to cold stress in mice, but little is known about the effect of PACAP directly at the adipocyte. Here we have shown that PAC1R mRNA expression may be important in the adipose acclimation to long-term cold exposure. PAC1R and VPAC1 mRNA were expressed in the three physiologically distinct adipose tissue depots investigated, and the pattern of expression differs depending on depot type and housing temperature. These receptors were also expressed in preadipocytes and differentiated adipocytes in cultures of all three depots, demonstrating for the first time PACAP receptor expression in adipocytes themselves. The lack of observed effect on the rates of lipolysis or oxygen consumption with acute pharmacological stimulation of PAC1R suggests that this receptor does not activate thermogenesis in mature adipocytes, but we have not tested the effects of chronic stimulation of the PAC1R on adipocyte differentiation and function. The work presented here has added to the growing body of literature that supports a role for PACAP in energy regulation including in the context of adaptive thermogenesis and will inform future work attempting to re-balance the energy equation for the treatment of obesity and diabetes.

Chapter Four: Concluding Remarks on AAV Development and the Expression of PACAP Receptors in Adipocytes

4.1 SUMMARY

This thesis was completed to **(A)** develop a viral gene therapy tool to study the effects of pituitary adenylate cyclase-activating polypeptide (PACAP) expression specifically in the ventromedial nucleus (VMH) of the hypothalamus and **(B)** address the hypothesis that PACAP may enhance adaptive thermogenesis by acting peripherally at the adipocyte.

The objectives of this research were the following:

1. Develop a stereotaxic injection protocol and perform intracerebral injections of adeno-associated virus (AAV).
2. Assess the performance of the AAV vector and accompanying plasmid pscAAV9-SF1-GFP for inducing enhanced green fluorescent protein (EGFP) gene expression in the VMH *in vivo*.
3. Produce a mouse model of maximal thermogenic activation and assess the genetic regulation of PACAP and PACAP receptor expression in adipose tissues.
4. Determine whether PACAP or its receptors are expressed specifically on mouse adipocytes.
5. Assess the lipolytic and thermogenic consequences of acute PACAP receptor activation on mouse adipocytes *in vitro*.

Chapter Two addressed objectives 1 and 2 above with the future aim of developing a tool (Figure 2.2) that could be used to restore PACAP expression specifically in the VMH of PACAP-null mice, thus providing a genetic model to assess the contribution of the VMH to energy balance including thermogenesis. The efficacy of the plasmid and its vector were assessed by detection and localization of EGFP expression using fluorescent microscopy. Results showed successful induction of EGFP expression in the VMH-targeted, but not intracerebroventricular-targeted strategy (Figure 2.4). Due to the high viral concentration used,

some off-target expression was detected (Figures 2.4 and 2.5) and thus I have recommended lower viral dosage to prevent steroidogenic factor 1 (SF1) promoter leakiness. EGFP was detected superior to the VMH, and thus I also recommend modification of the injection coordinates for future studies. The successful induction of EGFP expression in the hypothalamus was an important and positive step towards the larger goal of VMN-specific PACAP rescue in PACAP-null mice.

Chapter Three addressed objectives 3-5 above, which were designed to evaluate the potential for peripheral activation of thermogenesis by PACAP at the level of the adipose tissue. The mouse model of maximal thermogenic acclimation developed here was confirmed to meet the genetic, histological, and morphological changes expected based on previous work[64,72,177,179] (Figures 3.2-3.5). We then measured PACAP receptor expression in adipose tissues of this model and found that the results did not support our hypothesis that PAC1R mRNA expression would be significantly increased in cold-acclimated brown adipose tissue (BAT). However, these data show the first documented evidence of PAC1R expression in BAT and provide the first robust analysis of PACAP receptor expression in white adipose tissue and BAT under cold exposure (Figures 3.6-3.8). Interestingly, PACAP receptor expression was increased in inguinal and decreased in gonadal white adipose tissue, showing depot-specific patterning of the PAC1 receptor. Isolated mature adipocytes and preadipocytes of BAT showed expression of the PACAP-specific receptor, confirming adipocyte PAC1R expression. *In vitro* functional data did not support the hypothesis that PACAP could acutely induce lipolysis or thermogenesis via PAC1R alone, or in combination with adrenergic receptor agonism (Figures 3.9-3.16). Future work should address the possibility that long-term PACAP treatment could enhance the thermogenic capacity of adipocytes.

4.2 SIGNIFICANCE

Obesity and its comorbidities account for a significant portion of the health care burden, decrease quality of life for patients, and increase the risk of death. Current strategies of increasing exercise and decreasing food intake have not been successful in curbing the increasing prevalence of this disease. Environmental factors such as poor urban planning that prohibit active lifestyle choices have contributed to the obesity epidemic, but dysregulated energy metabolism is the driver of the disease and must be better understood in order to provide comprehensive treatment strategies. Energy metabolism is controlled by nutritional, hormonal, and neuronal signals working in concert. Hormonal regulation of energy balance has gained interest as a therapeutic target and this substantial field continues to expand with the identification of a number of extremely promising molecular targets to better understand and treat obesity and T2D.

Here we investigated two approaches to understanding energy balance under the influence of the therapeutically intriguing neuropeptide PACAP, which is involved in the regulation of sympathetic output to peripheral effector organs, including BAT, to alter energy expenditure. The first approach we used targeted the hypothalamic VMH, which is an essential energy regulating brain centre that is known to regulate food intake and energy expenditure to alter body mass. In the VMH, PACAP is localized to the same neurons as orexigenic and anorexigenic hormones such as proopiomelanocortin, neuropeptide Y, Agouti-related peptide, and brain-derived neurotrophic factor, suggesting that it may play an important role in the regulation or integration of energy-modulating pathways within this nucleus. Neuroanatomical and pharmacological evidence also implicate PACAP as an important neuropeptide in other hypothalamic nuclei, but it is difficult to discern the relative contribution and hierarchy of hypothalamic nuclei in thermogenic activation. Thus, we have proposed an AAV-mediated

genetic strategy to restore PACAP specifically in the VMH to assess its effectiveness in rescuing the thermogenically-impaired phenotype of PACAP-null mice. AAV-mediated gene therapy techniques are becoming more common in the clinical setting. While some technical difficulties remain, the work presented here has provided preliminary evidence that the virus and accompanying plasmid developed by the Gray lab are effective in inducing gene expression using the SF1 promoter. Future completion of VMH-specific genetic rescue of PACAP will be a powerful tool to understand the hypothalamic regulation of energy balance, including thermogenesis, and will help in understanding the mechanisms that can lead to negative energy balance and ameliorate obesity and its metabolic complications.

The second approach targets the adipose tissue directly to better elucidate PACAP's role in energy metabolism. Sympathetic outputs controlled by the hypothalamus have long been known to initiate thermogenesis in BAT, and central administration of PACAP has proven effective in activating adaptive thermogenesis, but the current literature does not address the possibility that PACAP may act as a peripheral activator of thermogenesis by binding directly to adipocytes. The data presented here are, to the best of our knowledge, the first documented evidence of PAC1R mRNA expression in BAT and provide the first robust analysis of PACAP receptor expression in adipose tissues of a model of thermogenic activation. The discovery of PAC1R mRNA in BAT provides an exciting opportunity to expand the understanding of hormonal regulation within this tissue and in the larger context of energy balance. Further, the significant regulation of a number of PACAP receptors across three functionally distinct adipose tissue in this model adds to the growing evidence that PACAP and its receptors are essential components at various levels of stress axes. The preliminary assessment of PAC1R function in adipose tissue did not provide evidence for acute lipolytic or thermogenic activation *in vitro*, but further work is required to fully understand the role of this receptor in adipose

function. The ability to target energy expenditure directly at the adipocyte may provide a promising therapeutic strategy due to the specificity of PAC1R splice variant expression across tissues.

In summary, this thesis has contributed to a more comprehensive understanding of the energy-regulating peptide PACAP and has aided the development of tools available to elucidate the roles of PACAP in hypothalamic nuclei, which will inform efforts to develop better anti-obesity strategies oriented towards novel molecular targets. Specificity is an essential component in the development of therapeutics and in understanding the complicated regulatory networks in the central nervous system. The viral reintroduction of PACAP specifically to the VMH and discovery of its highly spliced receptor PAC1R in BAT both provide opportunities to enhance the targeting of research and therapeutics that aim to utilize adaptive thermogenesis as an energy expenditure mechanism in the prevention and treatment of obesity and type 2 diabetes.

List of Abbreviations

AAV9	adeno-associated virus, serotype 9
Acetyl-CoA	acetyl-coenzyme A
ACTH	adrenocorticotropin-releasing hormone
ACUC	animal care and use committee
AgRP	Agouti-related peptide
ANS	autonomic nervous system
ARH	arcuate nucleus (of the hypothalamus)
ATP	adenosine triphosphate
BAT	brown adipose tissue
BDNF	brain-derived neurotropic factor
BMI	body mass index
BMP8B	bone morphogenic protein 8B
C/EBP	CCAAT enhancer binding protein
cAMP	cyclic adenosine monophosphate
CCK	cholecystokinin
CL316,243	disodium (R,R)-5-[2-[[2-(3-chlorophenyl)–2-hydroxyethyl]-amino]-propyl]-1,3-benzodi-oxazole-2,2-dicarboxylate
CMV	cytomegalovirus (promoter)
CNS	central nervous system
CREBP	cAMP response-element binding protein
CRH	corticotropin-releasing hormone
DMEM/F12	Dulbecco's Modified Eagle's Medium/Nutrient Mixture F-12 Ham

DMH	dorsomedial nucleus (of the hypothalamus)
EGFP	enhanced green fluorescent protein
FBS	fetal bovine serum
FCCP	carbonyl cyanide-4-phenylhydrazone
FFA	free fatty acids
FGF21	fibroblast growth factor 21
FKPM	fragments per kilobase million
GDP	guanosine diphosphate
GPCR	G-protein coupled receptor
GTP	guanosine triphosphate
gWAT	gonadal white adipose tissue
HEPES	(4-(2-hydroxyethyl)-1-piperazineethanesulfonic acid)
HOXC9	homeobox c9
HPA	hypothalamic-pituitary-adrenal axis
HSL	hormone-sensitive lipase
ICV	intracerebroventricular
IL-6	interleukin 6
ingWAT	inguinal white adipose tissue
IP_3	inositol triphosphate
MCP1	monocyte chemoattractant protein 1
NPY	neuropeptide Y
NR5A1	nuclear receptor subfamily 5 group A member 1
PACAP	pituitary adenylate cyclase-activating polypeptide

PKA	protein kinase A
PLC	phospholipase C
PNS	parasympathetic nervous system
POMC	proopiomelanocortin
PPAR-γ	peroxisome proliferator-activated receptor gamma
PVH	paraventricular nucleus (of the hypothalamus)
Rapgef4	Rap guanine nucleotide exchange factor 4
ROI	region of interest
scAAV9	self-complimentary adeno-associated virus, serotype 9
SF1	steroidogenic factor 1
SNS	sympathetic nervous system
SVF	stromal vascular fraction
T2D	type 2 diabetes
TD-NMR	Time-domain nuclear magnetic resonance
TNFα	tumor necrosis factor alpha
TRP	transient receptor potential
UCP1	uncoupling protein 1
VEGFA	vascular endothelial growth factor A
vg	viral genomes
VIP	vasoactive intestinal peptide
VMH	ventromedial nucleus (of the hypothalamus)
WAT	white adipose tissue
β_3-AR	beta-3 adrenergic receptor

Bibliography

1. Anis, A.H., Zhang, W., Bansback, N., Guh, D.P., Amarsi, Z. & Birmingham, C.L. Obesity and overweight in canada: An updated cost-of-illness study. *Obes Rev* **11**, 31-40 (2010).

2. Roberts, K.C., Shields, M., de Groh, M., Aziz, A. & Gilbert, J.A. Overweight and obesity in children and adolescents: Results from the 2009 to 2011 canadian health measures survey. *Health Rep* **23**, 37-41 (2012).

3. Katzmarzyk, P.T. & Mason, C. Prevalence of class i, ii and iii obesity in canada. *CMAJ* **174**, 156-157 (2006).

4. Ng, M., Fleming, T., Robinson, M., Thomson, B., Graetz, N., Margono, C., Mullany, E.C., Biryukov, S., Abbafati, C., Abera, S.F., Abraham, J.P., Abu-Rmeileh, N.M., Achoki, T., AlBuhairan, F.S., Alemu, Z.A., Alfonso, R., Ali, M.K., Ali, R., Guzman, N.A., Ammar, W.*, et al.* Global, regional, and national prevalence of overweight and obesity in children and adults during 1980-2013: A systematic analysis for the global burden of disease study 2013. *Lancet* **384**, 766-781 (2014).

5. Finkelstein, E.A., Trogdon, J.G., Cohen, J.W. & Dietz, W. Annual medical spending attributable to obesity: Payer-and service-specific estimates. *Health Aff (Millwood)* **28**, w822-831 (2009).

6. Cornier, M.A., Dabelea, D., Hernandez, T.L., Lindstrom, R.C., Steig, A.J., Stob, N.R., Van Pelt, R.E., Wang, H. & Eckel, R.H. The metabolic syndrome. *Endocr Rev* **29**, 777-822 (2008).

7. Giles-Corti, B. & Robertson-Wilson, J. The role of the changing built environment in shaping out shape. in *Geographies of obesity: Environmental understandings of the obesity epidemic* (eds. Wood, L. & Falconer, R.) 155-174 (Routledge, London, 2016).

8. Lavie, C.J., Milani, R.V. & Ventura, H.O. Obesity and cardiovascular disease: Risk factor, paradox, and impact of weight loss. *J Am Coll Cardiol* **53**, 1925-1932 (2009).

9. Apovian, C.M. Obesity: Definition, comorbidities, causes, and burden. *Am J Manag Care* **22**, s176-185 (2016).

10. Pickett, K.E., Kelly, S., Brunner, E., Lobstein, T. & Wilkinson, R.G. Wider income gaps, wider waistbands? An ecological study of obesity and income inequality. *J Epidemiol Community Health* **59**, 670-674 (2005).

11. Jonasson, M.E., Wicklow, B.A., Sellers, E.A.C., Dolinsky, V.W. & Doucette, C.A. Exploring the role of the hnf-1αg319s polymorphism in β cell failure and youth-onset type 2 diabetes: Lessons from mody and hnf-1α-deficient animal models. *Biochemistry and Cell Biology* **93**, 487-494 (2015).

12. Hall, K.D., Ayuketah, A., Brychta, R., Cai, H., Cassimatis, T., Chen, K.Y., Chung, S.T., Costa, E., Courville, A., Darcey, V., Fletcher, L.A., Forde, C.G., Gharib, A.M., Guo, J., Howard, R., Joseph, P.V., McGehee, S., Ouwerkerk, R., Raisinger, K., Rozga, I.*, et al.* Ultra-processed diets

cause excess calorie intake and weight gain: An inpatient randomized controlled trial of ad libitum food intake. *Cell Metab* **30**, 226 (2019).

13. LeBlanc, A.G., Katzmarzyk, P.T., Barreira, T.V., Broyles, S.T., Chaput, J.P., Church, T.S., Fogelholm, M., Harrington, D.M., Hu, G., Kuriyan, R., Kurpad, A., Lambert, E.V., Maher, C., Maia, J., Matsudo, V., Olds, T., Onywera, V., Sarmiento, O.L., Standage, M., Tudor-Locke, C.*, et al.* Correlates of total sedentary time and screen time in 9-11 year-old children around the world: The international study of childhood obesity, lifestyle and the environment. *PLoS One* **10**, e0129622 (2015).

14. Ling, C. & Rönn, T. Epigenetics in human obesity and type 2 diabetes. *Cell Metabolism* **29**, 1028-1044 (2019).

15. Kenny, P.J. Common cellular and molecular mechanisms in obesity and drug addiction. *Nat Rev Neurosci* **12**, 638-651 (2011).

16. Will, M.J., Pratt, W.E. & Kelley, A.E. Pharmacological characterization of high-fat feeding induced by opioid stimulation of the ventral striatum. *Physiology & Behavior* **89**, 226-234 (2006).

17. Woods, S.C. Gastrointestinal satiety signals i. An overview of gastrointestinal signals that influence food intake. *American Journal of Physiology-Gastrointestinal and Liver Physiology* **286**, G7-G13 (2004).

18. Matarazzo, V., Schaller, F., Nédélec, E., Benani, A., Pénicaud, L., Muscatelli, F., Moyse, E. & Bauer, S. Inactivation of socs3 in the hypothalamus enhances the hindbrain response to endogenous satiety signals via oxytocin signaling. *The Journal of Neuroscience* **32**, 17097 (2012).

19. Frederich, R.C., Hamann, A., Anderson, S., Lollmann, B., Lowell, B.B. & Flier, J.S. Leptin levels reflect body lipid content in mice: Evidence for diet-induced resistance to leptin action. *Nat Med* **1**, 1311-1314 (1995).

20. Cinaz, P., Bideci, A., Camurdan, M.O., Guven, A. & Gonen, S. Leptin and soluble leptin receptor levels in obese children in fasting and satiety states. *J Pediatr Endocrinol Metab* **18**, 303-307 (2005).

21. Paz-Filho, G., Mastronardi, C.A. & Licinio, J. Leptin treatment: Facts and expectations. *Metabolism* **64**, 146-156 (2015).

22. Uotani, S., Bjørbaek, C., Tornøe, J. & Flier, J.S. Functional properties of leptin receptor isoforms: Internalization and degradation of leptin and ligand-induced receptor downregulation. *Diabetes* **48**, 279 (1999).

23. Dunn, S.L., Björnholm, M., Bates, S.H., Chen, Z., Seifert, M. & Myers, M.G., Jr. Feedback inhibition of leptin receptor/jak2 signaling via tyr1138 of the leptin receptor and suppressor of cytokine signaling 3. *Molecular Endocrinology* **19**, 925-938 (2005).

24. Gesta, S. & Kahn, R. White adipose tissue in *Adipose tissue biology* (ed. Symonds, M.E.) 149-199 (Springer International Publishing, 2017).

25. Mei, M., Zhao, L., Li, Q., Chen, Y., Huang, A., Varghese, Z., Moorhead, J.F., Zhang, S., Powis, S.H., Li, Q. & Ruan, X.Z. Inflammatory stress exacerbates ectopic lipid deposition in c57bl/6j mice. *Lipids Health Dis* **10**, 110 (2011).

26. Garg, A. & Misra, A. Hepatic steatosis, insulin resistance, and adipose tissue disorders. *J Clin Endocrinol Metab* **87**, 3019-3022 (2002).

27. Bergström, J., Hermansen, L., Hultman, E. & Saltin, B. Diet, muscle glycogen and physical performance. *Acta Physiologica Scandinavica* **71**, 140-150 (1967).

28. Abdel-Hamid, T.K. Modeling the dynamics of human energy regulation and its implications for obesity treatment. *System Dynamics Review* **18**, 431-471 (2002).

29. Flatt, J.P. Use and storage of carbohydrate and fat. *The American Journal of Clinical Nutrition* **61**, 952S-959S (1995).

30. Carey, G.B. Mechanisms regulating adipocyte lipolysis. in *Skeletal muscle metabolism in exercise and diabetes* (eds. Richter, E.A., Kiens, B., Galbo, H. & Saltin, B.) 157-170 (Springer US, Boston, MA, 1998).

31. Vidal-Puig, A. Adipose tissue expandability, lipotoxicity and the metabolic syndrome. *Endocrinol Nutr* **60 Suppl 1**, 39-43 (2013).

32. Bartness, T.J., Liu, Y., Shrestha, Y.B. & Ryu, V. Neural innervation of white adipose tissue and the control of lipolysis. *Front Neuroendocrinol* **35**, 473-493 (2014).

33. Moustaid, N., Jones, B.H. & Taylor, J.W. Insulin increases lipogenic enzyme activity in human adipocytes in primary culture. *J Nutr* **126**, 865-870 (1996).

34. Bluher, M. & Mantzoros, C.S. From leptin to other adipokines in health and disease: Facts and expectations at the beginning of the 21st century. *Metabolism* **64**, 131-145 (2015).

35. Lau, W.B., Ohashi, K., Wang, Y., Ogawa, H., Murohara, T., Ma, X.L. & Ouchi, N. Role of adipokines in cardiovascular disease. *Circ J* **81**, 920-928 (2017).

36. Lehr, S., Hartwig, S. & Sell, H. Adipokines: A treasure trove for the discovery of biomarkers for metabolic disorders. *Proteomics Clin Appl* **6**, 91-101 (2012).

37. Smith, U. & Kahn, B.B. Adipose tissue regulates insulin sensitivity: Role of adipogenesis, de novo lipogenesis and novel lipids. *J Intern Med* **280**, 465-475 (2016).

38. de Souza Batista, C.M., Yang, R.Z., Lee, M.J., Glynn, N.M., Yu, D.Z., Pray, J., Ndubuizu, K., Patil, S., Schwartz, A., Kligman, M., Fried, S.K., Gong, D.W., Shuldiner, A.R., Pollin, T.I. & McLenithan, J.C. Omentin plasma levels and gene expression are decreased in obesity. *Diabetes* **56**, 1655-1661 (2007).

39. Eckel, J. *Chapter 2 - adipose tissue: A major secretory peptide*, (Academic Press 2018).

40. Hotamisligil, G.S., Shargill, N.S. & Spiegelman, B.M. Adipose expression of tumor necrosis factor-alpha: Direct role in obesity-linked insulin resistance. *Science* **259**, 87-91 (1993).

41. Zhang, Y., Proenca, R., Maffei, M., Barone, M., Leopold, L. & Friedman, J.M. Positional cloning of the mouse obese gene and its human homologue. *Nature* **372**, 425-432 (1994).

42. Smith, J.K. Exercise, obesity and cns control of metabolic homeostasis: A review. *Front Physiol* **9**, 574 (2018).

43. van Dielen, F.M., van 't Veer, C., Buurman, W.A. & Greve, J.W. Leptin and soluble leptin receptor levels in obese and weight-losing individuals. *J Clin Endocrinol Metab* **87**, 1708-1716 (2002).

44. Grattan, D.R., Ladyman, S.R. & Augustine, R.A. Hormonal induction of leptin resistance during pregnancy. *Physiology & Behavior* **91**, 366-374 (2007).

45. Townsend, K.L., Kunz, T.H. & Widmaier, E.P. Changes in body mass, serum leptin, and mrna levels of leptin receptor isoforms during the premigratory period in myotis lucifugus. *Journal of Comparative Physiology B* **178**, 217-223 (2008).

46. Brown, R.E. & Kuk, J.L. Consequences of obesity and weight loss: A devil's advocate position. *Obes Rev* **16**, 77-87 (2015).

47. Kim, J.Y., van de Wall, E., Laplante, M., Azzara, A., Trujillo, M.E., Hofmann, S.M., Schraw, T., Durand, J.L., Li, H., Li, G., Jelicks, L.A., Mehler, M.F., Hui, D.Y., Deshaies, Y., Shulman, G.I., Schwartz, G.J. & Scherer, P.E. Obesity-associated improvements in metabolic profile through expansion of adipose tissue. *J Clin Invest* **117**, 2621-2637 (2007).

48. Kratz, M., Coats, B.R., Hisert, K.B., Hagman, D., Mutskov, V., Peris, E., Schoenfelt, K.Q., Kuzma, J.N., Larson, I., Billing, P.S., Landerholm, R.W., Crouthamel, M., Gozal, D., Hwang, S., Singh, P.K. & Becker, L. Metabolic dysfunction drives a mechanistically distinct proinflammatory phenotype in adipose tissue macrophages. *Cell Metab* **20**, 614-625 (2014).

49. Moitra, J., Mason, M.M., Olive, M., Krylov, D., Gavrilova, O., Marcus-Samuels, B., Feigenbaum, L., Lee, E., Aoyama, T., Eckhaus, M., Reitman, M.L. & Vinson, C. Life without white fat: A transgenic mouse. *Genes Dev* **12**, 3168-3181 (1998).

50. White, U.A. & Stephens, J.M. Transcriptional factors that promote formation of white adipose tissue. *Mol Cell Endocrinol* **318**, 10-14 (2010).

51. Lumeng, C.N., Bodzin, J.L. & Saltiel, A.R. Obesity induces a phenotypic switch in adipose tissue macrophage polarization. *J Clin Invest* **117**, 175-184 (2007).

52. Solinas, G. & Becattini, B. Jnk at the crossroad of obesity, insulin resistance, and cell stress response. *Mol Metab* **6**, 174-184 (2017).

53. Langin, D. Adipose tissue lipolysis as a metabolic pathway to define pharmacological strategies against obesity and the metabolic syndrome. *Pharmacol Res* **53**, 482-491 (2006).

54. Boden, G. & Shulman, G.I. Free fatty acids in obesity and type 2 diabetes: Defining their role in the development of insulin resistance and beta-cell dysfunction. *Eur J Clin Invest* **32 Suppl 3**, 14-23 (2002).

55. Zhang, Y., Matheny, M., Zolotukhin, S., Tumer, N. & Scarpace, P.J. Regulation of adiponectin and leptin gene expression in white and brown adipose tissues: Influence of β3-adrenergic agonists, retinoic acid, leptin and fasting. *Biochimica et Biophysica Acta (BBA) - Molecular and Cell Biology of Lipids* **1584**, 115-122 (2002).

56. Tsuchida, A., Yamauchi, T., Ito, Y., Hada, Y., Maki, T., Takekawa, S., Kamon, J., Kobayashi, M., Suzuki, R., Hara, K., Kubota, N., Terauchi, Y., Froguel, P., Nakae, J., Kasuga, M., Accili, D., Tobe, K., Ueki, K., Nagai, R. & Kadowaki, T. Insulin/foxo1 pathway regulates expression levels of adiponectin receptors and adiponectin sensitivity. *J Biol Chem* **279**, 30817-30822 (2004).

57. Straub, L.G. & Schrerer, P.E. Metabolic messengers: Adiponectin. *Nature Metabolism* **1**, 334-339 (2019).

58. Marroqui, L., Gonzalez, A., Neco, P., Caballero-Garrido, E., Vieira, E., Ripoll, C., Nadal, A. & Quesada, I. Role of leptin in the pancreatic beta-cell: Effects and signaling pathways. *J Mol Endocrinol* **49**, R9-17 (2012).

59. Ye, R. & Scherer, P.E. Adiponectin, driver or passenger on the road to insulin sensitivity? *Molecular Metabolism* **2**, 133-141 (2013).

60. Ulian, M.D., Aburad, L., da Silva Oliveira, M.S., Poppe, A.C.M., Sabatini, F., Perez, I., Gualano, B., Benatti, F.B., Pinto, A.J., Roble, O.J., Vessoni, A., de Morais Sato, P., Unsain, R.F. & Baeza Scagliusi, F. Effects of health at every size(r) interventions on health-related outcomes of people with overweight and obesity: A systematic review. *Obes Rev* **19**, 1659-1666 (2018).

61. Attie, A.D. & Scherer, P.E. Adipocyte metabolism and obesity. *J Lipid Res* **50 Suppl**, S395-399 (2009).

62. Kim, S.H. & Plutzky, J. Brown fat and browning for the treatment of obesity and related metabolic disorders. *Diabetes Metab J* **40**, 12-21 (2016).

63. Herz, C.T. & Kiefer, F.W. Adipose tissue browning in mice and humans. *J Endocrinol* **241**, R97-R109 (2019).

64. Cannon, B. & Nedergaard, J. Brown adipose tissue: Function and physiological significance. *Physiol Rev* **84**, 277-359 (2004).

65. Lowell, B.B. & Spiegelman, B.M. Towards a molecular understanding of adaptive thermogenesis. *Nature* **404**, 652-660 (2000).

66. Hanssen, M.J.W., van der Lans, A.A.J.J., Brans, B., Hoeks, J., Jardon, K.M.C., Schaart, G., Mottaghy, F.M., Schrauwen, P. & van Marken Lichtenbelt, W.D. Short-term cold acclimation recruits brown adipose tissue in obese humans. *Diabetes* **65**, 1179 (2016).

67. Graja, A. & Schulz, T.J. Mechanisms of aging-related impairment of brown adipocyte development and function. *Gerontology* **61**, 211-217 (2015).

68. Leitner, B.P., Huang, S., Brychta, R.J., Duckworth, C.J., Baskin, A.S., McGehee, S., Tal, I., Dieckmann, W., Gupta, G., Kolodny, G.M., Pacak, K., Herscovitch, P., Cypess, A.M. & Chen, K.Y. Mapping of human brown adipose tissue in lean and obese young men. *Proceedings of the National Academy of Sciences* **114**, 8649 (2017).

69. Bartelt, A. & Heeren, J. Adipose tissue browning and metabolic health. *Nature Reviews Endocrinology* **10**, 24 (2013).

70. Harms, M. & Seale, P. Brown and beige fat: Development, function and therapeutic potential. *Nature Medicine* **19**, 1252 (2013).

71. Jespersen, N., Larsen, T., Peijs, L., Daugaard, S., Homøe, P., Loft, A., De Jong, J., Mathur, N., Cannon, B., Nedergaard, J., Pedersen, B., Møller, K. & Scheele, C. A classical brown adipose tissue mrna signature partly overlaps with brite in the supraclavicular region of adult humans. *Cell metabolism* **17**, 798-805 (2013).

72. Walden, T.B., Hansen, I.R., Timmons, J.A., Cannon, B. & Nedergaard, J. Recruited vs. Nonrecruited molecular signatures of brown, "brite," and white adipose tissues. *Am J Physiol Endocrinol Metab* **302**, E19-31 (2012).

73. Wu, J., Boström, P., Sparks, Lauren M., Ye, L., Choi, Jang H., Giang, A.-H., Khandekar, M., Virtanen, Kirsi A., Nuutila, P., Schaart, G., Huang, K., Tu, H., van Marken Lichtenbelt, Wouter D., Hoeks, J., Enerbäck, S., Schrauwen, P. & Spiegelman, Bruce M. Beige adipocytes are a distinct type of thermogenic fat cell in mouse and human. *Cell* **150**, 366-376 (2012).

74. Timmons, J.A., Wennmalm, K., Larsson, O., Walden, T.B., Lassmann, T., Petrovic, N., Hamilton, D.L., Gimeno, R.E., Wahlestedt, C., Baar, K., Nedergaard, J. & Cannon, B. Myogenic gene expression signature establishes that brown and white adipocytes originate from distinct cell lineages. *Proceedings of the National Academy of Sciences* **104**, 4401 (2007).

75. Enerbäck, S., Jacobsson, A., Simpson, E.M., Guerra, C., Yamashita, H., Harper, M.-E. & Kozak, L.P. Mice lacking mitochondrial uncoupling protein are cold-sensitive but not obese. *Nature* **387**, 90-94 (1997).

76. Matthias, A., Ohlson, K.B., Fredriksson, J.M., Jacobsson, A., Nedergaard, J. & Cannon, B. Thermogenic responses in brown fat cells are fully ucp1-dependent. Ucp2 or ucp3 do not substitute for ucp1 in adrenergically or fatty scid-induced thermogenesis. *J Biol Chem* **275**, 25073-25081 (2000).

77. Perkins, M.N., Rothwell, N.J., Stock, M.J. & Stone, T.W. Activation of brown adipose tissue thermogenesis by the ventromedial hypothalamus. *Nature* **289**, 401-402 (1981).

78. Amir, S. Stimulation of the paraventricular nucleus with glutamate activates interscapular brown adipose tissue thermogenesis in rats. *Brain Res* **508**, 152-155 (1990).

79. Martin, J. *Neuroanatomy: Text and atlas*, (McGraw-Hill Companies,Incorporated, 2003).

80. Rui, L. Brain regulation of energy balance and body weight. *Rev Endocr Metab Disord* **14**, 387-407 (2013).

81. Roh, E. & Kim, M.S. Brain regulation of energy metabolism. *Endocrinol Metab (Seoul)* **31**, 519-524 (2016).

82. Miyata, A., Arimura, A., Dahl, R.R., Minamino, N., Uehara, A., Jiang, L., Culler, M.D. & Coy, D.H. Isolation of a novel 38 residue-hypothalamic polypeptide which stimulates adenylate cyclase in pituitary cells. *Biochem Biophys Res Commun* **164**, 567-574 (1989).

83. Vaudry, D., Falluel-Morel, A., Bourgault, S., Basille, M., Burel, D., Wurtz, O., Fournier, A., Chow, B.K., Hashimoto, H., Galas, L. & Vaudry, H. Pituitary adenylate cyclase-activating polypeptide and its receptors: 20 years after the discovery. *Pharmacol Rev* **61**, 283-357 (2009).

84. Dickson, L. & Finlayson, K. Vpac and pac receptors: From ligands to function. *Pharmacology & therapeutics* **121**, 294-316 (2009).

85. Arimura, A., Somogyvari-Vigh, A., Miyata, A., Mizuno, K., Coy, D.H. & Kitada, C. Tissue distribution of pacap as determined by ria: Highly abundant in the rat brain and testes. *Endocrinology* **129**, 2787-2789 (1991).

86. Dow, R.C., Bennie, J. & Fink, G. Pituitary adenylate cyclase-activating peptide-38 (pacap)-38 is released into hypophysial portal blood in the normal male and female rat. *J Endocrinol* **142**, R1-4 (1994).

87. Eiden, L.E., Emery, A.C., Zhang, L. & Smith, C.B. Pacap signaling in stress: Insights from the chromaffin cell. *Pflugers Arch* **470**, 79-88 (2018).

88. Hamelink, C., Tjurmina, O., Damadzic, R., Young, W.S., Weihe, E., Lee, H.W. & Eiden, L.E. Pituitary adenylate cyclase-activating polypeptide is a sympathoadrenal neurotransmitter involved in catecholamine regulation and glucohomeostasis. *Proc Natl Acad Sci U S A* **99**, 461-466 (2002).

89. Mustafa, T., Walsh, J., Grimaldi, M. & Eiden, L.E. Pac1hop receptor activation facilitates catecholamine secretion selectively through 2-apb-sensitive ca(2+) channels in pc12 cells. *Cell Signal* **22**, 1420-1426 (2010).

90. Pisegna, J.R. & Wank, S.A. Molecular cloning and functional expression of the pituitary adenylate cyclase-activating polypeptide type i receptor. *Proceedings of the National Academy of Sciences of the United States of America* **90**, 6345-6349 (1993).

91. Sreedharan, S.P., Patel, D.R., Huang, J.X. & Goetzl, E.J. Cloning and functional expression of a human neuroendocrine vasoactive intestinal peptide receptor. *Biochem Biophys Res Commun* **193**, 546-553 (1993).

92. Adamou, J.E., Aiyar, N., Van Horn, S. & Elshourbagy, N.A. Cloning and functional characterization of the human vasoactive intestinal peptide (vip)-2 receptor. *Biochem Biophys Res Commun* **209**, 385-392 (1995).

93. Blechman, J. & Levkowitz, G. Alternative splicing of the pituitary adenylate cyclase-activating polypeptide receptor pac1: Mechanisms of fine tuning of brain activity. *Frontiers in Endocrinology* **4**, 55 (2013).

94. Spongier, D., Waeber, C., Pantaloni, C., Holsboer, F., Bockaert, J., Seeburgt, P.H. & Journot, L. Differential signal transduction by five splice variants of the pacap receptor. *Nature* **365**, 170-175 (1993).

95. Moro, O. & Lerner, E.A. Maxadilan, the vasodilator from sand flies, is a specific pituitary adenylate cyclase activating peptide type i receptor agonist. *J Biol Chem* **272**, 966-970 (1997).

96. Uchida, D., Tatsuno, I., Tanaka, T., Hirai, A., Saito, Y., Moro, O. & Tajima, M. Maxadilan is a specific agonist and its deleted peptide (m65) is a specific antagonist for pacap type 1 receptor. *Ann N Y Acad Sci* **865**, 253-258 (1998).

97. Emery, A.C., Xu, W., Eiden, M.V. & Eiden, L.E. Guanine nucleotide exchange factor epac2-dependent activation of the gtp-binding protein rap2a mediates camp-dependent growth arrest in neuroendocrine cells. *J Biol Chem* **292**, 12220-12231 (2017).

98. Sherwood, N.M., Krueckl, S.L. & McRory, J.E. The origin and function of the pituitary adenylate cyclase-activating polypeptide (pacap)/glucagon superfamily. *Endocrine reviews* **21**, 619-670 (2000).

99. Persson, K. & Ahren, B. The neuropeptide pacap contributes to the glucagon response to insulin-induced hypoglycaemia in mice. *Acta physiologica Scandinavica* **175**, 25-28 (2002).

100. Gray, S.L. & Cline, D.L. Chapter 21 - pacap: Regulator of the stress response. in *Stress: Physiology, biochemistry, and pathology* (ed. Fink, G.) 279-291 (Academic Press, 2019).

101. Mustafa, T., Jiang, S.Z., Eiden, A.M., Weihe, E., Thistlethwaite, I. & Eiden, L.E. Impact of pacap and pac1 receptor deficiency on the neurochemical and behavioral effects of acute and chronic restraint stress in male c57bl/6 mice. *Stress* **18**, 408-418 (2015).

102. Ressler, K.J., Mercer, K.B., Bradley, B., Jovanovic, T., Mahan, A., Kerley, K., Norrholm, S.D., Kilaru, V., Smith, A.K., Myers, A.J., Ramirez, M., Engel, A., Hammack, S.E., Toufexis, D., Braas, K.M., Binder, E.B. & May, V. Post-traumatic stress disorder is associated with pacap and the pac1 receptor. *Nature* **470**, 492-497 (2011).

103. Tsukiyama, N., Saida, Y., Kakuda, M., Shintani, N., Hayata, A., Morita, Y., Tanida, M., Tajiri, M., Hazama, K., Ogata, K., Hashimoto, H. & Baba, A. Pacap centrally mediates emotional stress-induced corticosterone responses in mice. *Stress* **14**, 368-375 (2011).

104. Mori, H., Nakamachi, T., Ohtaki, H., Yofu, S., Sato, A., Endo, K., Iso, Y., Suzuki, H., Takeyama, Y., Shintani, N., Hashimoto, H., Baba, A. & Shioda, S. Cardioprotective effect of endogenous pituitary adenylate cyclase-activating polypeptide on doxorubicin-induced cardiomyopathy in mice. *Circulation Journal* **74**, 1183-1190 (2010).

105. Lindberg, D., Chen, P. & Li, C. Conditional viral tracing reveals that steroidogenic factor 1-positive neurons of the dorsomedial subdivision of the ventromedial hypothalamus project to autonomic centers of the hypothalamus and hindbrain. *J Comp Neurol* **521**, 3167-3190 (2013).

106. Hawke, Z., Ivanov, T.R., Bechtold, D.A., Dhillon, H., Lowell, B.B. & Luckman, S.M. Pacap neurons in the hypothalamic ventromedial nucleus are targets of central leptin signaling. *The Journal of Neuroscience* **29**, 14828 (2009).

107. Diane, A., Nikolic, N., Rudecki, A.P., King, S.M., Bowie, D.J. & Gray, S.L. Pacap is essential for the adaptive thermogenic response of brown adipose tissue to cold exposure. *J Endocrinol* **222**, 327-339 (2014).

108. Gray, S.L., Cummings, K.J., Jirik, F.R. & Sherwood, N.M. Targeted disruption of the pituitary adenylate cyclase-activating polypeptide gene results in early postnatal death associated with dysfunction of lipid and carbohydrate metabolism. *Mol Endocrinol* **15**, 1739-1747 (2001).

109. Resch, J.M., Boisvert, J.P., Hourigan, A.E., Mueller, C.R., Yi, S.S. & Choi, S. Stimulation of the hypothalamic ventromedial nuclei by pituitary adenylate cyclase-activating polypeptide induces hypophagia and thermogenesis. *Am J Physiol Regul Integr Comp Physiol* **301**, R1625-1634 (2011).

110. Resch, J.M., Maunze, B., Gerhardt, A.K., Magnuson, S.K., Phillips, K.A. & Choi, S. Intrahypothalamic pituitary adenylate cyclase-activating polypeptide regulates energy balance via site-specific actions on feeding and metabolism. *American Journal of Physiology-Endocrinology and Metabolism* **305**, E1452-E1463 (2013).

111. Giustina, A., Frara, S., Spina, A. & Mortini, P. Chapter 9 - the hypothalamus. in *The pituitary (fourth edition)* (ed. Melmed, S.) 291-327 (Academic Press, 2017).

112. Bauer, H.G. Endocrine and metabolic conditions related to pathology in the hypothalamus: A review. *The Journal of Nervous and Mental Disease* **128**(1959).

113. Saper, C.B. & Lowell, B.B. The hypothalamus. *Current Biology* **24**, R1111-R1116 (2014).

114. Simpson, J.A. Chapter 25 - homoeostasis and general responses to stress. 247-257 (Elsevier Ltd, 1988).

115. Hofman, M.A. & Swaab, D.F. Neuroplasticity in the human hypothalamus during ageing. in *Neuroimmune biology*, Vol. 4 (eds. Straub, R.H. & Mocchegiani, E.) 105-121 (Elsevier, 2004).

116. Romanovsky, A.A. Thermoregulation: Some concepts have changed. Functional architecture of the thermoregulatory system. *American Journal of Physiology-Regulatory, Integrative and Comparative Physiology* **292**, R37-R46 (2007).

117. Balagura, S. & Devenport, L.D. Feeding patterns of normal and ventromedial hypothalamic lesioned male and female rats. *Journal of Comparative and Physiological Psychology* **71**, 357-364 (1970).

118. Brooks, C.M., Lockwood, R.A. & Wiggins, M.L. A study of the effect of hypothalamic lesions on the eating habits of the albino rat. *American Journal of Physiology-Legacy Content* **147**, 735-741 (1946).

119. Satoh, N., Ogawa, Y., Katsuura, G., Tsuji, T., Masuzaki, H., Hiraoka, J., Okazaki, T., Tamaki, M., Hayase, M., Yoshimasa, Y., Nishi, S., Hosoda, K. & Nakao, K. Pathophysiological significance of the obese gene product, leptin, in ventromedial hypothalamus (vmh)-lesioned rats: Evidence for loss of its satiety effect in vmh-lesioned rats*. *Endocrinology* **138**, 947-954 (1997).

120. Wang, C., Bomberg, E., Levine, A., Billington, C. & Kotz, C.M. Brain-derived neurotrophic factor in the ventromedial nucleus of the hypothalamus reduces energy intake. *American Journal of Physiology-Regulatory, Integrative and Comparative Physiology* **293**, R1037-R1045 (2007).

121. Thorleifsson, G., Walters, G.B., Gudbjartsson, D.F., Steinthorsdottir, V., Sulem, P., Helgadottir, A., Styrkarsdottir, U., Gretarsdottir, S., Thorlacius, S., Jonsdottir, I., Jonsdottir, T., Olafsdottir, E.J., Olafsdottir, G.H., Jonsson, T., Jonsson, F., Borch-Johnsen, K., Hansen, T., Andersen, G., Jorgensen, T., Lauritzen, T.*, et al.* Genome-wide association yields new sequence variants at seven loci that associate with measures of obesity. *Nature Genetics* **41**, 18-24 (2009).

122. Willer, C.J., Speliotes, E.K., Loos, R.J.F., Li, S., Lindgren, C.M., Heid, I.M., Berndt, S.I., Elliott, A.L., Jackson, A.U., Lamina, C., Lettre, G., Lim, N., Lyon, H.N., McCarroll, S.A., Papadakis, K., Qi, L., Randall, J.C., Roccasecca, R.M., Sanna, S., Scheet, P.*, et al.* Six new loci associated with body mass index highlight a neuronal influence on body weight regulation. *Nature Genetics* **41**, 25-34 (2009).

123. Rudecki, A.P. & Gray, S.L. Pacap in the defense of energy homeostasis. *Trends in Endocrinology & Metabolism* **27**, 620-632 (2016).

124. Resch, J.M., Maunze, B., Phillips, K.A. & Choi, S. Inhibition of food intake by pacap in the hypothalamic ventromedial nuclei is mediated by nmda receptors. *Physiology & Behavior* **133**, 230-235 (2014).

125. Trung, N., Kambe, Y., Kurihara, T. & Miyata, A. Sun-116 the endogenous pituitary adenylate cyclase-activating polypeptide increases food intake by modulating the expression of neuropeptides in the hypothalamus. *Journal of the Endocrine Society* **3**(2019).

126. Mounien, L., Bizet, P., Boutelet, I., Gourcerol, G., Basille, M., Gonzalez, B., Vaudry, H. & Jegou, S. Expression of pacap receptor mrnas by neuropeptide y neurons in the rat arcuate nucleus. *Annals of the New York Academy of Sciences* **1070**, 457-461 (2006).

127. Murase, T., Kondo, K., Arima, H., Iwasaki, Y., Ito, M., Miura, Y. & Oiso, Y. The expression of pituitary adenylate cyclase-activating polypeptide (pacap) mrna in rat brain: Possible role of endogenous pacap in vasopressin release. *Neuroscience Letters* **185**, 103-106 (1995).

128. Tan, C.L., Cooke, E.K., Leib, D.E., Lin, Y.-C., Daly, G.E., Zimmerman, C.A. & Knight, Z.A. Warm-sensitive neurons that control body temperature. *Cell* **167**, 47-59.e15 (2016).

129. Chen, X.-M., Hosono, T., Yoda, T., Fukuda, Y. & Kanosue, K. Efferent projection from the preoptic area for the control of non-shivering thermogenesis in rats. *The Journal of Physiology* **512**, 883-892 (1998).

130. Caterina, M.J. Transient receptor potential ion channels as participants in thermosensation and thermoregulation. *American Journal of Physiology-Regulatory, Integrative and Comparative Physiology* **292**, R64-R76 (2007).

131. Amir, S., Lagiorgia, M. & Pollock, R. Intra-ventromedial hypothalamic injection of insulin suppresses brown fat thermogenesis in the anaesthetized rat. *Brain Res* **480**, 340-343 (1989).

132. Zaretskaia, M.V., Zaretsky, D.V., Shekhar, A. & DiMicco, J.A. Chemical stimulation of the dorsomedial hypothalamus evokes non-shivering thermogenesis in anesthetized rats. *Brain Res* **928**, 113-125 (2002).

133. Bamshad, M., Song, C.K. & Bartness, T.J. Cns origins of the sympathetic nervous system outflow to brown adipose tissue. *American Journal of Physiology-Regulatory, Integrative and Comparative Physiology* **276**, R1569-R1578 (1999).

134. Bartness, T.J., Vaughan, C.H. & Song, C.K. Sympathetic and sensory innervation of brown adipose tissue. *International Journal of Obesity* **34**, S36-S42 (2010).

135. Oldfield, B.J., Giles, M.E., Watson, A., Anderson, C., Colvill, L.M. & McKinley, M.J. The neurochemical characterisation of hypothalamic pathways projecting polysynaptically to brown adipose tissue in the rat. *Neuroscience* **110**, 515-526 (2002).

136. Kim, K.W., Zhao, L., Donato, J., Jr., Kohno, D., Xu, Y., Elias, C.F., Lee, C., Parker, K.L. & Elmquist, J.K. Steroidogenic factor 1 directs programs regulating diet-induced thermogenesis and leptin action in the ventral medial hypothalamic nucleus. *Proc Natl Acad Sci U S A* **108**, 10673-10678 (2011).

137. Stefanidis, A., Wiedmann, N.M., Adler, E.S. & Oldfield, B.J. Hypothalamic control of adipose tissue. *Best Practice & Research Clinical Endocrinology & Metabolism* **28**, 685-701 (2014).

138. Kotterman, M.A. & Schaffer, D.V. Engineering adeno-associated viruses for clinical gene therapy. *Nature Reviews Genetics* **15**, 445-451 (2014).

139. Meyer, K., Ferraiuolo, L., Schmelzer, L., Braun, L., McGovern, V., Likhite, S., Michels, O., Govoni, A., Fitzgerald, J., Morales, P., Foust, K.D., Mendell, J.R., Burghes, A.H. & Kaspar, B.K. Improving single injection csf delivery of aav9-mediated gene therapy for sma: A dose-response study in mice and nonhuman primates. *Mol Ther* **23**, 477-487 (2015).

140. Naso, M.F., Tomkowicz, B., Perry, W.L. & Strohl, W.R. Adeno-associated virus (aav) as a vector for gene therapy. *BioDrugs* **31**, 317-334 (2017).

141. Hammond, S.L., Leek, A.N., Richman, E.H. & Tjalkens, R.B. Cellular selectivity of aav serotypes for gene delivery in neurons and astrocytes by neonatal intracerebroventricular injection. *PloS one* **12**, e0188830-e0188830 (2017).

142. Haberman, R.P. & McCown, T.J. Regulation of gene expression in adeno-associated virus vectors in the brain. *Methods* **28**, 219-226 (2002).

143. Kattenhorn, L.M., Tipper, C.H., Stoica, L., Geraghty, D.S., Wright, T.L., Clark, K.R. & Wadsworth, S.C. Adeno-associated virus gene therapy for liver disease. *Human Gene Therapy* **27**, 947-961 (2016).

144. Choi, Y.-H., Fujikawa, T., Lee, J., Reuter, A. & Kim, K.W. Revisiting the ventral medial nucleus of the hypothalamus: The roles of sf-1 neurons in energy homeostasis. *Frontiers in Neuroscience* **7**, 71 (2013).

145. Cheung, C.C., Kurrasch, D.M., Liang, J.K. & Ingraham, H.A. Genetic labeling of steroidogenic factor-1 (sf-1) neurons in mice reveals ventromedial nucleus of the hypothalamus (vmh) circuitry beginning at neurogenesis and development of a separate non-sf-1 neuronal cluster in the ventrolateral vmh. *J Comp Neurol* **521**, 1268-1288 (2013).

146. Zhao, L., Bakke, M., Krimkevich, Y., Cushman, L.J., Parlow, A.F., Camper, S.A. & Parker, K.L. Steroidogenic factor 1 (sf1) is essential for pituitary gonadotrope function. *Development* **128**, 147-154 (2001).

147. Woodson, K.G., Crawford, P.A., Sadovsky, Y. & Milbrandt, J. Characterization of the promoter of sf-1, an orphan nuclear receptor required for adrenal and gonadal development. *Mol Endocrinol* **11**, 117-126 (1997).

148. Xu, Y., Faulkner, L. & Hill, J. Cross-talk between metabolism and reproduction: The role of pomc and sf1 neurons. *Frontiers in Endocrinology* **2**, 98 (2012).

149. Strausberg, R.L., Feingold, E.A., Grouse, L.H., Derge, J.G., Klausner, R.D., Collins, F.S., Wagner, L., Shenmen, C.M., Schuler, G.D., Altschul, S.F., Zeeberg, B., Buetow, K.H., Schaefer, C.F., Bhat, N.K., Hopkins, R.F., Jordan, H., Moore, T., Max, S.I., Wang, J., Hsieh, F*., et al.* Generation and initial analysis of more than 15,000 full-length human and mouse cdna sequences. *Proc Natl Acad Sci U S A* **99**, 16899-16903 (2002).

150. Sadovsky, Y., Crawford, P.A., Woodson, K.G., Polish, J.A., Clements, M.A., Tourtellotte, L.M., Simburger, K. & Milbrandt, J. Mice deficient in the orphan receptor steroidogenic factor 1 lack adrenal glands and gonads but express p450 side-chain-cleavage enzyme in the placenta and have normal embryonic serum levels of corticosteroids. *Proc Natl Acad Sci U S A* **92**, 10939-10943 (1995).

151. Kinyua, A.W., Yang, D.J., Chang, I. & Kim, K.W. Steroidogenic factor 1 in the ventromedial nucleus of the hypothalamus regulates age-dependent obesity. *PLoS One* **11**, e0162352 (2016).

152. Jeyasuria, P., Ikeda, Y., Jamin, S.P., Zhao, L., De Rooij, D.G., Themmen, A.P., Behringer, R.R. & Parker, K.L. Cell-specific knockout of steroidogenic factor 1 reveals its essential roles in gonadal function. *Mol Endocrinol* **18**, 1610-1619 (2004).

153. Davis, A.M., Seney, M.L., Stallings, N.R., Zhao, L., Parker, K.L. & Tobet, S.A. Loss of steroidogenic factor 1 alters cellular topography in the mouse ventromedial nucleus of the hypothalamus. *Journal of Neurobiology* **60**, 424-436 (2004).

154. Büdefeld, T., Tobet, S.A. & Majdic, G. Altered position of cell bodies and fibers in the ventromedial region in sf-1 knockout mice. *Exp Neurol* **232**, 176-184 (2011).

155. Shioda, S., Ohtaki, H., Nakamachi, T., Dohi, K., Watanabe, J.U.N., Nakajo, S., Arata, S., Kitamura, S., Okuda, H., Takenoya, F. & Kitamura, Y. Pleiotropic functions of pacap in the cns. *Annals of the New York Academy of Sciences* **1070**, 550-560 (2006).

156. Gray, J.T. & Zolotukhin, S. Design and construction of functional aav vectors. in *Adeno-associated virus: Methods and protocols* (eds. Snyder, R.O. & Moullier, P.) 25-46 (Humana Press, Totowa, NJ, 2011).

157. McMillan, T.R. University of Northern British Columbia (2017).

158. Morley, J.E., Horowitz, M., Morley, P.M. & Flood, J.F. Pituitary adenylate cyclase activating polypeptide (pacap) reduces food intake in mice. *Peptides* **13**, 1133-1135 (1992).

159. Glascock, J.J., Osman, E.Y., Wetz, M.J., Krogman, M.M., Shababi, M. & Lorson, C.L. Decreasing disease severity in symptomatic, smn(-/-);smn2(+/+), spinal muscular atrophy mice following scaav9-smn delivery. *Hum Gene Ther* **23**, 330-335 (2012).

160. Badea, A., Ali-Sharief, A.A. & Johnson, G.A. Morphometric analysis of the c57bl/6j mouse brain. *Neuroimage* **37**, 683-693 (2007).

161. Lein, E.S., Hawrylycz, M.J., Ao, N., Ayres, M., Bensinger, A., Bernard, A., Boe, A.F., Boguski, M.S., Brockway, K.S., Byrnes, E.J., Chen, L., Chen, L., Chen, T.-M., Chi Chin, M., Chong, J., Crook, B.E., Czaplinska, A., Dang, C.N., Datta, S., Dee, N.R.*, et al.* Genome-wide atlas of gene expression in the adult mouse brain. *Nature* **445**, 168-176 (2007).

162. Huang, L., Yuan, Z., Liu, P. & Zhou, T. Effects of promoter leakage on dynamics of gene expression. *BMC Syst Biol* **9**, 16-16 (2015).

163. Rosano, G.L. & Ceccarelli, E.A. Recombinant protein expression in escherichia coli: Advances and challenges. *Front Microbiol* **5**, 172-172 (2014).

164. Gao, Y., Chen, T., Lei, X., Li, Y., Dai, X., Cao, Y., Ding, Q., Lei, X., Li, T. & Lin, X. Neuroprotective effects of polydatin against mitochondrial-dependent apoptosis in the rat cerebral cortex following ischemia/reperfusion injury. *Mol Med Rep* **14**, 5481-5488 (2016).

165. Catalano, S., Malivindi, R., Giordano, C., Gu, G., Panza, S., Bonofiglio, D., Lanzino, M., Sisci, D., Panno, M.L. & Ando, S. Farnesoid x receptor, through the binding with steroidogenic factor

1-responsive element, inhibits aromatase expression in tumor leydig cells. *J Biol Chem* **285**, 5581-5593 (2010).

166. Martin, D., Xu, J., Porretta, C. & Nichols, C.D. Neurocytometry: Flow cytometric sorting of specific neuronal populations from human and rodent brain. *ACS Chem Neurosci* **8**, 356-367 (2017).

167. Yamasaki, T., Suzuki, A., Hasebe, R. & Horiuchi, M. Flow cytometric detection of prp^{sc} in neurons and glial cells from prion-infected mouse brains. *Journal of Virology* **92**, e01457-01417 (2018).

168. Cline, D.L., Short, L.I., Forster, M.A.M. & Gray, S.L. Adipose tissue expression of pacap, vip, and their receptors in response to cold stress. *J Mol Neurosci* **68**, 427-438 (2019).

169. Gray, S.L. & Vidal-Puig, A.J. Adipose tissue expandability in the maintenance of metabolic homeostasis. *Nutr Rev* **65**, S7-12 (2007).

170. Pellegrinelli, V., Carobbio, S. & Vidal-Puig, A. Adipose tissue plasticity: How fat depots respond differently to pathophysiological cues. *Diabetologia* **59**, 1075-1088 (2016).

171. Boss, O. & Farmer, S.R. Recruitment of brown adipose tissue as a therapy for obesity-associated diseases. *Front Endocrinol (Lausanne)* **3**, 14 (2012).

172. Soler-Vazquez, M.C., Mera, P., Zagmutt, S., Serra, D. & Herrero, L. New approaches targeting brown adipose tissue transplantation as a therapy in obesity. *Biochem Pharmacol* **155**, 346-355 (2018).

173. Stanford, K.I., Middelbeek, R.J., Townsend, K.L., An, D., Nygaard, E.B., Hitchcox, K.M., Markan, K.R., Nakano, K., Hirshman, M.F., Tseng, Y.H. & Goodyear, L.J. Brown adipose tissue regulates glucose homeostasis and insulin sensitivity. *J Clin Invest* **123**, 215-223 (2013).

174. Himms-Hagen, J., Cui, J., Danforth, E., Jr., Taatjes, D.J., Lang, S.S., Waters, B.L. & Claus, T.H. Effect of cl-316,243, a thermogenic beta 3-agonist, on energy balance and brown and white adipose tissues in rats. *Am J Physiol* **266**, R1371-1382 (1994).

175. Klaus, S., Seivert, A. & Boeuf, S. Effect of the beta(3)-adrenergic agonist cl316,243 on functional differentiation of white and brown adipocytes in primary cell culture. *Biochim Biophys Acta* **1539**, 85-92 (2001).

176. Nicholls, D.G. & Locke, R.M. Thermogenic mechanisms in brown fat. *Physiol Rev* **64**, 1-64 (1984).

177. Nedergaard, J. & Lindberg, O. The brown fat cell. *Int Rev Cytol* **74**, 187-286 (1982).

178. Shabalina, I.G., Petrovic, N., de Jong, J.M., Kalinovich, A.V., Cannon, B. & Nedergaard, J. Ucp1 in brite/beige adipose tissue mitochondria is functionally thermogenic. *Cell Rep* **5**, 1196-1203 (2013).

179. Nedergaard, J., Golozoubova, V., Matthias, A., Asadi, A., Jacobsson, A. & Cannon, B. Ucp1: The only protein able to mediate adaptive non-shivering thermogenesis and metabolic inefficiency. *Biochim Biophys Acta* **1504**, 82-106 (2001).

180. Bukowiecki, L., Collet, A.J., Follea, N., Guay, G. & Jahjah, L. Brown adipose tissue hyperplasia: A fundamental mechanism of adaptation to cold and hyperphagia. *Am J Physiol* **242**, E353-359 (1982).

181. Picard, F., Gehin, M., Annicotte, J., Rocchi, S., Champy, M.F., O'Malley, B.W., Chambon, P. & Auwerx, J. Src-1 and tif2 control energy balance between white and brown adipose tissues. *Cell* **111**, 931-941 (2002).

182. Jia, R., Luo, X.Q., Wang, G., Lin, C.X., Qiao, H., Wang, N., Yao, T., Barclay, J.L., Whitehead, J.P., Luo, X. & Yan, J.Q. Characterization of cold-induced remodelling reveals depot-specific differences across and within brown and white adipose tissues in mice. *Acta Physiol (Oxf)* **217**, 311-324 (2016).

183. Harms, M.J., Li, Q., Lee, S., Zhang, C., Kull, B., Hallen, S., Thorell, A., Alexandersson, I., Hagberg, C.E., Peng, X.R., Mardinoglu, A., Spalding, K.L. & Boucher, J. Mature human white adipocytes cultured under membranes maintain identity, function, and can transdifferentiate into brown-like adipocytes. *Cell Rep* **27**, 213-225 e215 (2019).

184. Kiefer, F.W. Browning and thermogenic programing of adipose tissue. *Best Pract Res Clin Endocrinol Metab* **30**, 479-485 (2016).

185. Ghosh, A.K., Mau, T., O'Brien, M. & Yung, R. Novel role of autophagy-associated pik3c3 gene in gonadal white adipose tissue browning in aged c57/bl6 male mice. *Aging (Albany NY)* **10**, 764-774 (2018).

186. Guerra, C., Koza, R.A., Walsh, K., Kurtz, D.M., Wood, P.A. & Kozak, L.P. Abnormal nonshivering thermogenesis in mice with inherited defects of fatty acid oxidation. *J Clin Invest* **102**, 1724-1731 (1998).

187. Tolwani, R.J., Hamm, D.A., Tian, L., Sharer, J.D., Vockley, J., Rinaldo, P., Matern, D., Schoeb, T.R. & Wood, P.A. Medium-chain acyl-coa dehydrogenase deficiency in gene-targeted mice. *PLoS Genet* **1**, e23 (2005).

188. Olsen, J.M., Csikasz, R.I., Dehvari, N., Lu, L., Sandstrom, A., Oberg, A.I., Nedergaard, J., Stone-Elander, S. & Bengtsson, T. Beta3-adrenergically induced glucose uptake in brown adipose tissue is independent of ucp1 presence or activity: Mediation through the mtor pathway. *Mol Metab* **6**, 611-619 (2017).

189. Prusiner, S.B., Cannon, B. & Lindberg, O. Oxidative metabolism in cells isolated from brown adipose tissue. 1. Catecholamine and fatty acid stimulation of respiration. *Eur J Biochem* **6**, 15-22 (1968).

190. Nedergaard, J., Alexson, S. & Cannon, B. Cold adaptation in the rat: Increased brown fat peroxisomal beta-oxidation relative to maximal mitochondrial oxidative capacity. *Am J Physiol* **239**, C208-216 (1980).

191. Shore, A.M., Karamitri, A., Kemp, P., Speakman, J.R., Graham, N.S. & Lomax, M.A. Cold-induced changes in gene expression in brown adipose tissue, white adipose tissue and liver. *PLoS One* **8**, e68933 (2013).

192. Inagaki, T., Sakai, J. & Kajimura, S. Transcriptional and epigenetic control of brown and beige adipose cell fate and function. *Nat Rev Mol Cell Biol* **17**, 480-495 (2016).

193. Hilton, C., Karpe, F. & Pinnick, K.E. Role of developmental transcription factors in white, brown and beige adipose tissues. *Biochim Biophys Acta* **1851**, 686-696 (2015).

194. Wang, W. & Seale, P. Control of brown and beige fat development. *Nat Rev Mol Cell Biol* **17**, 691-702 (2016).

195. Francois, M., Qualls-Creekmore, E., Berthoud, H.R., Munzberg, H. & Yu, S. Genetics-based manipulation of adipose tissue sympathetic innervation. *Physiol Behav* **190**, 21-27 (2018).

196. Whittle, A.J., Carobbio, S., Martins, L., Slawik, M., Hondares, E., Vazquez, M.J., Morgan, D., Csikasz, R.I., Gallego, R., Rodriguez-Cuenca, S., Dale, M., Virtue, S., Villarroya, F., Cannon, B., Rahmouni, K., Lopez, M. & Vidal-Puig, A. Bmp8b increases brown adipose tissue thermogenesis through both central and peripheral actions. *Cell* **149**, 871-885 (2012).

197. Chartoumpekis, D.V., Habeos, I.G., Ziros, P.G., Psyrogiannis, A.I., Kyriazopoulou, V.E. & Papavassiliou, A.G. Brown adipose tissue responds to cold and adrenergic stimulation by induction of fgf21. *Mol Med* **17**, 736-740 (2011).

198. Fisher, F.M., Kleiner, S., Douris, N., Fox, E.C., Mepani, R.J., Verdeguer, F., Wu, J., Kharitonenkov, A., Flier, J.S., Maratos-Flier, E. & Spiegelman, B.M. Fgf21 regulates pgc-1alpha and browning of white adipose tissues in adaptive thermogenesis. *Genes Dev* **26**, 271-281 (2012).

199. Sun, K., Kusminski, C.M., Luby-Phelps, K., Spurgin, S.B., An, Y.A., Wang, Q.A., Holland, W.L. & Scherer, P.E. Brown adipose tissue derived vegf-a modulates cold tolerance and energy expenditure. *Mol Metab* **3**, 474-483 (2014).

200. Mahdaviani, K., Chess, D., Wu, Y., Shirihai, O. & Aprahamian, T.R. Autocrine effect of vascular endothelial growth factor-a is essential for mitochondrial function in brown adipocytes. *Metabolism* **65**, 26-35 (2016).

201. Bianco, A.C. & Silva, J.E. Intracellular conversion of thyroxine to triiodothyronine is required for the optimal thermogenic function of brown adipose tissue. *J Clin Invest* **79**, 295-300 (1987).

202. Filipsson, K., Sundler, F., Hannibal, J. & Ahren, B. Pacap and pacap receptors in insulin producing tissues: Localization and effects. *Regul Pept* **74**, 167-175 (1998).

203. Åkesson, L., Ahren, B., Edgren, G. & Degerman, E. Vpac2-r mediates the lipolytic effects of pituitary adenylate cyclase-activating polypeptide/vasoactive intestinal polypeptide in primary rat adipocytes. *Endocrinology* **146**, 744-750 (2005).

204. Wei, Y. & Mojsov, S. Tissue specific expression of different human receptor types for pituitary adenylate cyclase activating polypeptide and vasoactive intestinal polypeptide: Implications for their role in human physiology. *J Neuroendocrinol* **8**, 811-817 (1996).

205. Peirce, V., Carobbio, S. & Vidal-Puig, A. The different shades of fat. *Nature* **510**, 76-83 (2014).

206. Bustin, S.A., Benes, V., Garson, J.A., Hellemans, J., Huggett, J., Kubista, M., Mueller, R., Nolan, T., Pfaffl, M.W., Shipley, G.L., Vandesompele, J. & Wittwer, C.T. The miqe guidelines: Minimum information for publication of quantitative real-time pcr experiments. *Clin Chem* **55**, 611-622 (2009).

207. Trapnell, C., Roberts, A., Goff, L., Pertea, G., Kim, D., Kelley, D.R., Pimentel, H., Salzberg, S.L., Rinn, J.L. & Pachter, L. Differential gene and transcript expression analysis of rna-seq experiments with tophat and cufflinks. *Nat Protoc* **7**, 562-578 (2012).

208. Kim, S., Scheffler, K., Halpern, A.L., Bekritsky, M.A., Noh, E., Kallberg, M., Chen, X., Kim, Y., Beyter, D., Krusche, P. & Saunders, C.T. Strelka2: Fast and accurate calling of germline and somatic variants. *Nat Methods* **15**, 591-594 (2018).

209. Atgie, C., Faintrenie, G., Carpene, C., Bukowiecki, L.J. & Geloen, A. Effects of chronic treatment with noradrenaline or a specific beta3-adrenergic agonist, cl 316 243, on energy expenditure and epididymal adipocyte lipolytic activity in rat. *Comp Biochem Physiol A Mol Integr Physiol* **119**, 629-636 (1998).

210. Greenberg, A.S., Shen, W.J., Muliro, K., Patel, S., Souza, S.C., Roth, R.A. & Kraemer, F.B. Stimulation of lipolysis and hormone-sensitive lipase via the extracellular signal-regulated kinase pathway. *J Biol Chem* **276**, 45456-45461 (2001).

211. Smith, R.E. & Roberts, J.C. Thermogenesis of brown adipose tissue in cold-acclimated rats. *American Journal of Physiology-Legacy Content* **206**, 143-148 (1964).

212. Calvo, J.R., Montilla, M.L., Guerrero, J.M. & Segura, J.J. Expression of vip receptors in mouse peritoneal macrophages: Functional and molecular characterization. *J Neuroimmunol* **50**, 85-93 (1994).

213. Petrovic, N., Walden, T.B., Shabalina, I.G., Timmons, J.A., Cannon, B. & Nedergaard, J. Chronic peroxisome proliferator-activated receptor gamma (ppargamma) activation of epididymally derived white adipocyte cultures reveals a population of thermogenically competent, ucp1-containing adipocytes molecularly distinct from classic brown adipocytes. *J Biol Chem* **285**, 7153-7164 (2010).

214. Yang, Y.S., Song, H.D., Li, R.Y., Zhou, L.B., Zhu, Z.D., Hu, R.M., Han, Z.G. & Chen, J.L. The gene expression profiling of human visceral adipose tissue and its secretory functions. *Biochem Biophys Res Commun* **300**, 839-846 (2003).

215. Young, J.B., Saville, E., Rothwell, N.J., Stock, M.J. & Landsberg, L. Effect of diet and cold exposure on norepinephrine turnover in brown adipose tissue of the rat. *J Clin Invest* **69**, 1061-1071 (1982).

216. Sekar, R., Wang, L. & Chow, B.K.C. Central control of feeding behavior by the secretin, pacap, and glucagon family of peptides. *Frontiers in Endocrinology* **8**, 18 (2017).

217. Warner, A., Kjellstedt, A., Carreras, A., Bottcher, G., Peng, X.R., Seale, P., Oakes, N. & Linden, D. Activation of beta3-adrenoceptors increases in vivo free fatty acid uptake and utilization in brown but not white fat depots in high-fat-fed rats. *Am J Physiol Endocrinol Metab* **311**, E901-E910 (2016).

218. Unelius, L., Bronnikov, G., Mohell, N. & Nedergaard, J. Physiological desensitization of beta 3-adrenergic responses in brown fat cells: Involvement of a postreceptor process. *Am J Physiol* **265**, C1340-1348 (1993).

219. Raajendiran, A., Tsiloulis, T. & Watt, Matthew J. Adipose tissue development and the molecular regulation of lipid metabolism. *Essays in Biochemistry* **60**, 437-450 (2016).

220. Moreno-Navarrete, J.M. & Fernández-Real, J.M. Adipocyte differentiation. in *Adipose tissue biology* (ed. Symonds, M.E.) 69-90 (Springer International Publishing, Cham, 2017).